Geophysical Investigations of Salinization along the Upper Colorado River between Lake Thomas and Ivie Reservoir, Texas

by

Jeffrey G. Paine, Edward W. Collins, and H. S. Nance

Bureau of Economic Geology

Scott W. Tinker, Director

John A. and Katherine G. Jackson School of Geosciences

The University of Texas at Austin

Austin, Texas 78713-8924

August 2005

GEOPHYSICAL INVESTIGATIONS OF SALINIZATION ALONG THE UPPER COLORADO RIVER BETWEEN LAKE THOMAS AND IVIE RESERVOIR, TEXAS

by

Jeffrey G. Paine, Edward W. Collins, and H. S. Nance
Bureau of Economic Geology
John A. and Katherine G. Jackson School of Geosciences
The University of Texas at Austin

Mail address:
University Station, Box X
Austin, Texas 78713-8924

Street address:
J. J. Pickle Research Campus, Building 130
10100 Burnet Road
Austin, Texas 78758-4445
jeff.paine@beg.utexas.edu

Prepared for

Texas Commission on Environmental Quality
P.O. Box 13087
MC 203
Austin, Texas 78711-3087

Contract No. 582-4-56385
Work Order No. 6

August 2005
Revised January 2006

Recommended citation: Paine, J. G., Collins, E. W., and Nance, H. S., 2005, Geophysical investigations of salinization along the upper Colorado River between Lake Thomas and Ivie Reservoir, Texas: The University of Texas at Austin, Bureau of Economic Geology, report prepared for Texas Commission on Environmental Quality, under contract no. 582-4-56385, 113 p.

Page intentionally blank

CONTENTS

FIGURES

TABLES

Page intentionally blank

SUMMARY

We conducted an airborne geophysical survey of the upper Colorado River and its tributaries from Lake Thomas to Ivie Reservoir. The purpose of this survey and supporting ground-based geophysical measurements and chemical analyses of surface water was to delineate the lateral extent and assess the degree and possible sources of salinization that contribute to the failure of the Colorado River to meet surface water quality standards for total dissolved solids (TDS), chloride, and sulfate along segment 1426 below Spence Reservoir.

The airborne electromagnetic (EM) survey, flown in February 2005, measured the electrical conductivity of the ground at multiple exploration depths along stream-axis flight lines on the Colorado River between Lake Thomas and Spence Reservoir, Spence Reservoir and Ivie Reservoir, and on Beals Creek, a high-salinity tributary, from Big Spring to the Colorado River confluence. Block surveys were flown centered on the Colorado River in the Silver and Machae Creek areas to provide more detailed conductivity data in these salinized areas. Because the electrical conductivity of the ground increases with increasing salinity, conductivity data from ground and airborne EM surveys can be used to rapidly assess salinization over large areas such as the upper Colorado River basin.

Ground-based and airborne EM data show that the area upstream from Spence Reservoir is generally more conductive (and more saline) than segment 1426 downstream from Spence Reservoir. The survey identified 11 high-conductivity areas of the Colorado River and Beals Creek that each are likely to increase the TDS, chloride, and sulfate load carried by the Colorado River. There are four high-conductivity segments on the Colorado River above Spence Reservoir (the Sharon Ridge, Canyon Creek, Barber Reservoir, and Silver areas), three on Beals Creek (but only two of these, the Moss Creek Lake and Spade Ranch areas, show significant evidence of ground salinization), and four between Spence Reservoir and Ballinger on segment 1426 (the Machae Creek, Maverick, Bull Hollow, and Valley Creek areas, in downstream order).

We used geophysical data to choose key water-sampling locations that included low-flow-stage river samples near the upstream and downstream ends of the four conductive areas along segment 1426. These data verified that TDS, chloride, and sulfate loads carried by the river do increase along these conductive areas. Loading estimates based on April 2005 data suggest that the Maverick and Valley Creek segments are receiving relatively sulfate-rich discharges that likely represent dominant flow contributions from naturally dissolving evaporite deposits. The Machae Creek and Bull Hollow areas are receiving relatively chloride-rich load increases that may be caused by nearby produced-water sources in adjacent oil fields. All segments show apparent ground conductivities that increase with depth, implying that ground-water salinities increase downward within the exploration depth of the instrument. Baseflow contributions to the river from the regional, largely naturally saline aquifers are a major control on Colorado River salinity, but this dominance appears to be modified locally near other sources of near-surface salinity such as produced water from the Sharon Ridge Oil Field (Sharon Ridge and Canyon Creek areas), the Jameson–Strawn Oil Field (Silver area), the Snyder Oil Field (Moss Creek Lake area), and the Wendkirk Oil Field (the Machae Creek area). Impacts range from local, near-surface salinization along the river near tributaries that drain parts of the fields to deeper infiltration from past surface discharge or leaking wells and possible lateral migration and discharge at riverbank seeps or into adjacent alluvial sediments.

INTRODUCTION

This report summarizes geophysical investigations of surface-water salinity and shallow electrical ground conductivity along and above segment 1426 of the upper Colorado River near San Angelo, Texas (fig. 1). Segment 1426 extends more than 100 km from its upstream limit at the Robert Lee Dam impounding E. V. Spence Reservoir in Coke County to several kilometers downstream from the Mustang Creek confluence below Ballinger in Runnels County. Several governmental agencies have monitored and analyzed surface water quality along segment 1426, including the Lower Colorado River Authority, the Upper Colorado River Authority, the Colorado River Municipal Water District, the U.S. Geological Survey, and the Texas Commission on Environmental Quality (TCEQ) and its subcontractors (EA Engineering, Science, and Technology, 2002). Surface-water monitoring has revealed periodic and repeated high salinity values at several monitoring sites along this segment, at times exceeding the 2,000 milligrams per liter (mg/L) criterion for total dissolved solids (TDS). Other related constituents of concern include chloride and sulfate (EA Engineering, Science, and Technology, 2002).

The Bureau of Economic Geology (Bureau) conducted an airborne geophysical survey using a multi-frequency electromagnetic induction (EM) instrument to delineate the extent and intensity of salinization and identify salinity sources that degrade surface-water quality in the upper Colorado River (segment 1426) between Spence Reservoir near Robert Lee and Ivie Reservoir below Ballinger. Data were acquired in February 2005 (a) along the axis of the Colorado River between Lake Thomas and Ivie Reservoir; (b) along Beals Creek between its confluence with the Colorado River and Big Spring, and (c) along closely spaced flight lines within two small corridors centered on the Colorado River near Robert Lee (the Machae Creek block) and Silver (the Silver block). We converted processed data into images showing trends and variations in apparent conductivity laterally and with depth along and near the creek. Because salinization is a key factor controlling the electrical conductivity of the ground, we used lateral and vertical conductivity trends to interpret the extent and intensity of salinization, whether it has shallow or deep sources, and, by combining geophysical patterns with chemical surface-water patterns, we interpreted the likely salinization source type.

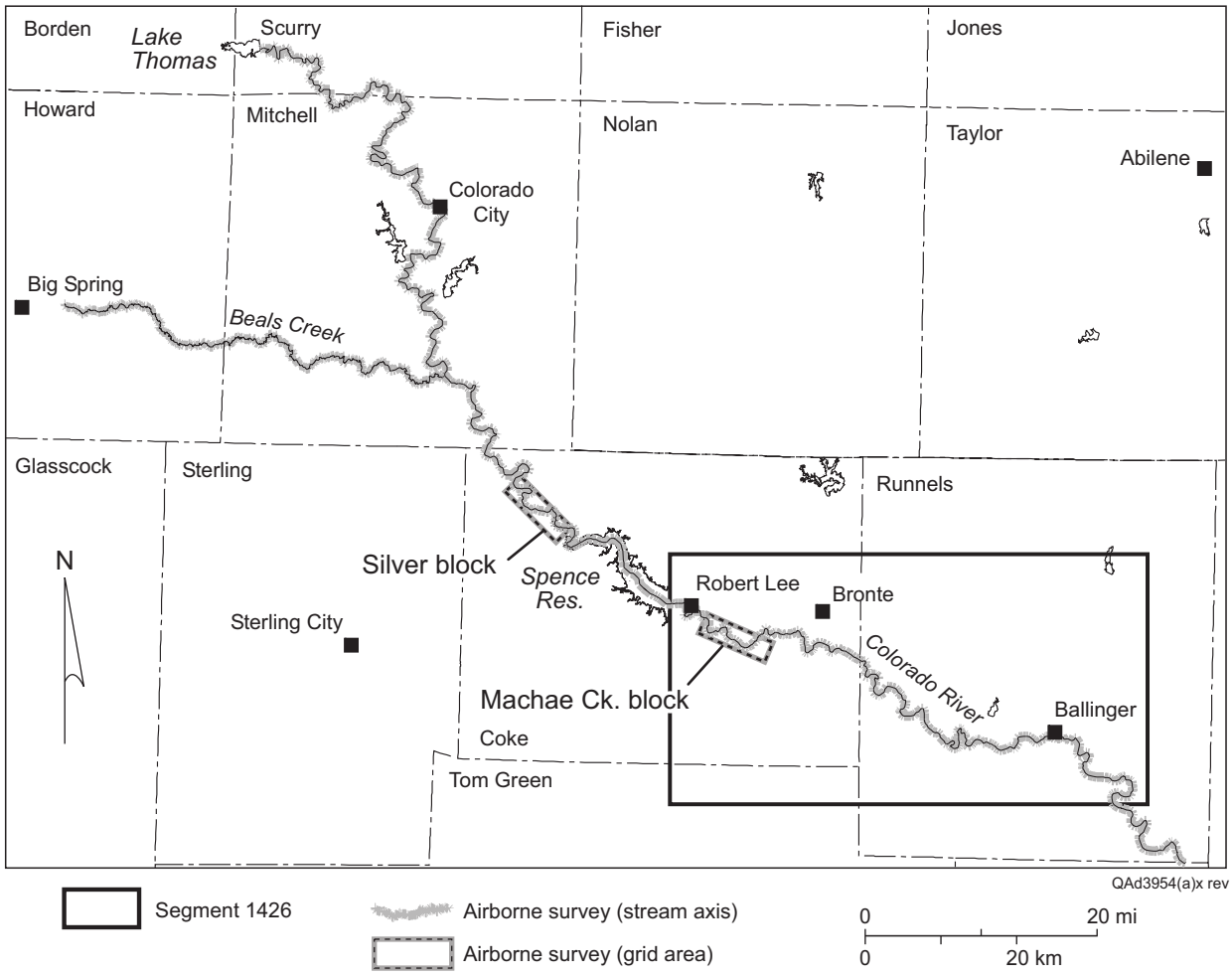

Figure 1. Map of the upper Colorado River region and the area surrounding segment 1426, west Texas. Also shown are the locations of the airborne geophysical survey along the axes of the Colorado River and Beals Creek and the Silver and Machae Creek airborne survey blocks.

Geology

The Colorado River between Lake J. B. Thomas and Ballinger lies within a broad alluvial valley that has eroded into Triassic and Permian bedrock (fig. 2). Surficial deposits of the region include thin remnants of older Pleistocene alluvial deposits that exist within the margins of the river valley. Along the Colorado River and its tributaries, thin accumulations of sand, gravel, silt, and clay have been deposited in upper Pleistocene and Holocene terrace, floodplain, and channel environments. Alluvium, vegetation, and water commonly obscure bedrock deposits although bedrock is exposed in some places within the river channel and along its banks, verifying the minor thickness of the alluvium within and adjacent to the river bed.

Geologic cross-sections along the river's path (figs. 3 and 4) illustrate that the bedrock deposits dip gently westward and that successively older deposits are incised by the river. Between Lake Thomas and Spence Reservoir, the river cuts into sandstone and mudstone of the Triassic Dockum Group and sandstone, shale, and gypsum of the Permian Quartermaster and Whitehorse Group. Downstream from Spence Reservoir toward Ballinger, the river erodes into sandstone, shale, dolomite, limestone, and gypsum of the Blaine and Clear Fork units. Downstream from Ballinger, limestone and lesser shale of the Permian Leuders, Talpa, Grape Creek, and Bead Mountain Formations are cut by the river.

The region has a long history of exploration and production of hydrocarbons and evaluation of the rocks for industrial and construction materials such as gypsum, sand, and gravel. During the early 1900's, geologists identified locations of thick gypsum beds and sand and gravel deposits, and they noted that oil occurred within some of the rocks at the surface in Coke County (Beede and Waite, 1918). Specific sites of naturally occurring oil mentioned by Beede and Bentley (1918) and later by the west Texas-San Angelo Geological Societies (1961) include south Pecan Creek, which drains into Spence Reservoir, and Mountain Creek, a tributary of the Colorado River east of Robert Lee. Hydrocarbon exploration and production boomed during the 1900s and is still active throughout the region.

Previous geologic mapping and stratigraphic studies of the area provided much of the geologic information used to evaluate the geologic framework. Reports of early geologic surveys within Coke

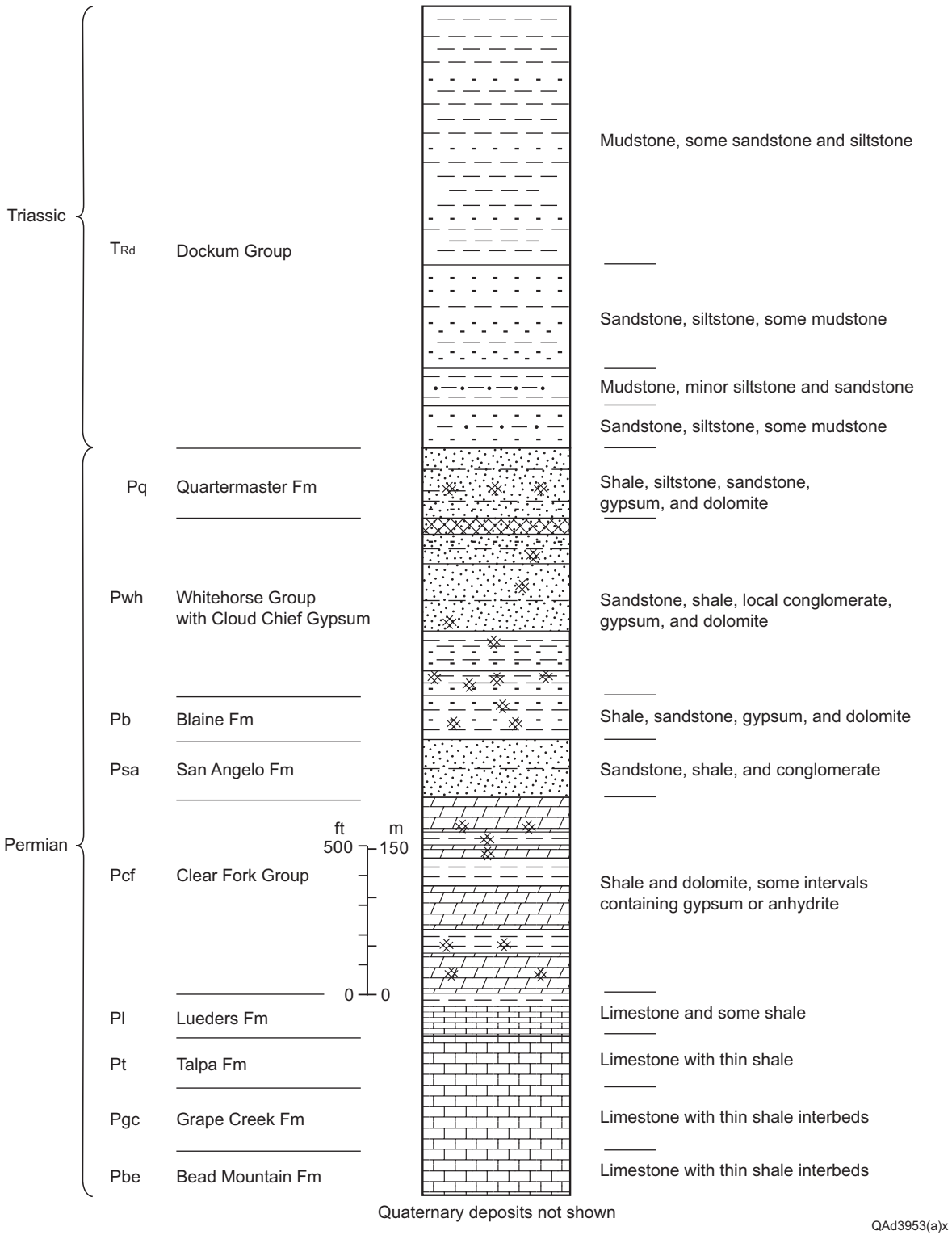

Figure 2. Generalized stratigraphic column and rock type for Permian and Triassic units cropping out along the Colorado River in the study area. Because these units dip regionally to the west, outcropping units become older in the downstream direction.

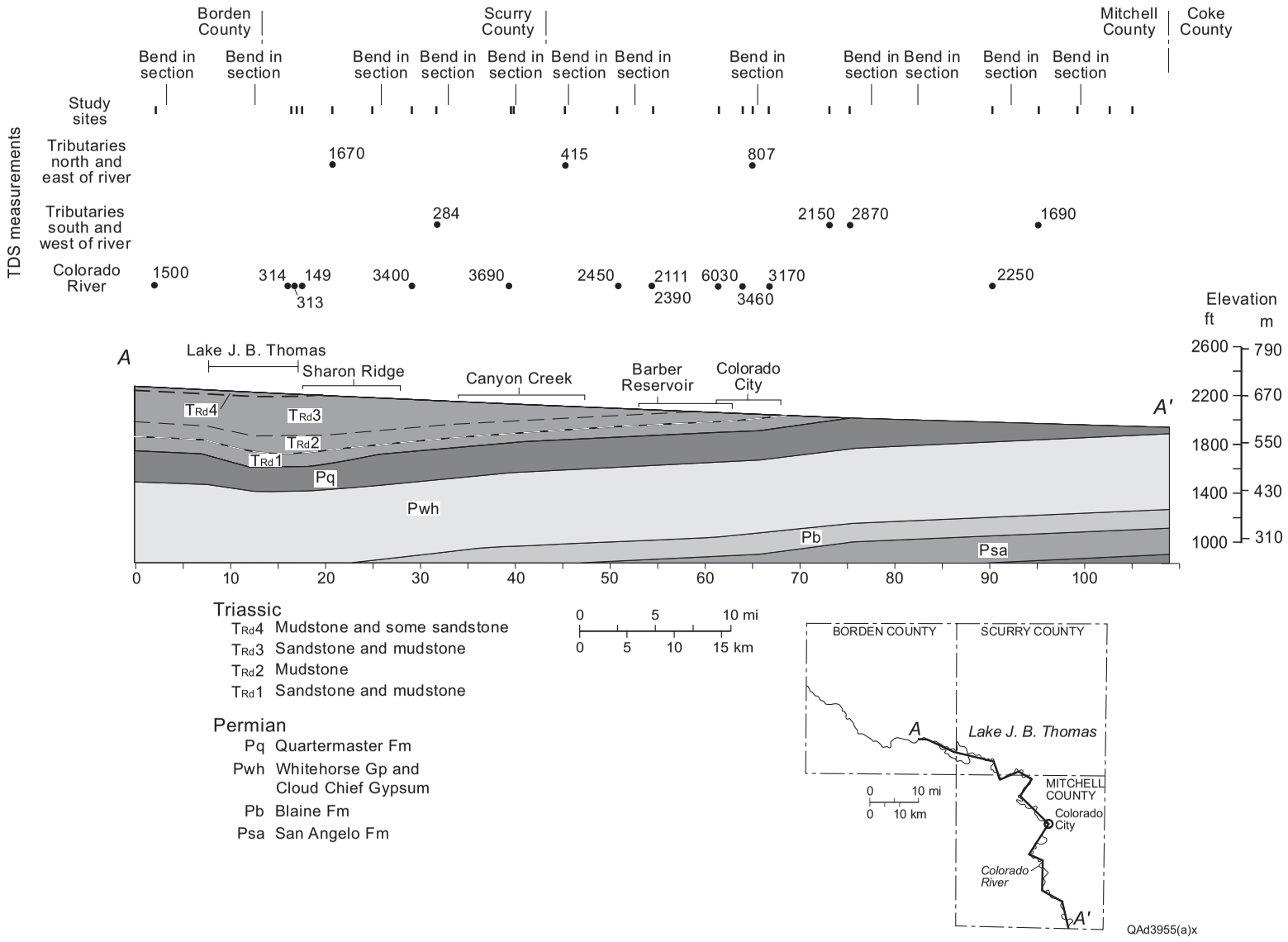

Figure 3. Geologic cross section A–A′ along the Colorado River in southeast Borden, Scurry, and Mitchell Counties. TDS measurements were collected during October 26-28, 2004 (appendix B).

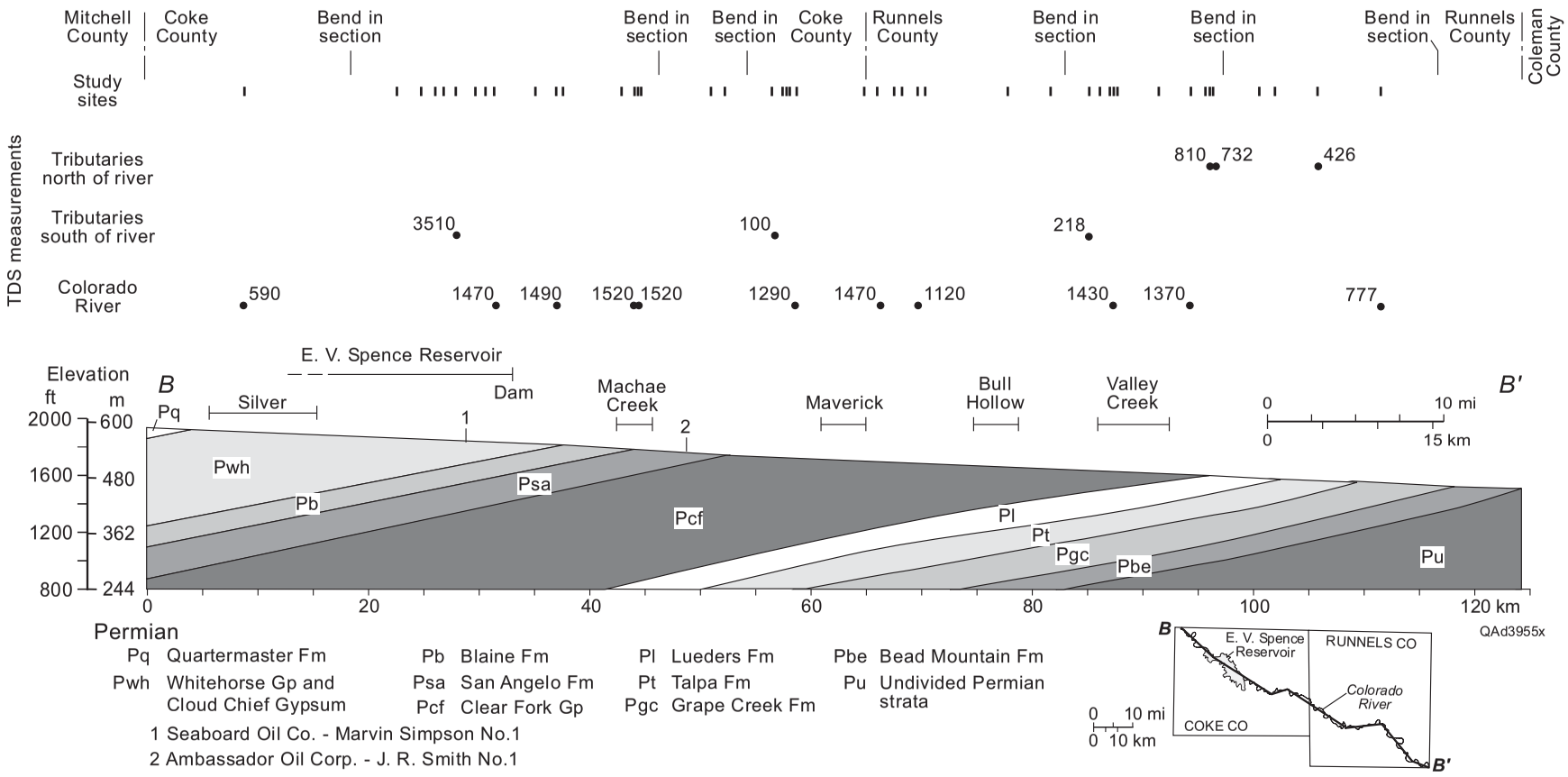

Figure 4. Geologic cross section B–B′ along the Colorado River in Coke and Runnels Counties. TDS measurements were collected during August 2-3, 2004 and October 25-26, 2004 (appendix B).

and Runnels Counties by Beede and Waite (1918) and Beede and Bentley (1918) contain descriptions of rocks near the river. Regional geologic maps constructed during the 1970's (Eifler and others, 1974; Eifler and others, 1975; Kier and others, 1976) and the results of stratigraphic studies by Mear (1963), Lehman (1994), and Lucas and others (1994) provided data on the modern stratigraphic nomenclature and general lithologies of the geologic units. Hydrogeologic works by Shamburger (1967), Mount and others (1967), Wilson (1973), and Johnson (2002) also provided a geologic framework for this investigation.

Surface-Water Quality

There have been many investigations of factors affecting relatively poor surface- and ground-water quality along this segment of the Colorado (including Mount and others, 1967; Leifeste and Lansford, 1968; Richter and others, 1990; Slade and Buszka, 1994; Paine and others, 1999). Most previous studies attribute degraded surface- and ground-water quality in the upper Colorado River area to a combination of effects, including (a) natural dissolution of evaporite deposits and subsequent migration of saline water to the surface, and (b) oilfield-related introduction of highly saline formation water into the surface and near-surface environment through surface discharge of produced water into pits or through unplugged or leaking oil and gas wells.

Recent water sampling and analysis by the Colorado River Municipal Water District (CRMWD) and others has repeatedly documented elevated concentrations of total dissolved solids (TDS), chloride, and sulfate in the Colorado River along and upstream from segment 1426. Chemical analyses of surface water flowing in the river conducted in support of the airborne survey allow the following general observations:

1. Specific conductivity (hence, TDS) values vary along the stream course. Variations do not generally reflect direction of flow, suggesting that there are local sources of more-highly saline water and that dilution lowers salinity downstream from locations that show elevated salinity.

2. Groundwater salinity varies in similar patterns to stream salinity. Areas characterized by higher and lower groundwater salinities are configured as northeast-southwest elongate bands that probably reflect Permian and Triassic stratigraphic and structural strike. Areas of locally elevated river salinity appear to lie within northeast-southwest elongate zones that are characterized by locally elevated groundwater salinity. These correspondences strongly suggest a connection between groundwater and surface water systems.

3. Stream salinities are higher during lower-flow conditions than during higher-flow conditions. This suggests that groundwater base-flow is the primary source of elevated salinity rather than contaminants entrained in precipitation runoff. Sampling during two recent visits (January and April 2005) were during relatively low-flow conditions that are typical of the river except during, and for a week or so after, storm events.

4. The Colorado River has been generally a gaining stream during recent low-flow conditions. Elevated-salinity correspondences between the groundwater and stream probably reflect contamination of the river by groundwater rather than groundwater contamination by the river.

METHODS

This study uses instruments based on the electromagnetic induction method to acquire information on the electrical conductivity of the shallow subsurface along and near the Colorado River. Most sediment, soil, and rock types are poor electrical conductors (McNeill, 1980a). The electrical conductivity of water is strongly influenced by its TDS concentration (Robinove and others, 1958); its conductivity increases almost linearly as TDS increases. When saline water infiltrates generally nonconductive strata, the bulk conductivity of the strata increases as the salinity of the pore water increases. Conductivity measurements are thus a useful proxy for salinization intensity in most strata.

We supplemented available surface-water quality data with reconnaissance measurements of the electrical conductivity of the ground and surface water in an attempt to identify critical stream segments where highly salinized ground may contribute to the degradation of surface-water quality. Where possible, we acquired ground-conductivity measurements along the axis of main and tributary streams. If the stream axis was not accessible, we measured ground conductivity along the stream bank. In places along the Colorado River, there was sufficient water depth to allow travel by canoe to isolated stream and tributary segments. Elsewhere, stream access was by foot from road or bridge crossings. A hand-held GPS receiver provided locations for all ground- and water-conductivity measurements.

Results from ground-based investigations helped design an airborne geophysical survey that included stream-axis flight lines along the Colorado River and Beals Creek and small block surveys in two areas near Spence Reservoir (fig. 1). We combined results from ground-based and airborne geophysical surveys with water-quality data to identify salinized areas and assess salinity sources.

Ground-Based EM Survey

We used the frequency-domain electromagnetic induction (EM) method to measure apparent electrical conductivity of the ground in the study area. Frequency-domain EM methods employ a changing primary magnetic field created around a transmitter coil to induce current to flow in the ground or in the annulus around a borehole, which in turn creates a secondary magnetic field that is sensed by

the receiver coil (Parasnis, 1986; Frischknecht and others, 1991; West and Macnae, 1991). The strength of the secondary field is a complex function of EM frequency and ground conductivity (McNeill, 1980b), but generally increases with ground conductivity at constant frequency.

We used a Geonics EM31 ground conductivity meter (fig. 5) to measure the apparent conductivity of the ground. This instrument operates at a primary EM frequency of 9.8 kHz, measuring apparent conductivity to a depth of about 3 m (horizontal dipole [HD] orientation) and 6 m (vertical dipole [VD] orientation) using transmitter and receiver coils that are separated by 3.7 m. The instrument has a useful conductivity range of less than 1 millisiemens/m (mS/m) to 1,000 mS/m.

We acquired ground conductivity measurements at 344 sites along the upper Colorado River and its significant tributaries between Lake Thomas and Ivie Reservoir in July, August, and October 2004 and March 2005 (appendix A). At most locations, we acquired several measurements at various intervals along the stream bank (if the stream was flowing) or along the stream axis (if the stream was dry).

The EM31 was calibrated at the beginning of each field day. Measurements of apparent ground conductivity were acquired by (1) placing the instrument on the ground (or holding it just above the surface of the water) in the VD orientation; (2) noting the apparent conductivity reading; (3) rotating the instrument into the HD orientation; (4) noting the apparent conductivity reading; and (5) obtaining a latitude and longitude coordinate for the measurement using the GPS receiver. All conductivity measurements were entered into a geographic information system database (ArcMap by ESRI) for analysis and comparison with water-quality and airborne-survey data.

Airborne EM Survey

We used an airborne implementation of the frequency-domain EM method to measure apparent electrical conductivity of the ground along the Colorado River axis from Ivie Reservoir to Lake Thomas, along the Beals Creek axis from the confluence with the Colorado River to Big Spring, and in two corridors near Spence Reservoir. Geophex provided the technical survey crew and their GEM-2A

Figure 5. Geonics EM31 ground conductivity meter.

airborne instrument (fig. 6) and Airlift Helicopters provided a flight crew and helicopter to tow the instrument.

The GEM-2A is an EM instrument that employs a single pair of transmitter and receiver induction coils in horizontal coplanar orientation that operates at multiple effective frequencies (and exploration depths) simultaneously (Won and others, 2003). We chose to use five primary frequencies: 450, 1350, 4170, 12,810, and 39,030 Hz, that yield exploration depths ranging from a few meters at the highest frequency to several tens of meters at the lowest frequency (table 1). EM calibration procedures included recording ambient noise at the chosen primary frequencies and pre- and post-flight checks of instrument phase response using a ferrite rod and amplitude response using a Q-coil. Instrument response and drift were compensated by raising the instrument above 300 m at the beginning and end of each flight to minimize the instrument's response to the ground.

Also included in the instrument (table 1) are a cesium-vapor magnetometer that measures the strength of the Earth's magnetic field and a GPS receiver that provides the location of the instrument to an accuracy of 5 m or better. The helicopter flew at a nominal height of 60 m, towing the instrument at a height of about 30 m. Barometric and radar altimeters were installed in the helicopter to provide flight-height data. Altimeter height was combined with the length and orientation of the tow cable to calculate the height of the instrument above ground. The final sampling rate for EM and magnetic field data was 10 Hz. Average flight speeds of 143 to 225 km/hr translate to an approximate on-the-ground sample spacing of 4 to 6 m.

Geophex acquired airborne EM and magnetic field data along a total distance of more than 700 km in the upper Colorado River region on February 2 and 3, 2005. This distance included a single line 351 km long along the axis of the Colorado between Lake Thomas and Ivie Reservoir (including all of segment 1426), a single line 86 km long along the axis of Beals Creek between Big Spring and the confluence with the Colorado River, and 133 km in each of two 3×10 km corridors centered on the Colorado River upstream from Spence Reservoir in the Silver area and downstream from Spence Reservoir near Robert Lee. We flew 11 main lines spaced 300 m apart and two tie lines spaced 5 km apart in each of these corridors to provide more detailed spatial coverage.

Figure 6. Geophex GEM-2A in flight above the Colorado River near Robert Lee, Texas.

Table 1. Summary of acquisition parameters for the airborne geophysical survey of the upper Colorado River area flown by Geophex, Ltd. (Geophex, 2005).

Dates	February 2–3, 2005	
Aircraft	Helicopter, Hughes 369D	
Flight height	60	m
Flight speed (average per flight)	143 to 225	km/hr
Flight lengths (total)	703	km
Colorado River, Lake Thomas to Spence Res.	207	km
Colorado River, Spence Res. to Ivie Res.	144	km
Beals Creek, Big Spring to Colorado River	86	km
Machae Creek block (3 x 10 km, 300 m line spacing)	133	km
Silver block (3 x 10 km, 300 m line spacing)	133	km
EM instrument	GEM-2A	
Bird height	30	m
Frequencies (5)	450, 1350, 4170, 12,810, 39,030	Hz
Sample rate and spacing	10	Hz
Sample spacing (average)	4 to 6.3	m
Magnetometer (airborne)	Cesium vapor, Geometrics G823A	
Height	30	m
Sample rate	10	Hz
Sample spacing (average)	4 to 6.3	m
Sensitivity	0.01	nT
Magnetometer (ground)	Cesium vapor, Geometrics G858	
Sensitivity	0.1	nT
Sample rate	1	Hz
Navigation	Differential GPS, receiver mounted on bird	

Geophex provided preliminary, unprocessed geophysical data after each stream-axis flight that allowed us to choose detailed survey corridor locations. Geophex processed the airborne survey data to calculate apparent conductivities and depths along the flight lines for each frequency using a pseudo-layer half-space model algorithm (Sengpiel, 1988; Geophex, 2005). We produced apparent conductivity images at each frequency along stream axes by classifying values according to their mean and standard deviation for the stream segment. We also generated stream-axis pseudo cross sections in selected areas using the data processing software ERMapper, considering distance along the stream as one variable and apparent conductivity at each frequency as the other variable. These sections are useful for depicting the lateral extent of salinization and the relative depths of likely salinity sources.

For the Machae Creek and Silver blocks, we gridded apparent conductivity data for each frequency using ERMapper to produce apparent conductivity maps for each survey area. These data were gridded using a 25 m cell size and triangulation interpolation between grid points. Five apparent conductivity measurements at each of the 33,389 measurement locations in the Machae Creek block and 32,868 locations in the Silver block were used to create the grid images, which were then imported into a GIS data base for analysis.

Water Conductivity, TDS, and Hydrochemical Analyses

We measured the electrical conductivity of water samples at 45 locations along the upper Colorado River, along Beals Creek and other significant tributaries, and at lakes (appendix B) using a Corning Checkmate 90 conductivity and TDS probe. Measurements were taken in August and October 2004. This instrument measures the temperature and electrical conductivity of the water sample and calculates the resulting TDS concentration. All temperature, conductivity, and TDS measurements were entered into a GIS data base for comparison with ground-conductivity data.

Additional TDS measurements and surface-water sampling were completed during and after the airborne geophysical survey. For these activities, field locations were determined using a hand-held Garmin GPS receiver. Field measurements of stream water for specific electrical conductivity (SC), pH,

and temperature were performed with a Hydrolab Quanta multiparameter probe system. Calibrations for SC and pH were performed with certified calibration solutions. Measurements with the Quanta were occasionally compared to measurements of the same samples performed with Oakton Con (SC) and Orion 250A+ (pH) laboratory instruments.

Eighteen stream samples and one produced-water sample (appendix C) were collected for laboratory analyses following protocols provided by the Kansas Geological Survey (KGS) where the analyses were performed (Donald Whittemore, pers. comm., 2005). The produced-water sample was collected in October 2005 from a storage tank containing commingled brine produced from Cisco reservoir wells in the Wendkirk Oil Field. Two splits were acquired for each sample. For major anion analyses, 500 ml of water was passed through a 0.45 mL Whatman syringe filter and collected in a 500-ml nalgene bottle that had been rinsed with filtered sample. For major cation analyses, 200 ml of water were passed through a 0.45 mL filter and 2 ml of 6N HCl were added to maintain metals in solution. In each split headspace was minimized. Samples were kept on ice and shipped for overnight delivery to the KGS laboratory in Lawrence, Kansas.

RECONNAISSANCE SURFACE-WATER MEASUREMENTS

We supplemented existing data on surface-water quality in the upper Colorado River area with (a) reconnaissance measurements of water conductivity and TDS concentration and (b) measurements of apparent ground conductivity. These complementary data sets reveal a snapshot of salinity in the Colorado River and its tributaries and impoundments and likely salinity source areas in alluvial deposits adjacent to the river and were used to establish upstream and downstream boundaries for the airborne geophysical survey.

TDS concentration in surface-water samples from the Colorado River and its lakes and tributaries is highly variable (fig. 7; appendix B). Concentrations measured during this study range from fresh (100 mg/L) to very saline (more than 10,000 mg/L), averaging about 1900 mg/L for all samples.

Colorado River above Spence Reservoir

October 2004 samples show that Colorado River salinity is more variable from one location to another between Lake Thomas and Spence Reservoir than it is along segment 1426 (fig. 7). At the most upstream location measured, the Colorado River had a TDS concentration of 1500 mg/L at the FM 1205 bridge above Lake Thomas (location C246, fig. 7; appendix B). Lake Thomas water was fresh (about 315 mg/L, locations C248 and C249); farther downstream, Spence Reservoir water was slightly saline (1330 mg/L, location C279). Between these reservoirs, Colorado River salinity ranged from 1540 (location C280 at RR 2059 above Spence Reservoir) to 6030 mg/L (location C302 at the I-20 bridge near Colorado City). Notable salinity increases occurred over relatively short distances along the river. Colorado River salinity increased from the Cedar Bend bridge (2390 mg/L at C305) to the highest measured river values at the I-20 bridge only 12 km downstream (6030 mg/L at C302).

The highest October 2004 salinities were measured along Beals Creek, a significant Colorado River tributary (fig. 7; appendix B). Near the upper end of the creek at the FM 700 bridge in Big Spring, salinity exceeded the upper limit of the instrument at more than 10,000 mg/L (location C305). There was a general downstream decrease in salinity along Beals Creek: 8160 mg/L at Midway Road

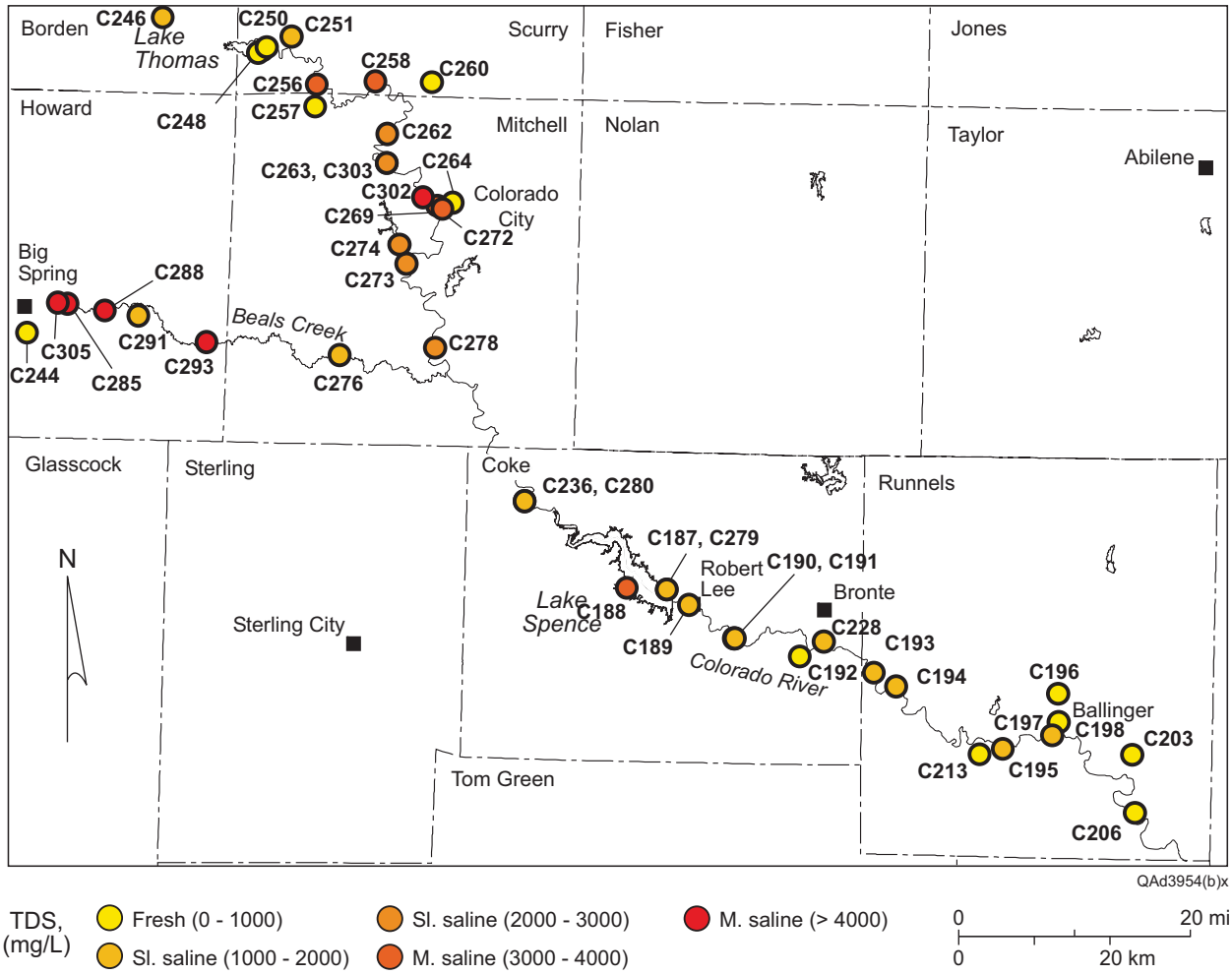

Figure 7. Map of the upper Colorado River region, West Texas (including TMDL segment 1426 below Spence Reservoir), depicting TDS concentrations measured in the Colorado River and its tributaries in August and October 2004. Symbol labels indicate measurement locations listed in appendix B. Salinity classification from Robinove and others (1958).

(C285), 4550 mg/L at Moss Lake Road (C288), 5040 mg/L at FM 821 (C291), and 1690 mg/L at Texas 163 (C276). Salinities in other Colorado tributaries (in downstream order) include 1670 mg/L at FM 2085 on Bull Creek (C251), 284 mg/L on ponded Willow Creek at FM 1229 (C257), 415 mg/L on Deep Creek at Scurry County Road 4138 (C260), 807 mg/L on Lone Wolf Creek at Colorado City (C264), and 2870 mg/L on ponded Morgan Creek at Texas 163 (C273).

Colorado River at and below Spence Reservoir

Surface-water salinity measured in August 2004 revealed highly variable water quality across the area. Spence Reservoir had a slightly saline TDS concentration of 1470 mg/L at the Lakeview Recreation Area on the north shore of the lake (fig. 8; location C187, appendix B). Colorado River water flowing into Spence Reservoir was considerably less saline at a TDS value of 590 mg/L (area B, fig. 8; location C236, appendix B) despite flowing through alluvial deposits with efflorescence (evaporite mineral crusts) and a dense growth of salt cedar. Runoff from recent rainfall may have temporarily lowered the TDS concentration of the Colorado River in this area.

At Salt Creek on the southern shore of Spence Reservoir, we measured a higher, moderately saline TDS concentration of 3510 mg/L in ponded water. The stream name, its salinity, and the presence of gypsum rock fragments in the stream bed all suggest that Salt Creek contributes to the elevated salinity of Spence Reservoir.

We tested flowing Colorado River water at nine locations downstream from Spence Reservoir (fig. 8; appendix B). Upstream from Ballinger (above the confluence with Elm Creek), measured TDS concentrations were similar to those measured in Spence Reservoir, ranging from 1120 mg/L at the FM 3115 bridge (fig. 8; location C194, appendix B) to 1520 mg/L near a gravel quarry where efflorescence was noted on alluvial deposits adjacent to the river (area C, fig. 8; location C191, appendix B). At Ballinger, Elm Creek contributed a significant amount of fresh water (732 to 810 mg/L TDS, fig. 8; locations C196 and C197, appendix B) to the Colorado River. Downstream from Ballinger at the

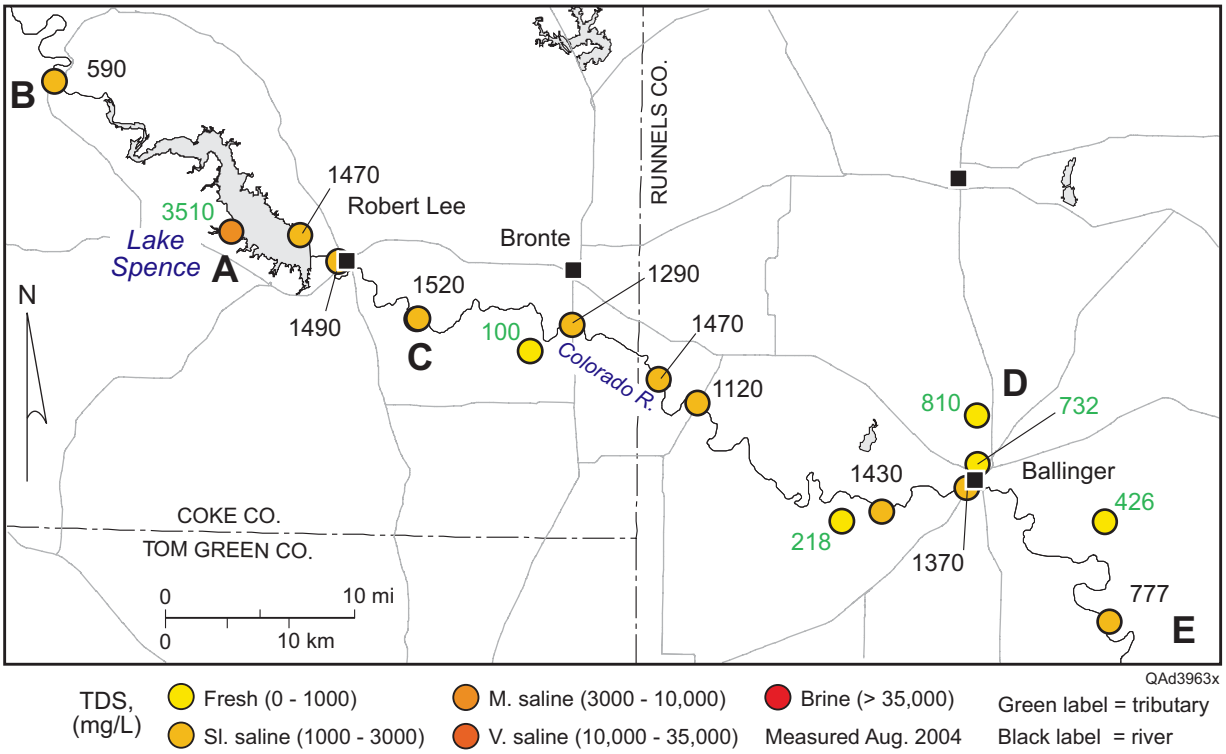

Figure 8. Map of the upper Colorado River segment 1426 study area depicting TDS concentration measured in August 2004 (appendix B).

Runnels County Road 129 bridge, Colorado River water was fresh at 777 mg/L (area E, fig. 8; location C206, appendix B).

Measurements of TDS concentration taken in ponded water along minor, non-flowing Colorado River tributaries were relatively fresh, ranging from 100 mg/L on Live Oak Creek south of Bronte (fig. 8; location C228, appendix B) to 426 mg/L on Mustang Creek near Ballinger (fig. 8; location 203, appendix B). Neither Elm Creek nor these tributaries appear to contribute significant amounts of highly saline water to the Colorado River despite draining areas where significant hydrocarbon exploration and production has occurred.

GROUND CONDUCTIVITY MEASUREMENTS

We acquired ground conductivity measurements at 344 representative sites along the upper Colorado River and its tributaries between Lake Thomas and Ivie Reservoir to better understand the extent and intensity of ground salinization and its possible contribution to elevated salinity concentrations in segment 1426 of the Colorado River (fig. 9; table 2; appendix A).

In general, measured apparent ground conductivity is relatively low in this area. In the horizontal dipole (HD) instrument orientation, which measures apparent conductivity in the upper 3 m of the subsurface, measured values ranged from 7 to 528 millisiemens per meter (mS/m) and averaged 106 mS/m (table 2). A similar average (108 mS/m) was obtained in the vertical dipole (VD) orientation, where the instrument explores to a depth of about 6 m.

We classified HD and VD apparent conductivities into five categories. VD values between 8 and 70 mS/m were considered low, 71 to 111 mS/m were low to moderate, 112 to 176 mS/m were moderate, 177 to 286 mS/m were moderate to high, and values of 287 mS/m and above were high (fig. 9). HD and VD values are highly correlated such that sites with high VD values also had high HD values (appendix A). Despite the limited access to the river and its tributaries, we recorded elevated conductivities at several sites that are consistent with near-surface salinization that may contributed to degraded Colorado River water quality.

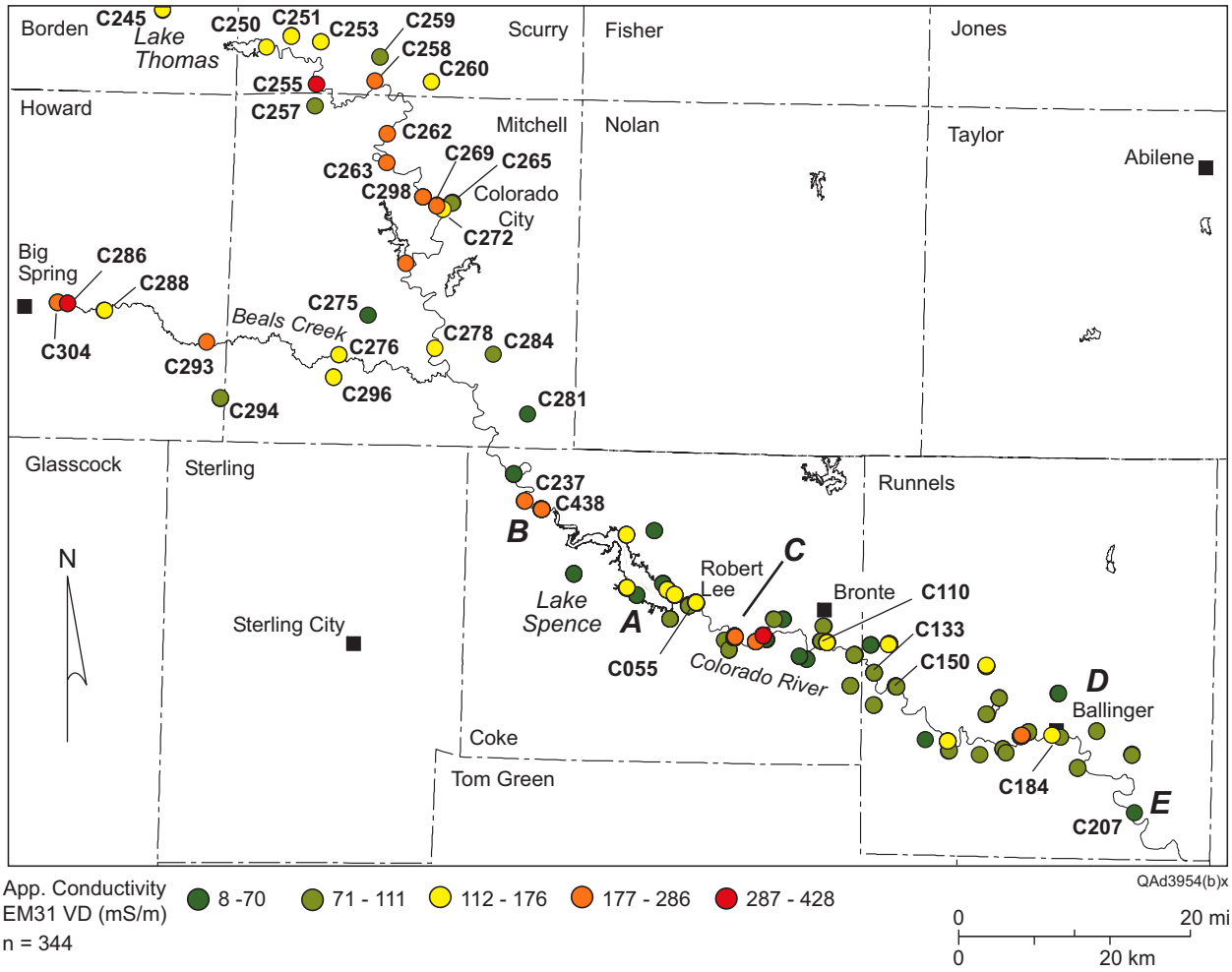

Figure 9. Upper Colorado River area apparent conductivity measured using an EM31 ground-conductivity meter in the vertical dipole (VD) mode. Symbol labels indicate measurement locations listed in appendix A.

Table 2. Statistical parameters for apparent ground conductivity measurements acquired in July, August, and October 2004 and March 2005 in the upper Colorado River area (appendix A) using a Geonics EM31 instrument (fig. 5). Horizontal-dipole (HD) measurements represent the upper 3 m of the subsurface; vertical-dipole (VD) measurements represent the upper 6 m.

All measurements, Lake Thomas to Ivie Reservoir

Instrument Orientation	Number	Average (mS/m)	Minimum (mS/m)	Maximum (mS/m)	Std. Dev. (mS/m)
HD	344	106	7	528	80
VD	344	108	8	428	60

Lake Thomas to Spence Reservoir, Borden, Scurry, Howard, Mitchell, and Coke counties

Instrument Orientation	Number	Average (mS/m)	Minimum (mS/m)	Maximum (mS/m)	Std. Dev. (mS/m)
HD	111	124	7	474	89
VD	111	121	8	428	77

Below Spence Reservoir, Coke and Runnels counties

Instrument Orientation	Number	Average (mS/m)	Minimum (mS/m)	Maximum (mS/m)	Std. Dev. (mS/m)
HD	233	97	20	528	74
VD	233	102	25	336	49

Colorado River, Lake Thomas to Spence Reservoir

Ground-conductivity measurements along the Colorado River itself are consistently higher between Lake Thomas and Spence Reservoir than they are between Spence Reservoir and the most downstream point below Ballinger (fig. 9; table 3; appendix A). Measurements along the Colorado River between Lake Thomas and Spence Reservoir range from 121 to 425 mS/m in the deeper (VD) mode and 137 to 376 mS/m in the shallower (HD) mode. Highest values upstream from Spence Reservoir were measured at the Texas 350 bridge in Scurry County (425 mS/m at location C255), near the I-20 and State Spur 377 bridges at Colorado City (as high as 376 mS/m at C298 to C301 and C269 to C271), and at the RR 2059 bridge upstream from Spence Reservoir (298 mS/m at C237 to C238). We measured slightly lower conductivity values upstream from Lake Thomas (47 to 154 mS/m at C245 and C246), just below Lake Thomas at the FM 1298 bridge (121 to 153 mS/m at C250), and below Colorado City at the Texas 163 and Mitchell County Road 337 bridges (123 to 139 mS/m at C272 and C278).

Colorado River Tributaries, Lake Thomas to Spence Reservoir

We measured ground conductivity at 30 locations along 13 tributaries to the Colorado River between Lake Thomas and Spence Reservoir (fig. 9; table 4; appendix A). Ground conductivities along these tributaries range from 61 to 474 mS/m, generally higher than conductivities measured along most Colorado tributaries below Spence Reservoir.

The highest conductivities were measured at several locations along Beals Creek, which also contributed the highest surface-water salinity concentrations. Beals Creek ground conductivities near Big Spring ranged from 214 to 397 mS/m at FM 700 (locations C304 and C305) and 389 to 474 mS/m at Midway Road (C286 and C287). Farther downstream, conductivities remained elevated at Moss Lake Road (135 to 215 mS/m at C288 to C290) and FM 821 (206 to 280 mS/m at C293). We measured the lowest conductivities along Beals Creek at the most downstream location (123 to 139 mS/m at C276 to C277).

Table 3. Apparent ground conductivity ranges in the HD and VD instrument orientations along the Colorado River, listed in downstream order. Individual locations and measurements are listed in appendix A and shown on fig. 9.

Colorado River Segment	Locations	VD mS/m	HD mS/m
Near FM 1205 bridge upstream from L. Thomas	C245 to C246	56-146	47-154
Near FM 1298 bridge downstream from L. Thomas	C250	121	153
Near Texas 350 bridge	C255	425	275
Near FM 2835 bridge	C258	246	203
Near FM 1808 bridge	C262	220	260
Near Mitchell Co. Road 167	C263	207	155
Near I-20 bridge at Colorado City	C298 to C301	204-265	238-376
Near State Spur 377 bridge, Colorado City	C269 to C271	154-286	158-186
Near Texas 163 bridge, Colorado City	C272	124	137
Near Mitchell Co. Road 337	C278	123	139
Near RR 2059 bridge upstream from L. Spence	C237 to C238	170-180	200-298
Robert Lee	C055 to C064	64-108	48-119
Gravel quarry at Machae Creek	C077 to C089	126-267	95-528
Near U.S. 277 bridge (upstream)	C123 to C128	85-96	76-90
Near U.S. 277 bridge (downstream)	C110 to C111	88-90	78-110
Near Kickapoo Creek confluence	C117 to C121	69-128	115-131
Runnels County road crossing	C132 to C137	56-102	40-98
Near FM 3115 bridge	C150 to C159	62-86	65-88
Near FM 2111 bridge (downstream side)	C173 to C176	78-88	74-114
U.S. 67 and U.S. 83 bridges, Ballinger	C184 to C186	90-163	62-105
Runnels County Road 129 bridge	C207	56	46

Table 4. Apparent ground conductivity ranges in the HD and VD instrument orientations along Colorado River tributaries on the north (N) and south (S) side of the river, listed in downstream order. Individual locations and measurements are listed in appendix A and shown on fig. 9.

Tributary Segment	Locations	VD mS/m	HD mS/m
Bull Creek at FM 2085 (N)	C251 to C252	109-142	122-158
Bluff Creek at FM 1606 (N)	C253 to C254	109-114	98-101
Willow Creek (S)	C257	103	97
Canyon Creek (N)	C259	78	92
Deep Creek (N)	C260 to C261	136-138	107-125
Lone Wolf Creek (N)	C265 to C268	61-110	45-110
Morgan Creek (S)	C273	205	215
Wildhorse Creek (S)	C275	61	60
Beals Creek at FM 700	C304 to C305	214-225	367-397
Beals Creek at Midway Road	C286 to C287	389-428	407-474
Beals Creek at Moss Lake Road	C288 to C290	135-174	138-215
Beals Creek at FM 821	C293	280	206
Bull Creek at FM 2183 (S; Beals Creek tributary)	C294 to C295	74-87	57-62
Hackberry Creek (S; Beals Creek tributary)	C296 to C297	134-150	93-132
Beals Creek at Texas 163	C276 to C277	128-137	123-139
Red Bank Creek (N)	C284	100	81
Walnut Creek (N)	C281	70	47
Pecan Creek (S, Lake Spence)	C042 to C045	46-54	40-46
Rough Creek (N, Lake Spence)	C239 to C243	71-135	64-107
Yellow Wolf Creek (N, Lake Spence)	C053 to C054	47-58	30-39
Salt Creek (S, Lake Spence)	C028 to C041	71-109	67-192
Paint Creek (S, Lake Spence	C046 to C048	46-53	32-39
Wildcat Creek (S, Lake Spence)	C020 to C027	59-85	45-61
Messbox Creek (N)	C013 to C018	65-121	75-100
Mountain Creek (N, Robert Lee)	C065 to C075	66-120	49-120
Jack Miles Creek (S)	C229 to C230	94-99	66-74
Machae Creek (N)	C091 to C101	73-205	62-224
Buffalo Creek (S)	C231 to C235	42-80	34-51
Turkey Creek (N)	C102 to C103	72-85	47-62
Double Barrel Creek (N)	C104 to C105	55-60	31-40
Live Oak Creek (S)	C225 to C227	25-30	20-24
Live Oak Creek tributary (S)	C223 to C224	34	26-30
Kickapoo Creek at U.S. 277 (N)	C106 to C109	73-83	54-63
Kickapoo Creek at Colorado River (N)	C112 to C116	99-137	78-211
Hog Creek (N)	C129 to C131	53-60	41-48
Oak Creek (N)	C138 to C149	101-126	89-124
Juniper Creek (S)	C220 to C222	63-88	65-95
Mule Creek (S)	C218 to C219	75-85	60-65
Antelope Creek (S)	C216 to C217	55-71	56-58

Red Bank Creek (S)	C214 to C215	98-111	103-129
Indian Creek (S)	C213	101	84
Quarry Creek (N)	C169 to C171	92-109	65-88
Valley Creek, upstream (N)	C160 to C164	99-125	75-116
Valley Creek, downstream (N)	C165 to C168	87-89	57-72
Rocky Creek (S)	C211 to C212	72-78	54-56
Los Arroyos (N)	C177 to C180	97-105	101-147
Elm Creek (N)	C181 to C183	55 to 64	41 to 50
Bears Foot Creek (N)	C199 to C200	85-93	78-97
Spur Creek (S)	C209 to C210	89-102	81-111
Mustang Creek (N)	C201 to C205	75-86	49-69

Morgan Creek below Lake Colorado City was the only other tributary where we measured conductivities exceeding 200 mS/m (location C273). Other tributaries having moderate ground conductivities above 100 mS/m include, in downstream order, Bull Creek at FM 2085 near Lake Thomas (109 to 158 mS/m at C251 to C252), Bluff Creek at FM 1606 (98 to 114 mS/m at C253 to C254), Willow Creek at FM 1229 (97 to 103 mS/m at C257), Deep Creek at Scurry County Road 4138 (107 to 138 mS/m at C260 to C261), Lone Wolf Creek at Colorado City (45 to 110 mS/m at C265 to C268), and Hackberry Creek (a Beals Creek tributary) at FM 2183 (93 to 150 mS/m at C296 to C297). High ground conductivities in places along Beals Creek and these tributaries indicate varying degrees of near-surface salinization that can degrade surface-water quality.

We measured relatively low ground conductivities at the remaining tributaries, including (in downstream order) Canyon Creek at FM 1606 (78 to 92 mS/m at C259), Wildhorse Creek at Mitchell County Road 337 (60 to 61 mS/m at C275), Bull Creek (a Beals Creek tributary) at FM 2183 (57 to 87 mS/m at C294 to C295), Red Bank Creek at Mitchell County Road 337 (81 to 100 mS/m at C284), and Walnut Creek at Texas 208 (47 to 70 mS/m at C281). It is unlikely that these tributaries contribute significant saline water to the Colorado River from sources upstream from the measurement points.

Spence Reservoir Area

Spence Reservoir is not part of TMDL segment 1426, but its relatively poor water quality is a strong control on water quality in the Colorado River downstream from the lake. We measured apparent ground conductivity along several tributaries adjacent to the lake, including the Colorado River (fig. 9).

Moderate to high apparent conductivities were recorded along Salt Creek at the Paint Creek Recreation Area (area A, fig. 9; locations C028 ot C039, appendix A). An apparent conductivity profile along the stream (figs. 10 and 11) depicts elevated conductivities ranging from 122 to 192 mS/m in the shallower HD orientation and 71 to 116 mS/m in the deeper VD mode, suggesting surface salinization

Figure 10. Photograph looking upstream along Salt Creek at Lake Spence.

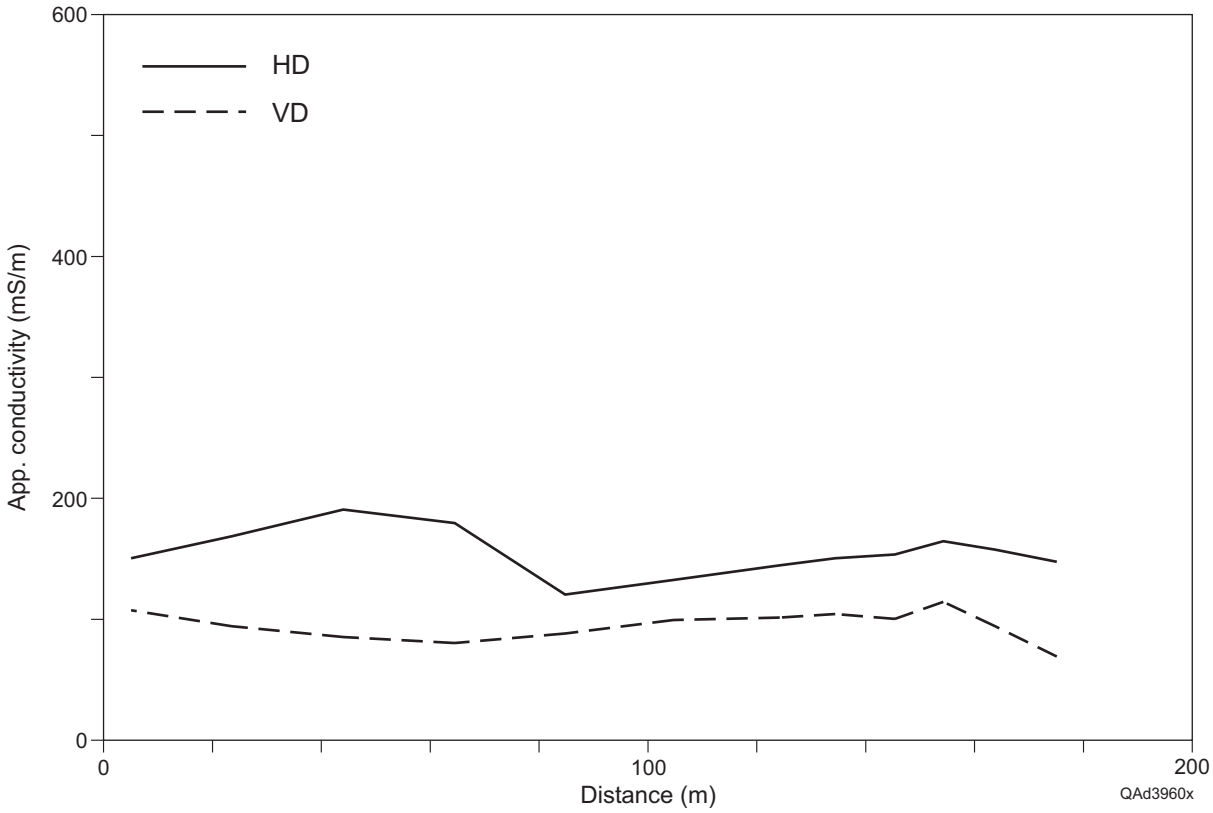

Figure 11. Apparent ground conductivity profile downstream along Salt Creek at Spence Reservoir.

associated with evaporative concentration or the presence of contributing salinity sources farther upstream. Surface water at this location was moderately saline in August 2004 (fig. 8).

The highest ground conductivities measured in the Spence Reservoir area were located along the Colorado River upstream from Spence Reservoir at the RR 2059 bridge (area B, fig. 9; locations C237 and C238, appendix A). These elevated conductivities coincided with efflorescence and dense growth of salt cedar on streambank alluvial deposits, but surface-water measurements at this site indicated fresh water flowing in the river. This area has undergone extensive historic hydrocarbon exploration and production that is a possible source for the observed ground salinization, as are other possible sources farther upstream.

Relatively low apparent conductivity was measured along most other tributaries surrounding Spence Reservoir (fig. 9), including Wildcat Creek (45 to 85 mS/m at locations C020 to C027, appendix A), Pecan Creek (40 to 54 mS/m at locations C042 to C045), Paint Creek (32 to 53 mS/m at locations C046 to C048), and Yellow Wolf Creek (30 to 58 mS/m at locations C053 to C054). Moderate conductivities (64 to 235 mS/m at locations C239 to C243) were measured along Rough Creek where it crosses an oil field on the north side of Spence Reservoir.

Colorado River Downstream from Spence Reservoir

With a few exceptions, apparent ground conductivity measured in the HD and VD orientations along 10 segments of the Colorado River downstream from Spence Reservoir are in the low to moderate categories (fig. 9; table 3) and are generally less than 100 mS/m. The first Colorado River segment below Spence Reservoir where anomalously high apparent conductivity was recorded was at a gravel quarry near the confluence with Machae Creek (area C, fig. 9). In addition to surface evidence of salinization that included efflorescence visible on alluvial deposits adjacent to the river (fig. 12), we measured apparent conductivities that increased from near-background levels of about 100 mS/m upstream from the apparent saline seep area to values as high as 528 mS/m in the shallower HD orientation and 267 mS/m in the deeper VD orientation (fig. 13). We also measured the highest Colorado

Figure 12. Photograph of efflorescence on the bank of the Colorado River in a salinized area near Machae Creek.

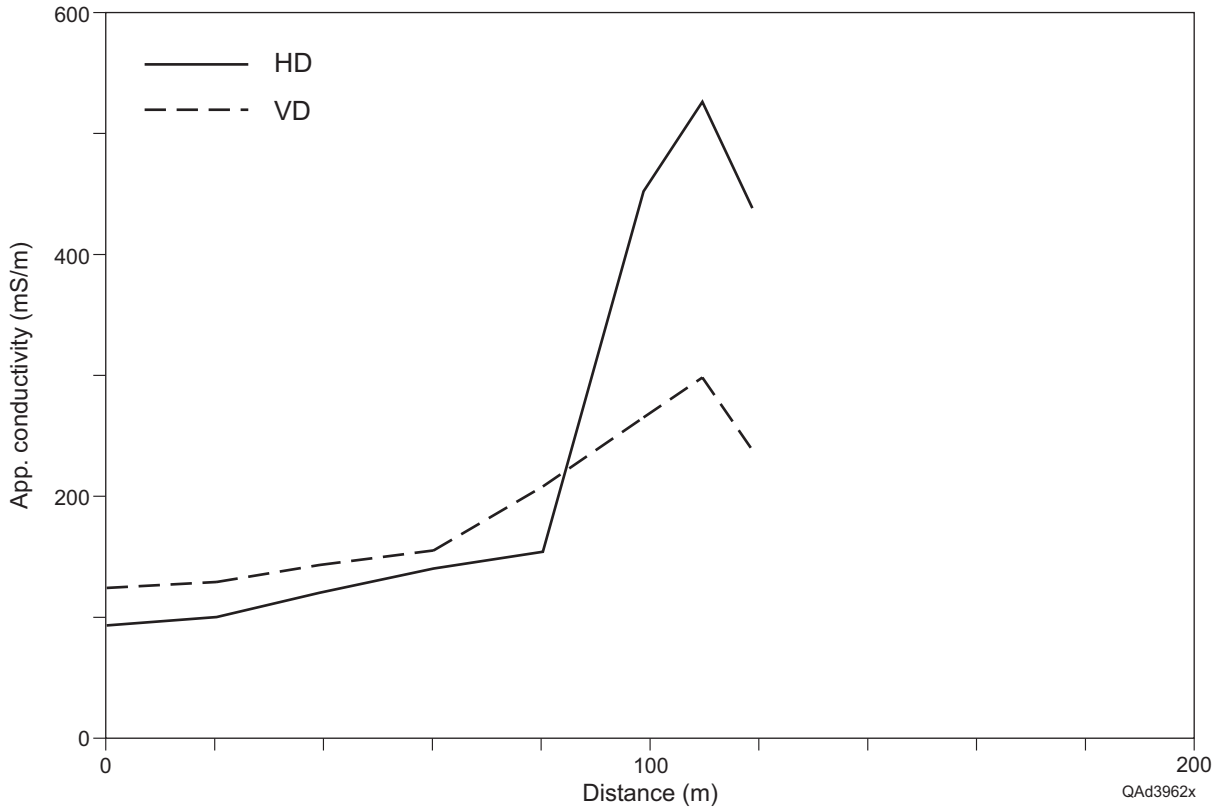

Figure 13. Apparent ground conductivity profile downstream along the Colorado River near Machae Creek.

River water salinity below Spence Reservoir at this site (1520 mg/L at locations C190 and C191, appendix B). Possible sources of salinity in this area include natural discharge of saline ground water and nearby oilfield-related discharge.

Apparent conductivities in the low to moderate range were measured along the Colorado River at the U.S. 277 bridge south of Bronte (fig. 9; table 3). Slightly higher apparent conductivities, reaching 128 to 131 mS/m, were measured a short distance downstream near the Kickapoo Creek confluence.

Farther downstream, measured apparent conductivity remained mostly in the low to moderate ranges at county road and highway crossings where the river is accessible, such as FM 3115 and FM 2111 bridges between Bronte and Ballinger (fig. 9; table 3). A single moderately high conductivity was measured along the river beneath the U.S. 67 bridge at Ballinger (163 mS/m at location C186, appendix A) that may be affected by cultural noise and not imply a local increase in ground conductivity or salinity.

Apparent conductivities measured along the Colorado River at the Runnels County Road 129 bridge, the most downstream location visited, are 46 to 56 mS/m (area E, fig. 9; table 3), virtually the lowest values measured along the river. These values are consistent with low-TDS concentration measured in water samples at this site (location C206, appendix B), reflecting the significant addition of fresh water to the Colorado River at the Elm Creek confluence in Ballinger.

Colorado River Tributaries Below Spence Reservoir

We measured apparent conductivity at one or more locations along 27 tributaries on the north and south sides of the Colorado River below Spence Reservoir (fig. 9; table 4; appendix A) in an attempt to identify salinized tributaries that might contribute high-TDS water to the Colorado River. Most of the tributaries were not flowing during our survey, but we expect that apparent ground conductivity measured in dry stream beds will remain elevated if the stream carries saline water when it does flow. Low apparent ground conductivity is expected along relatively fresh creeks; high apparent conductivity should be measured along relatively saline creeks.

In downstream order on the north side of the Colorado, we acquired data along Messbox and Mountain creeks near Robert Lee, Machae, Turkey, and Double Barrel creeks between Robert Lee and Bronte, Kickapoo, Hog, Oak, Quarry, and Valley creeks and Los Arroyos between Bronte and Ballinger, and Elm, Bears Foot, and Mustang creeks below Ballinger (table 4; fig. 9). On the south side of the Colorado, we acquired data along Jack Miles, Buffalo, and Live Oak creeks between Robert Lee and Bronte, Juniper, Antelope, Red Bank, Indian, and Rocky Creek between Bronte and Ballinger, and Spur Creek downstream from Ballinger.

Out of the 16 creek segments on the north side of the Colorado, we recorded apparent ground conductivities above 100 mS/m along only seven (Messbox, Mountain, Machae, Kickapoo, Oak, and Valley creeks and Los Arroyos). The highest values were measured at Machae Creek (as great as 224 mS/m near area C, fig. 9; table 4) at locations near its confluence with the Colorado River where high TDS values were measured in water samples, efflorescence was observed on the ground adjacent to the river, and elevated ground conductivities were measured. This is an area where oil-field activities continue and represent a possible salinity source.

The only other northern tributary where anomalously high apparent conductivities were measured was the downstream end of Kickapoo Creek near Bronte (fig. 9), where highest measured values reached 211 mS/m. These values are somewhat higher than those measured along the Colorado River in this area, suggesting possible minor salinization along Kickapoo Creek downstream from Bronte.

A short segment along the dry stream bed of Mountain Creek near Robert Lee also exceeded 100 mS/m (fig. 14). Relatively low peaks such as these that extend only a short distance along a stream bed are unlikely to represent major salinity sources.

Apparent ground conductivity exceeded 100 mS/m at only two creeks on the south side of the Colorado. Peak values reached 129 mS/m on Red Bank Creek and 111 mS/m on Spur Creek (fig. 9; table 4). Conductivities measured at all remaining measured creek segments on the north and south sides of the Colorado were below 100 mS/m, suggesting that major salinity sources are unlikely to exist upstream from the measurement points on these tributaries.

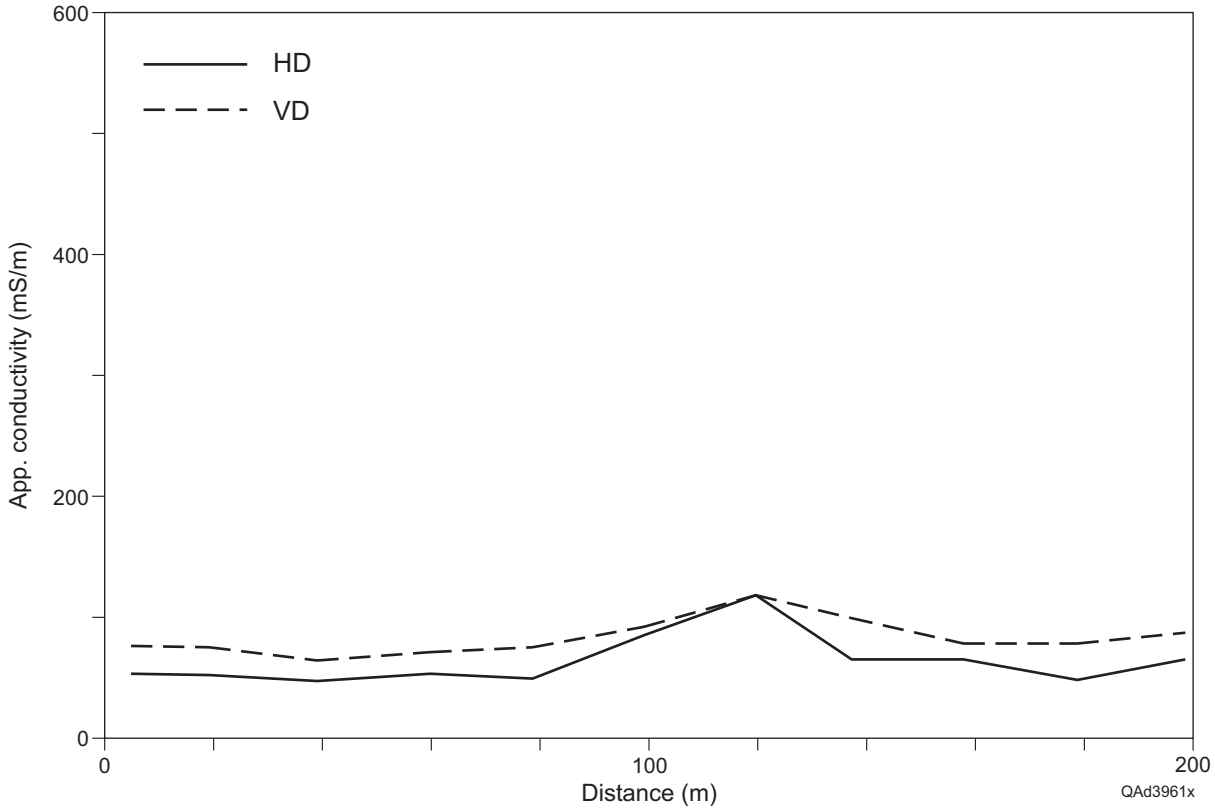

Figure 14. Apparent ground conductivity profile downstream along Mountain Creek (dry) at Robert Lee.

AIRBORNE GEOPHYSICAL SURVEY

Because significant sources affecting Colorado River salinity may exist between the Colorado River and the most downstream measurement location on each tributary, as well as along segments of the Colorado River and its tributaries that were inaccessible by foot, vehicle, or canoe during the field survey, we conducted an airborne geophysical survey to provide continuous ground-conductivity measurements along the river at multiple exploration depths.

The exploration depth of the airborne EM instrument is governed by instrument frequency and ground conductivity. The GEM-2A instrument (fig. 6) used in our airborne survey operated at five primary (transmitter) frequencies that ranged from 450 Hz to 39,030 Hz. Because the exploration depth of these instruments decreases as either frequency or ground conductivity increases, coils operating at different primary frequencies will measure different apparent conductivities over ground where the actual conductivity varies with depth. Exploration depth is approximated by "skin" depth, which is defined as the depth at which the field strength generated by the transmitter coil is reduced to 1/e times its original value. Skin depth is calculated using the equation

$$d = k\,(r / f)^{0.5}$$

where d = skin depth (in m), k = 500 (m/ohm-s)$^{0.5}$, r = resistivity (in ohm-m), and f = EM frequency (in cycles/s) (Telford and others, 1990). Recast into equivalent, reciprocal conductivity terms, this equation becomes

$$d = k\,(1 / \sigma f)^{0.5}$$

where k = 15,681 (m-mS/s)$^{0.5}$, σ = conductivity (in mS/m), and f = EM frequency.

We used the ground conductivity measurements made in the survey area with our ground-based instruments (table 2; appendix A) to estimate the exploration depths reached by the airborne instrument (fig. 15). Estimated exploration depth over the most conductive ground (528 mS/m) is the shallowest, increasing from as much as 3 m at the highest frequency (39 kHz) to 33 m at the lowest frequency (450 Hz). Exploration depths are greatest over the most poorly conductive ground (7 mS/m), ranging from about 30 m at 39 kHz to more than 200 m at 450 Hz. Increasing conductivities with depth, weak

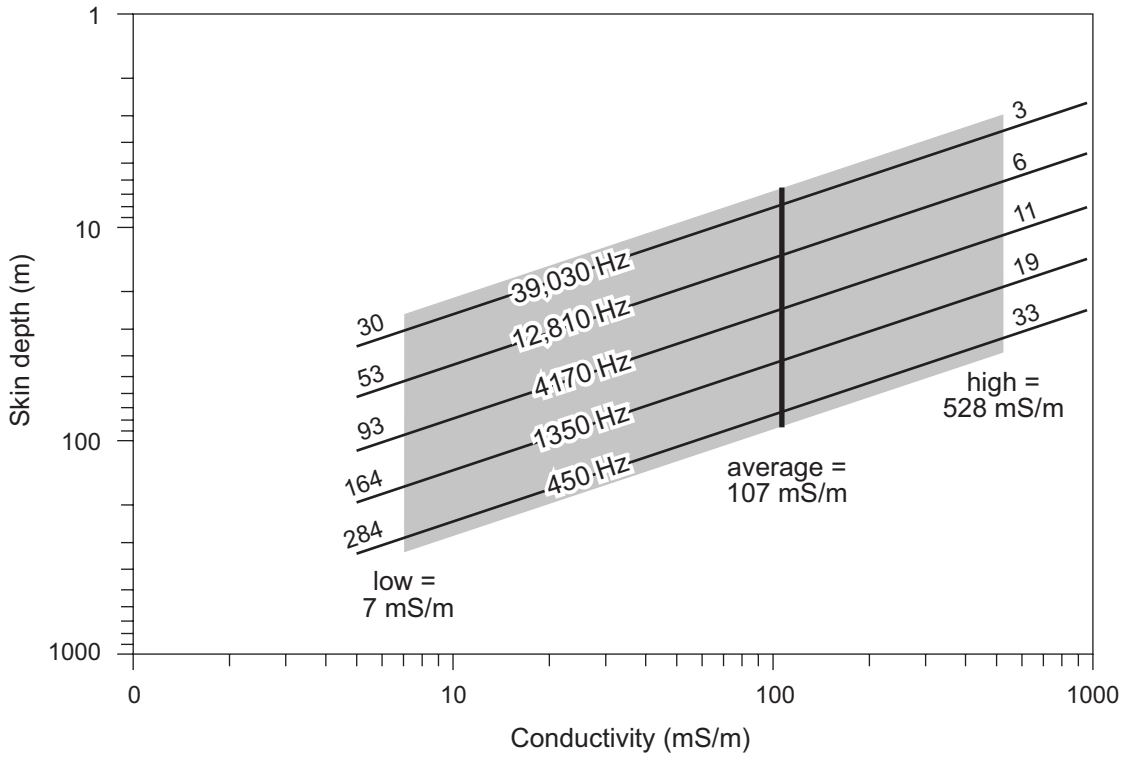

Figure 15. Approximate exploration (skin) depths for the five frequencies used in the Colorado River airborne EM survey. The shaded area represents the range of apparent conductivity values measured using a ground-based instrument (table 2). The heavy vertical line is the average conductivity value for all ground-based measurements. The actual apparent conductivities calculated from airborne-instrument data represent a bulk value that is influenced by electrical properties of the ground between the ground surface and the exploration depth for that frequency.

induced ground currents, and cultural noise can all combine to reduce the actual exploration depth achieved in a survey. We can produce a reasonable exploration depth estimate for the area and instrument by using the average measured ground conductivity (107 mS/m), which yields maximum exploration depths of 8 m at 39,030 Hz, 14 m at 12,810 Hz, 24 m at 4170 Hz, 42 m at 1350 Hz, and 73 m at 450 Hz.

Colorado River Above Spence Reservoir

The airborne geophysical survey extended above the upstream limit of segment 1426 at Spence Reservoir because previous studies have repeatedly shown that there are significant salinized areas upstream that degrade water quality in Spence Reservoir. This water in turn affects water quality below Spence Reservoir, particularly during low-flow conditions when releases from Spence can dominate downstream flow. Ground-based conductivity measurements made along the Colorado River and its tributaries upstream from Spence Reservoir are statistically higher than those measured farther downstream (table 2), suggesting generally greater ground salinization above Spence Reservoir. Airborne geophysical data acquired above Spence Reservoir include (a) 206 km along the axis of the Colorado River, (b) 86 km along Beals Creek, a major Colorado River tributary, and (c) 133 km within the Silver block a short distance upstream from Spence Reservoir (fig. 16).

Stream-axis apparent conductivities measured during the airborne survey are also generally higher at all frequencies above Spence Reservoir than they are farther downstream, as are average conductivities calculated for each major stream segment (figs. 16 and 17; table 5). Depending on the frequency, average ground conductivities are more than two to more than four times higher along the axis of the Colorado River above Spence Reservoir than they are along the Colorado River farther downstream. Average conductivities measured along Beals Creek are lower than values measured along the Colorado River above Spence Reservoir at all but the highest (shallowest-exploring) frequency, but also remain higher than Colorado River stream-axis values downstream from Spence Reservoir (table 5).

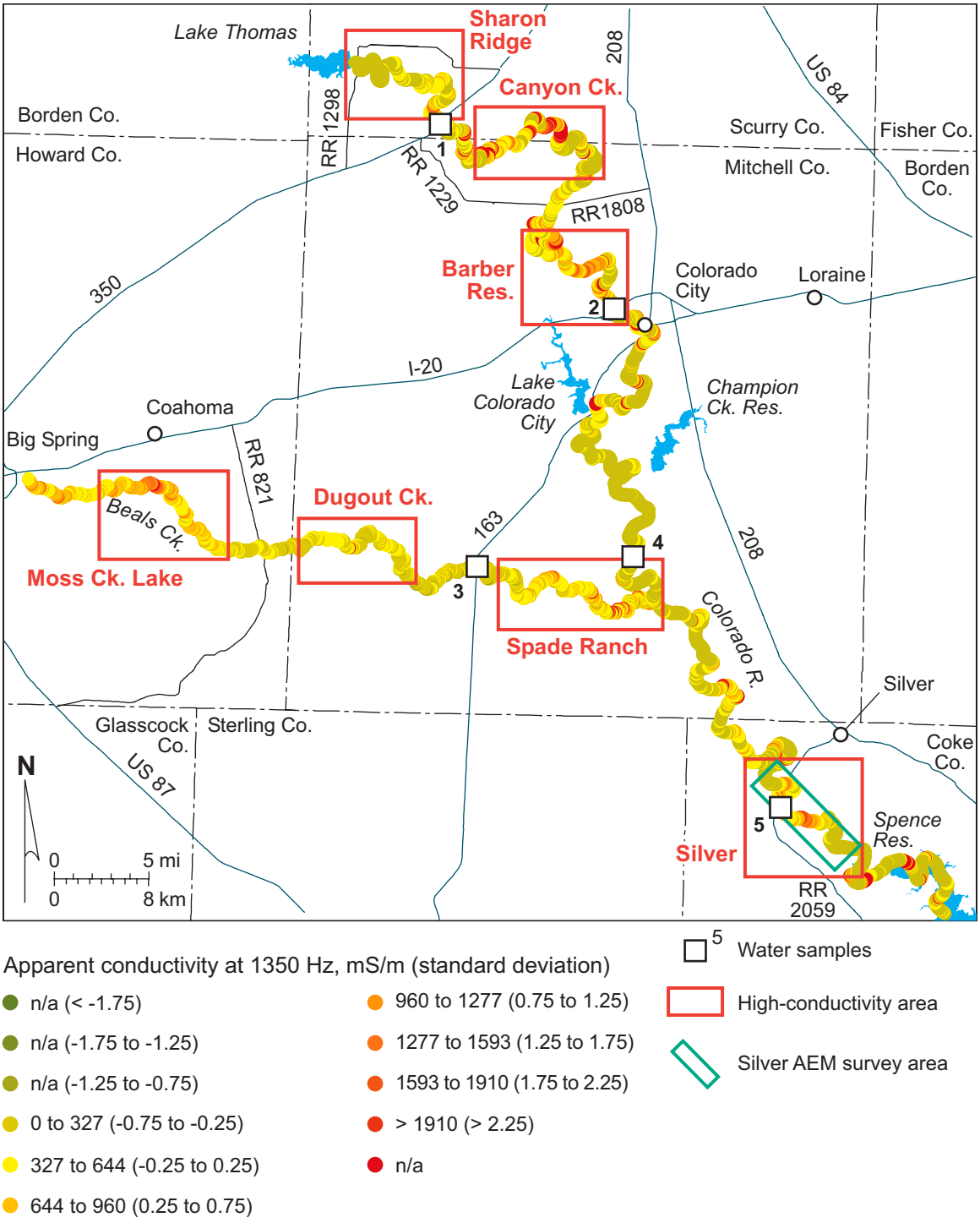

Figure 16. Apparent conductivity measured at 1350 Hz during the airborne geophysical survey along Beals Creek and the Colorado River between Lake Thomas and Spence Reservoir (colored dots). Also shown are the Sharon Ridge, Canyon Creek, Barber Reservoir, Silver, Moss Creek Lake, Dugout Creek, and Spade Ranch high-conductivity areas (red rectangles). The 1350-Hz frequency explores from the land surface to an average depth of about 20 m, estimated from the average river-axis conductivity at this frequency (table 5).

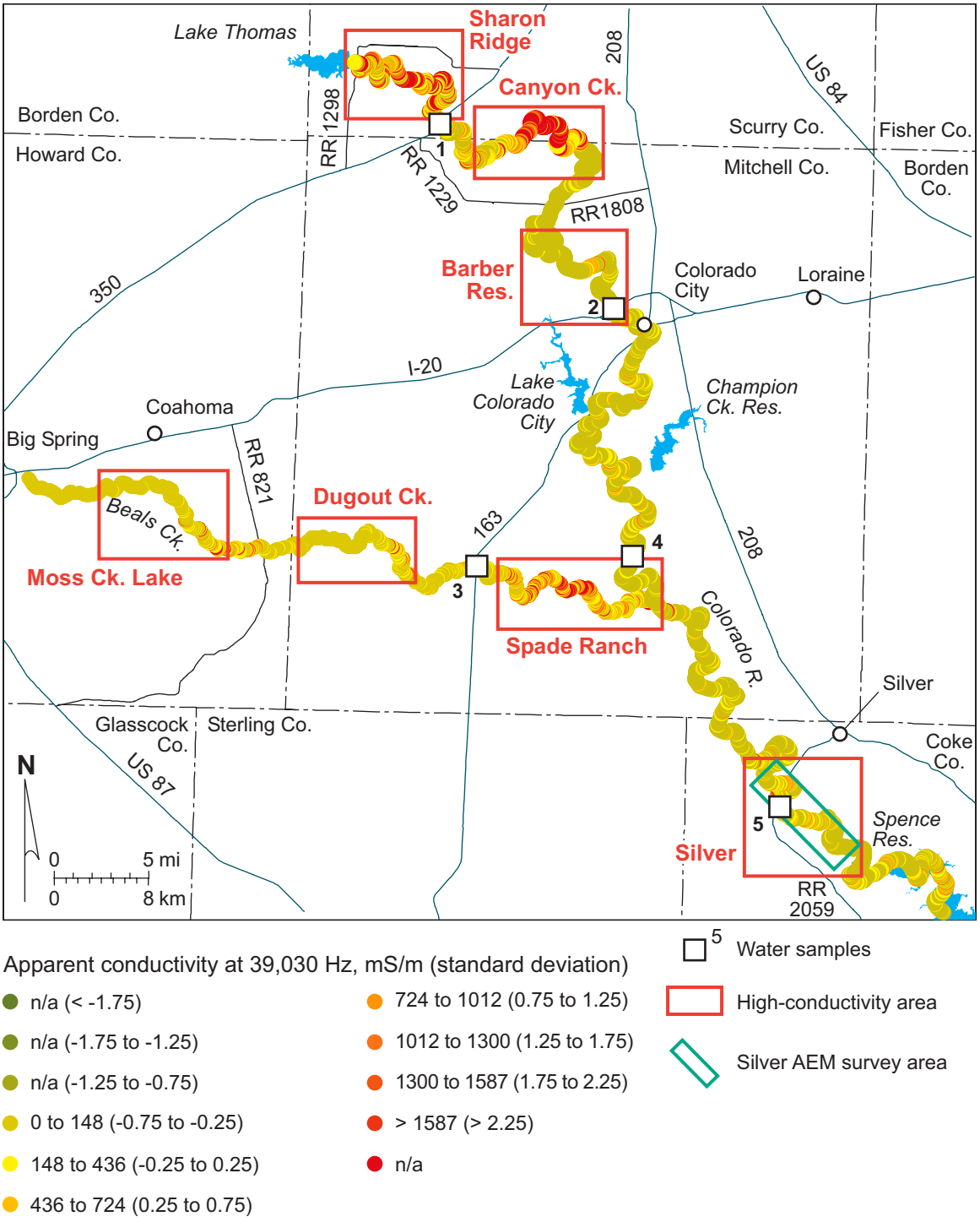

Figure 17. Apparent conductivity measured at 39,030 Hz along Beals Creek and the Colorado River between Lake Thomas and Spence Reservoir (colored dots). Also shown are the Sharon Ridge, Canyon Creek, Barber Reservoir, Silver, Moss Creek Lake, Dugout Creek, and Spade Ranch high-conductivity areas (red rectangles). The 39,030-Hz frequency explores from the land surface to an average depth of about 5 m, estimated from the average river-axis conductivity at this frequency (table 5).

Table 5. Average apparent conductivities measured at each frequency during the airborne geophysical survey of the upper Colorado River.

	EM frequency (Hz)				
Segment	**450**	**1350**	**4170**	**12,810**	**39,030**
Colorado River, Thomas to Spence	983	485	264	199	292
Sharon Ridge area	368	342	104	73	845
Canyon Creek area	1284	862	355	176	906
Barber Reservoir area	1439	805	345	190	79
Silver area	1270	420	762	694	173
Silver AEM block	994	664	571	566	453
Beals Creek	430	132	79	43	324
Moss Creek Lake area	334	187	132	49	201
Dugout Creek area	349	84	64	32	185
Spade Ranch area	721	165	82	62	642
Colorado River, Spence to Ivie	195	100	56	43	133
Machae Creek area	147	114	75	83	423
Machae AEM block	128	116	50	31	58
Maverick area	264	110	47	19	23
Bull Hollow area	196	131	74	49	99
Valley Creek area	293	153	62	44	43

Average conductivities for the Colorado River and Beals Creek areas show a similar trend of having the highest conductivities at the lowest (deepest-exploring) frequency (450 Hz), progressively lower apparent conductivities as frequency increases and exploration depth decreases, and high conductivities again at the highest (shallowest-exploring) frequency (39,030 Hz). This suggests that, within the exploration depth of this instrument, high salinities can be found both in near-surface accumulations (possibly without deeper sources) as well as within deeper zones that likely represent more saline ground water that may or may not extend upward to the river.

Maps of stream-axis apparent conductivity at representative low and high (deep and shallow) frequencies illustrate the differing instrument response to lateral and vertical extent and intensity of salinization. At a low frequency (1350 Hz), the Canyon Creek, Barber Reservoir, and Silver areas along the Colorado River and the Moss Creek Lake and Spade Ranch areas along Beals Creek are the most significant segments of elevated conductivity where relatively deep salinization exists (fig. 16). At the highest frequency (39,030 Hz), the Sharon Ridge, Canyon Creek, and Silver areas along the Colorado River and the Spade Ranch area along Beals Creek are the most significant segments of elevated conductivity, indicating likely near-surface salinization along these segments and relatively minor or local near-surface salinization in other areas. The Canyon Creek and Silver areas on the Colorado River and the Spade Ranch area on Beals Creek exhibit elevated conductivities at low and high frequencies, indicating the likely presence of both near-surface and deeper salinization.

Sharon Ridge Area

The Sharon Ridge area of elevated conductivity is a 20-km-long segment of the Colorado River between Lake Thomas and Texas 350 (fig. 18). It lies within an interval of the Dockum Group that contains sandstone and mudstone (figs. 2 and 3) and is adjacent to the densely developed Sharon Ridge Oil Field to the northeast. Bull Creek crosses the oil field and enters the Colorado River between 7 and 8 km from the upstream end of the segment. Bluff Creek also crosses the oil field, entering the Colorado River at about 14 km.

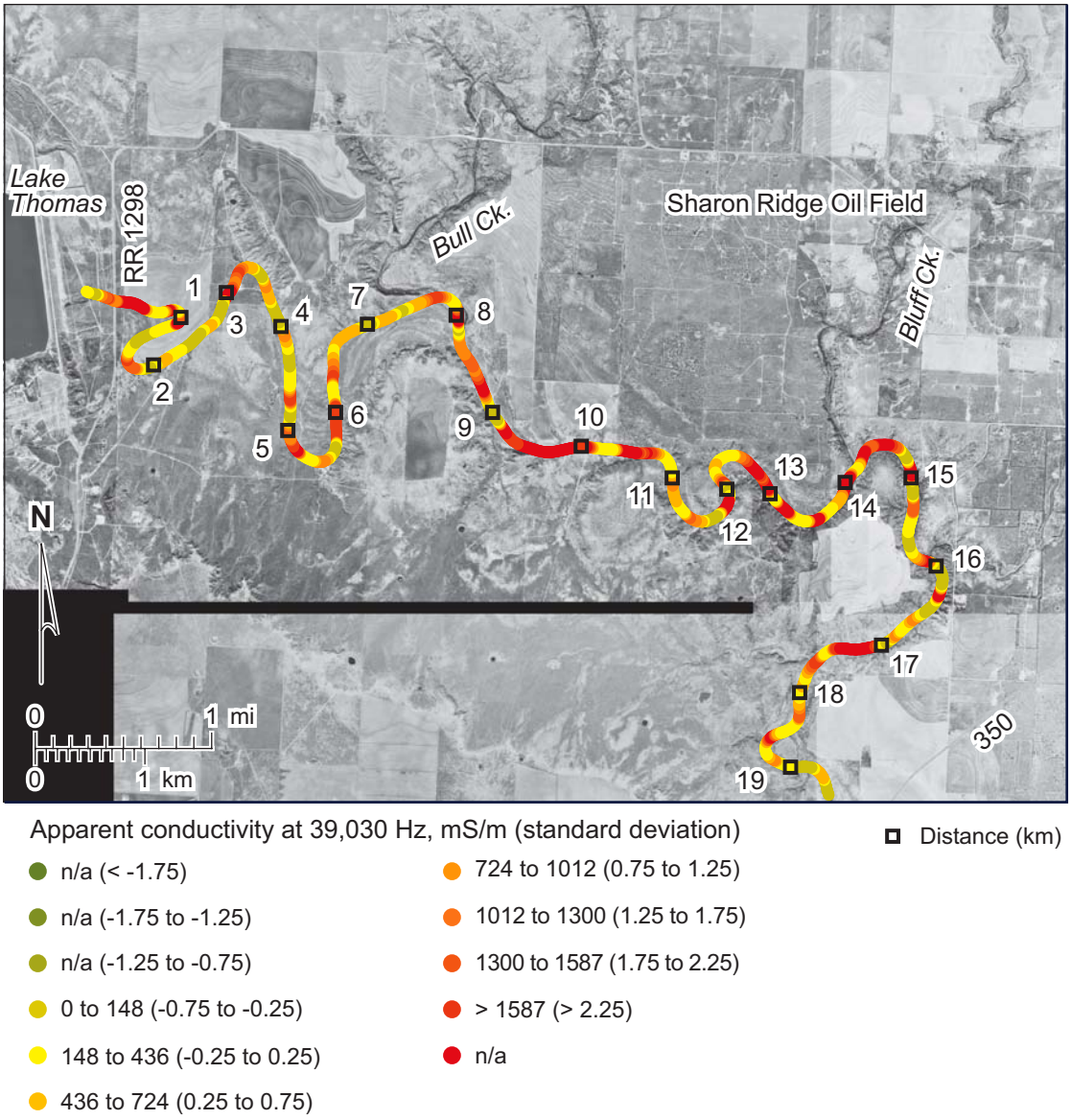

Figure 18. Map of the Sharon Ridge area (fig. 17) depicting apparent conductivity measured at 39,030 Hz (colored dots). The numbered points are the distance (in km) along the stream segment. The 39,030-Hz frequency explores from the land surface to an average depth of about 5 m, estimated from the average river-axis conductivity at this frequency (table 5).

Maps of stream-axis apparent conductivity show that this segment is dominated by elevated conductivity at the highest frequency (figs. 16 to 18). This segment had the second-highest average conductivity at 39,030 Hz of any surveyed stream segment, but the lowest average conductivities for all deeper-exploring frequencies than any other segment above Spence Reservoir. An image that combines apparent conductivity data from all frequencies along this segment as a pseudo-cross-section (fig. 19) shows extensive elevated conductivity at the highest (shallowest-exploring) frequency (39,030 Hz), particularly at and downstream from Bull Creek (8 to 11 km) and upstream and downstream from Bluff Creek (13 to 16 km). At the two lowest frequencies (450 and 1350 Hz), the pseudosection shows a second zone of elevated conductivity that extends across the segment and appears to shallow downstream, mimicking the regional geologic dip.

Elevated conductivities at the highest frequency likely represent near-surface salinization produced by surface transport and perhaps evaporative or transpirative concentration. The association with Bull and Bluff creeks suggests that these creeks may have transported saline water to the Colorado River, either from natural sources or from the Sharon Ridge Oil Field. The deeper "dipping" zone probably represents a geologic unit carrying saline ground water as part of the regional flow system. Baseflow discharge of saline ground water is most likely to occur at and downstream from Bluff Creek.

Canyon Creek Area

The Canyon Creek elevated conductivity segment extends about 21 km along the Colorado River between Texas 350 and RR 1808 (figs. 16, 17, and 20). It begins downstream from Willow Creek and passes through the densely developed Sharon Ridge Oil Field through much of its length. Canyon Creek enters the river near 11 km downstream; Deep Creek enters the Colorado near the end of the segment at 19 km. Like the Sharon Ridge area, the Canyon Creek segment lies within an interval of the Dockum Group that contains sandstone and mudstone (figs. 2 and 3).

The Canyon Creek segment is relatively conductive at low (deep) and high (shallow) frequencies (figs. 16 and 17). Average conductivity at the highest frequency is the highest of all segments examined

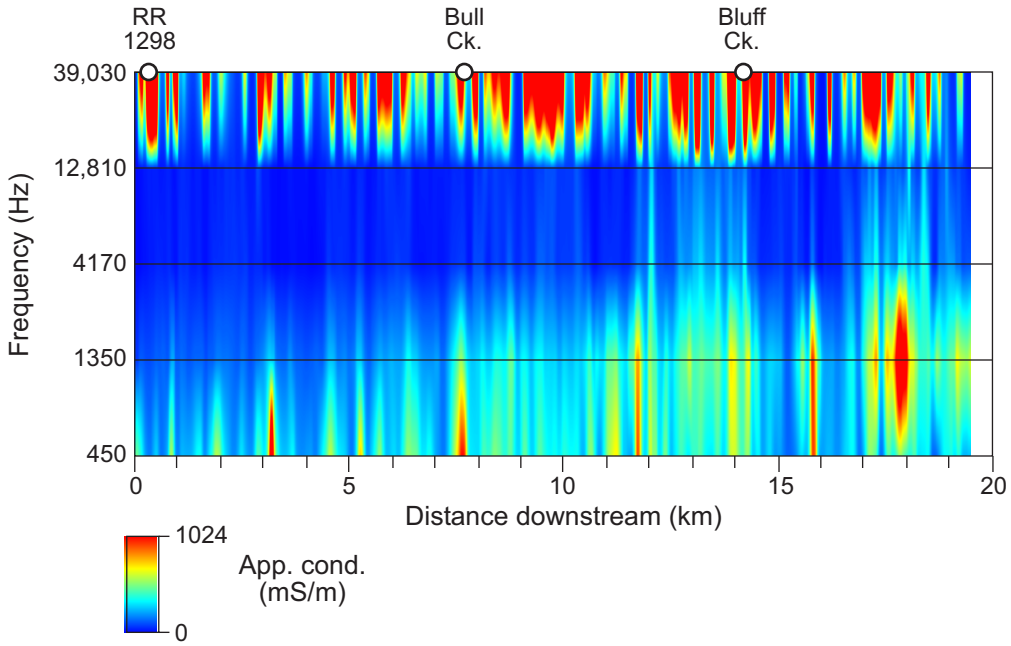

Figure 19. Combined apparent conductivity pseudosection along the Sharon Ridge segment of the Colorado River from all airborne survey frequencies. The shallowest-exploring frequency is along the top of the image and the deepest-exploring frequency is along the bottom.

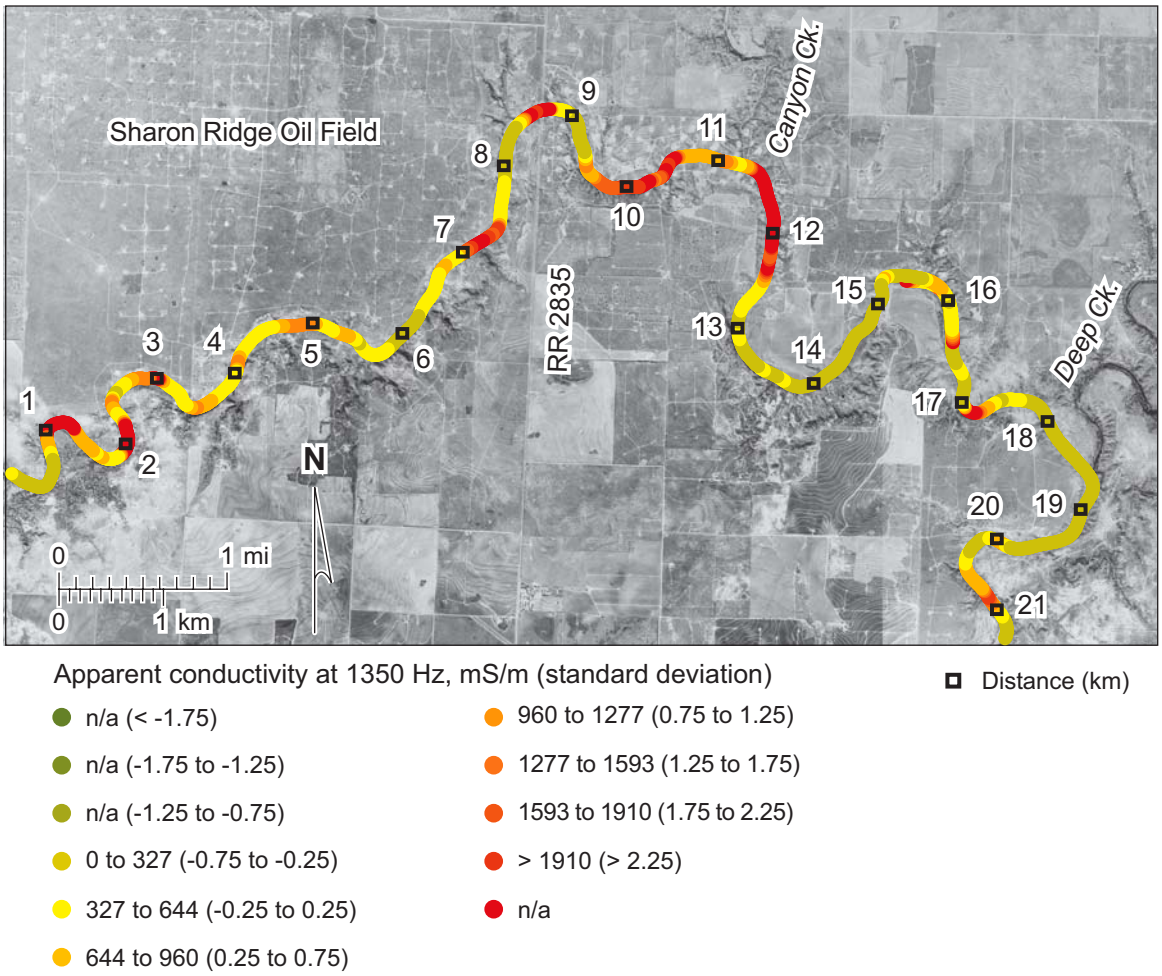

Figure 20. Map of the Canyon Creek area (fig. 16) depicting apparent conductivity measured at 1350 Hz (colored dots). The numbered points are the distance (in km) along the stream segment. The 1350-Hz frequency explores from the land surface to an average depth of about 20 m, estimated from the average river-axis conductivity at this frequency (table 5).

(table 5), but this segment also had very high average conductivities at the two lowest frequencies. Highest conductivities at the low frequencies were measured between RR 2835 and Canyon Creek (8 to 12 km, figs. 20 and 21) and between Canyon Creek and Deep Creek (14 to 17 km). Elevated conductivity at the highest frequency was measured where the river crosses the Sharon Ridge Oil Field (2 to 12 km, figs. 20 and 21). Local areas of elevated conductivity at single frequencies on the pseudosection (fig. 21) are probably caused by infrastructure such as pipelines, power lines, and metal structures.

High conductivities at the highest frequency indicate near-surface salinization adjacent to the Sharon Ridge Oil Field between 2 and 12 km that may be related to oil-field activities. High conductivities at lower frequencies (450 and 1350 Hz) between the upstream end of the segment and the confluence with Canyon Creek appear to shallow downstream, suggesting deep-source salinization within geologic units that dip westward and may contribute saline ground water to the Colorado River in places.

Barber Reservoir Area

The Barber Reservoir high-conductivity segment extends 21 km from Cedar Bend to Colorado City (figs. 16, 17, and 22). The upper 9 km of this segment passes through a densely developed oil field. Barber Reservoir, operated by CRMWD to store relatively high-salinity water diverted from the Colorado River, lies adjacent to the river on an alluvial terrace between 14 and 16 km (fig. 22). Bone Hollow enters the Colorado at 15 km. The Colorado River has mostly eroded an interval of the Dockum Group that is dominated by sandstone and mudstone. The southeastern part of the segment cuts Dockum mudstones (fig. 2 and 3).

Compared to other high-conductivity segments, average conductivities in the Barber Reservoir area are relatively low at the two highest frequencies and are relatively high at the two lowest frequencies (table 5). Elevated conductivities along this segment are highest and most extensive at the lowest frequencies (450 and 1350 Hz), particularly between 1 and 4 km, 7 and 14 km, and 16 and 19 km

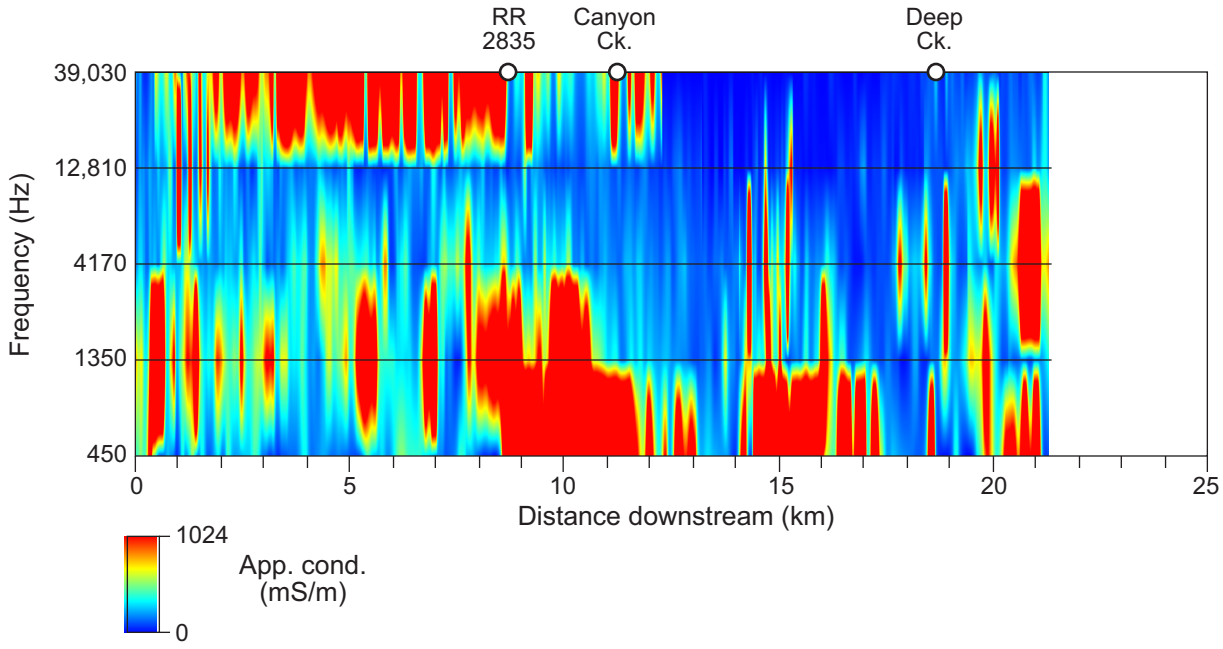

Figure 21. Combined apparent conductivity pseudosection along the Canyon Creek segment of the Colorado River from all airborne survey frequencies. The shallowest-exploring frequency is along the top of the image and the deepest-exploring frequency is along the bottom.

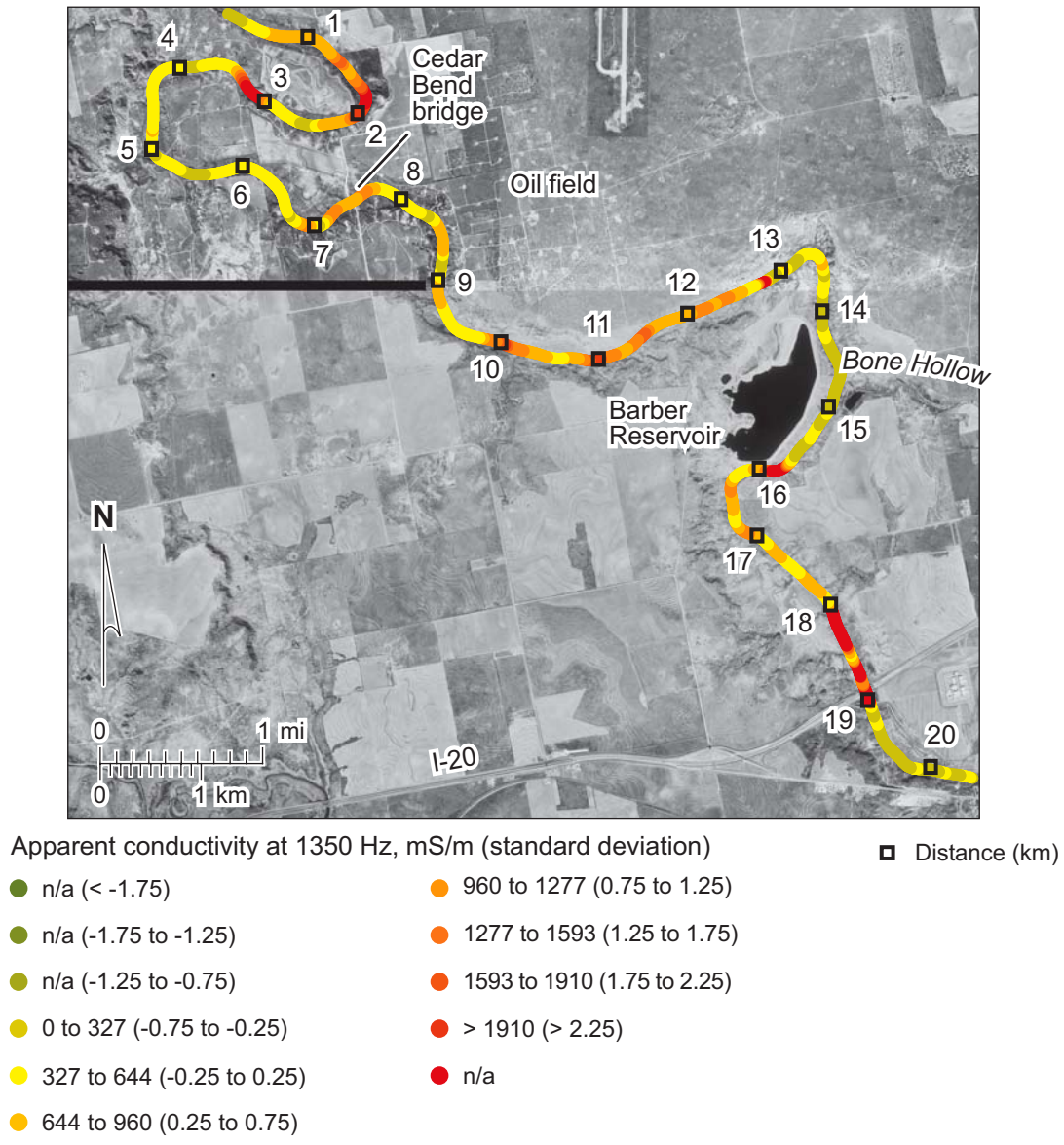

Figure 22. Map of the Barber Reservoir area (fig. 16) depicting apparent conductivity measured at 1350 Hz (colored dots). The numbered points are the distance (in km) along the stream segment. The 1350-Hz frequency explores from the land surface to an average depth of about 20 m, estimated from the average river-axis conductivity at this frequency (table 5).

(figs. 22 and 23). At higher, shallower-exploring frequencies, the only significant area of elevated conductivity is northwest of Barber Reservoir (10 to13 km). These data suggest that deep-source salinization exists in ground water beneath the river between 1 and 4 km, 7 and 14 km, and 16 and 19 km. Contributions to stream flow are likely to be most significant between 10 and 13 km, where shallow apparent conductivities are highest (fig. 23). The relatively recent age of the oil field combined with sparse oil-field activity downstream from 9 km suggests that the source of deep salinization is largely natural. It is possible that near-surface salinization evident between 11 and 13 km is augmented by diverted saline water in Barber Reservoir that could migrate northwestward toward the Colorado River through permeable Triassic sandstones that crop out between the reservoir and the river.

Silver Area

The Silver area encloses the most downstream segment of high apparent conductivities along the Colorado River axis above Spence Reservoir (figs. 16 and 17). This 19-km-long segment straddles RR 2059 and passes through the densely developed Jameson–Strawn Oil Field (fig. 24), flowing within a valley eroded into sandstone, shale, gypsum, dolomite, and local conglomerate of the Whitehorse Group and Cloud Chief Gypsum (figs. 2 and 4). Rough Creek enters the river at 7 km after passing through part of the oil field west of the river. Sand Creek drains another part of the oil field northeast of the river, entering the Colorado at 13 km. Bitter Creek enters the river at 17 km after crossing a sparsely developed part of the oil field west of the river. In-the-field analysis of airborne geophysical data between stream-axis flights showed this area to be anomalously conductive. We used the field data to define the boundaries of a gridded airborne survey (fig. 24).

Compared to other segments, the stream-axis flight line in the Silver area has the highest average conductivities at 4170 and 12,810 Hz as well as a very high average conductivity at the lowest frequency (table 5). At the two lowest frequencies, an extensive zone of high conductivity extends from 3 km to the Sand Creek confluence at about 13 km, coinciding with the most heavily developed part of the Jameson–Strawn field (figs. 24 and 25). Less extensive high conductivities at intermediate frequen-

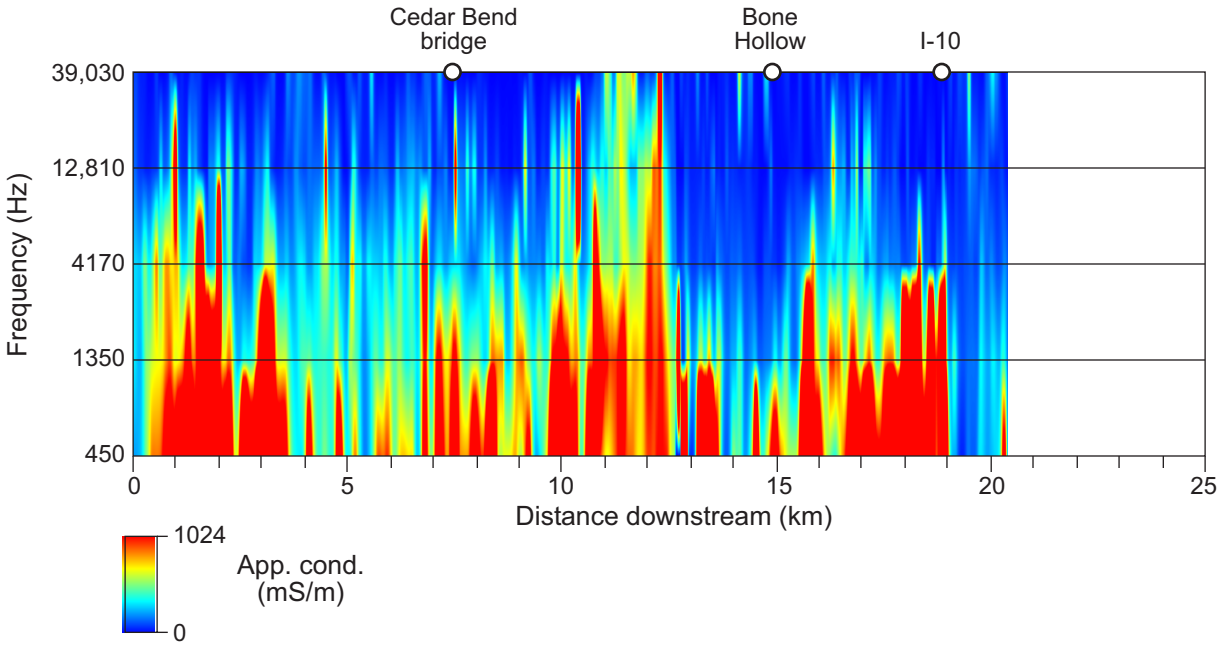

Figure 23. Combined apparent conductivity pseudosection along the Barber Reservoir segment of the Colorado River from all airborne survey frequencies. The shallowest-exploring frequency is along the top of the image and the deepest-exploring frequency is along the bottom.

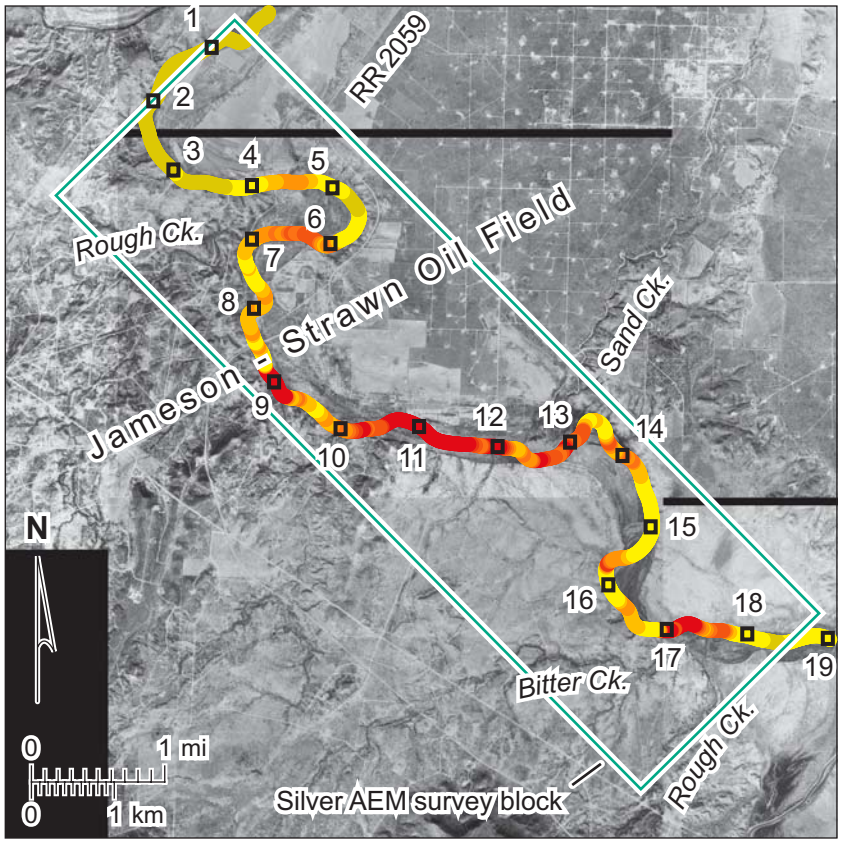

Figure 24. Map of the Silver area (fig. 16) depicting apparent conductivity measured at 4170 Hz (colored dots). The numbered points are the distance (in km) along the stream segment. The 4170-Hz frequency explores from the land surface to an average depth of about 15 m, estimated from the average river-axis conductivity at this frequency (table 5).

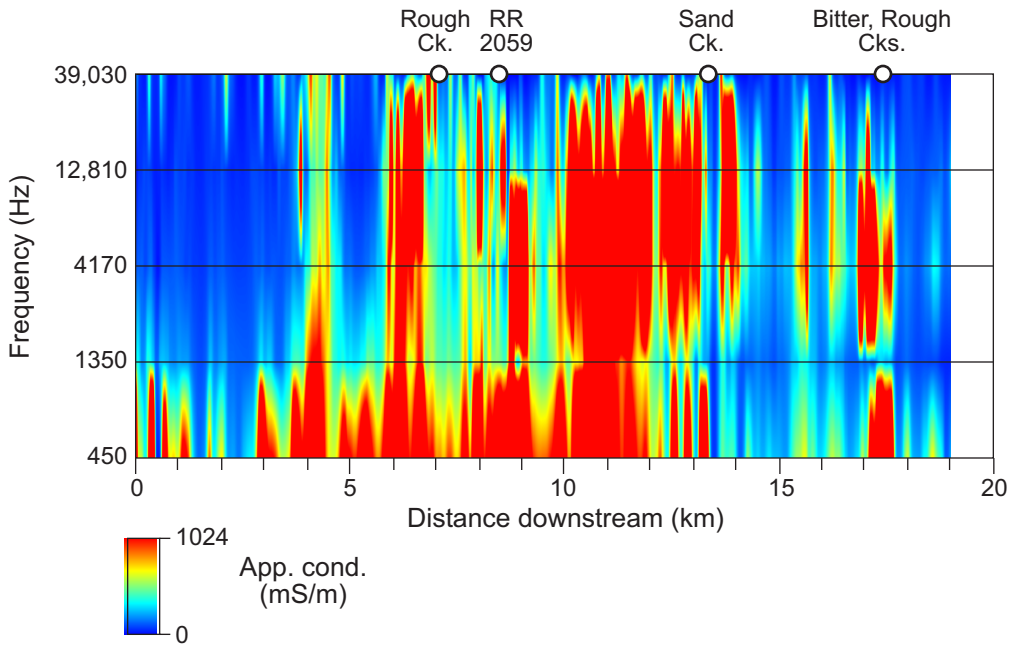

Figure 25. Combined apparent conductivity pseudosection along the Silver segment of the Colorado River from all airborne survey frequencies. The shallowest-exploring frequency is along the top of the image and the deepest-exploring frequency is along the bottom.

cies are shifted farther downstream from 6 to about 14 km. Elevated conductivities at the highest frequencies were also measured between 6 and 14 km.

Elevated conductivities at both high and low frequencies indicate the presence of shallow and deep salinization in this area. Although the elevated conductivities at the lowest frequency may delineate the lateral extent of dominantly natural sources of salinization, the elevated conductivities at higher frequencies indicate near-surface salinization that is likely to be oil-field related and probably contributes saline water to the Colorado River. The most significant zone of likely inflow appears to be between 6 and 14 km.

Moss Creek Lake Area, Beals Creek

In general, stream-axis conductivities along Beals Creek are lower than those along the Colorado River above Spence Reservoir at all but the highest frequency (table 5). The Moss Creek Lake area encloses the most upstream of the three high-conductivity areas identified along Beals Creek (figs. 16 and 17). Tributaries joining this 17-km-long segment of Beals Creek include Sandy Hollow (at 4 km) and Guthrie Draw (at 7.5 km) from the north and Moss Creek (at 8 km) and Powell Creek (at 14 km) from the south (fig. 26). Beals Creek cuts Dockum Group sandstone and mudstone (fig. 2 and 3) and crosses into the western part of the Snyder Oil Field near the downstream end of this segment (near 16 km). In addition to the extensive and heavily developed Snyder Oil Field, less dense oil-field development has occurred along the entire segment.

The Moss Creek Lake segment has the highest average conductivities measured along Beals Creek at intermediate to low frequencies (4170 and 1350 Hz, table 5; figs. 26 and 27). At these frequencies, high conductivities are mapped between 0 and 13 km and are particularly high between Sandy Hollow and Moss Creek (5 to 8 km). High conductivities at the highest frequencies begin between Moss Creek and Powell Creek, extending to the downstream end of the segment (11 to 17 km). Highest values were measured below Powell Creek adjacent to the Snyder Oil Field.

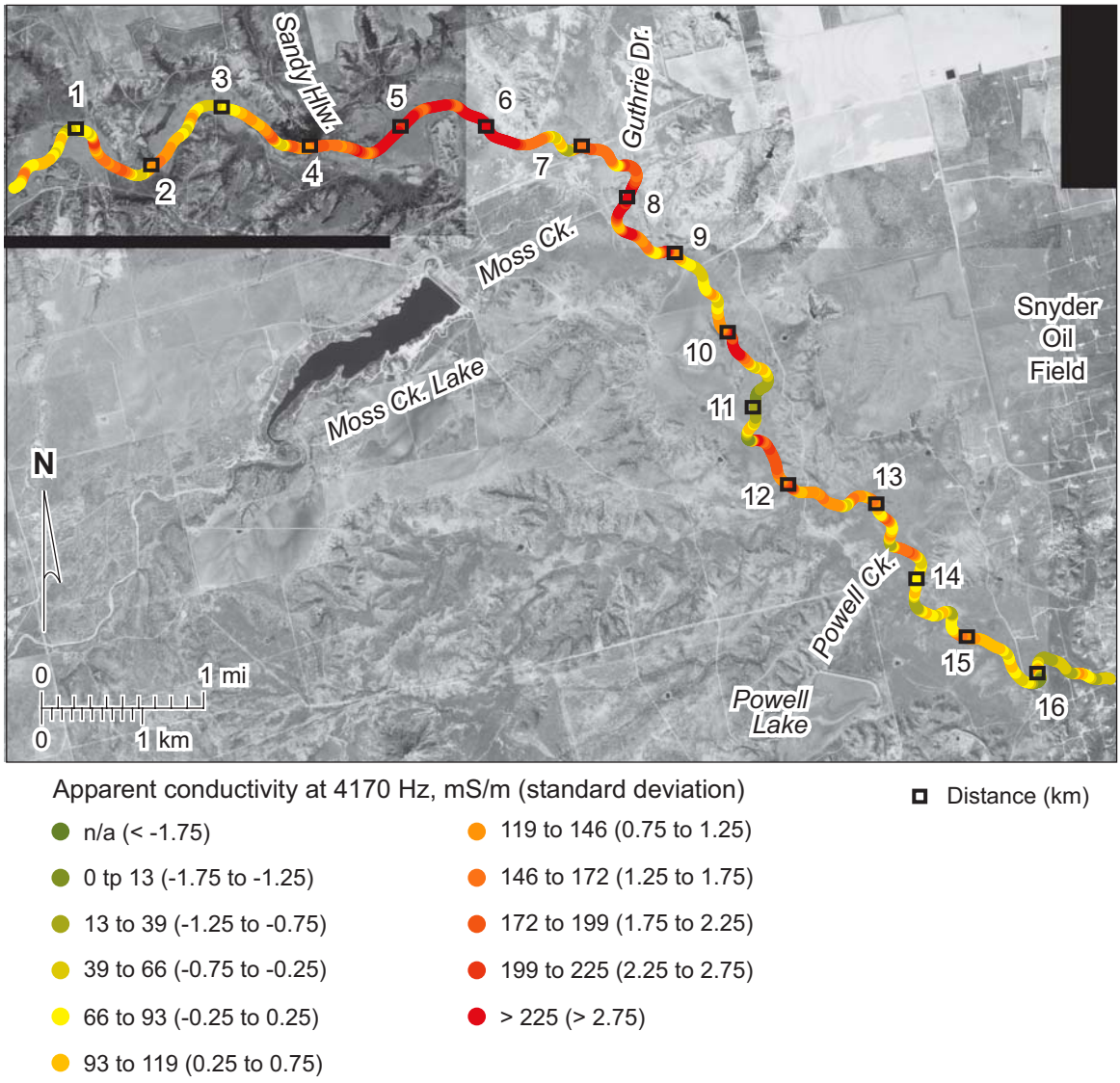

Figure 26. Map of the Moss Creek Lake area (fig. 16) along Beals Creek depicting apparent conductivity measured at 4170 Hz (colored dots). The numbered points are the distance (in km) along the stream segment. The 4170-Hz frequency explores from the land surface to an average depth of about 28 m, estimated from average conductivity measured at this frequency along Beals Creek (table 5).

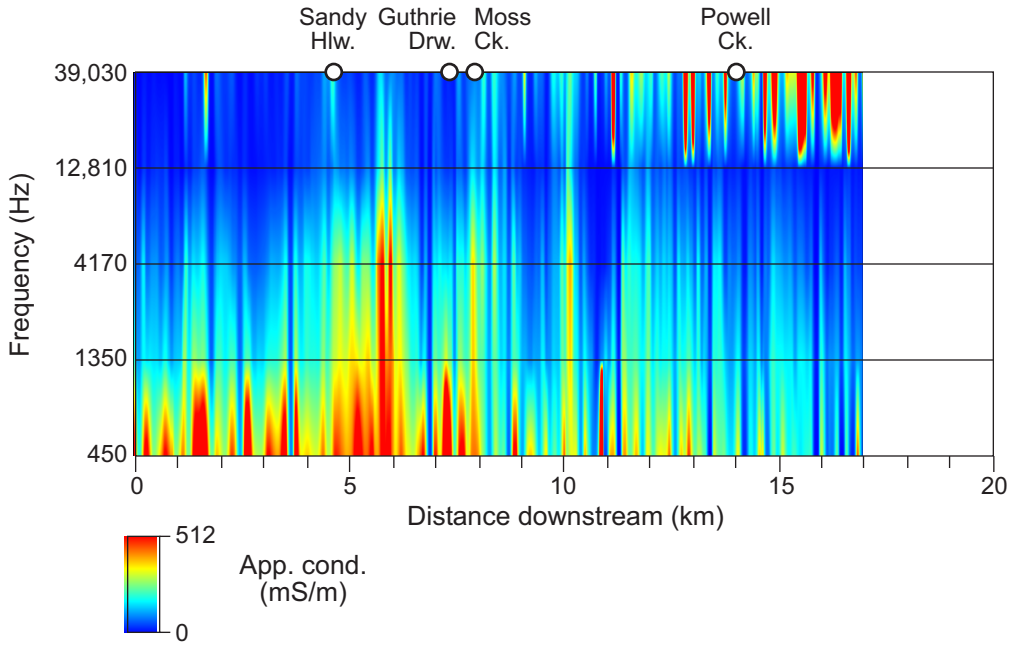

Figure 27. Combined apparent conductivity pseudosection along the Moss Creek Lake segment of Beals Creek from all airborne survey frequencies. The shallowest-exploring frequency is along the top of the image and the deepest-exploring frequency is along the bottom.

Conductivity patterns indicate there is evidence for shallow and deep salinization along the Moss Creek Lake segment. Deeper salinization extends from 0 to at least 13 km, probably representing ground water with high natural salinities. Contributions of saline ground water to Beals Creek are most likely between Sandy Hollow and Moss Creek. These contributions may combine with oil-field sources of salinity below Powell Creek (Sullivan and others, 1999) to produce the near-surface salinization evident there.

Dugout Creek Area, Beals Creek

The Dugout Creek segment of Beals Creek (figs. 16 and 17) is of interest because Dugout Creek crosses a heavily developed part of the Snyder Oil Field and joins Beals Creek 3 km downstream from the upper end of this segment (fig. 28). Here Beals Creek flows on Dockum Group sandstone and mudstone (fig. 2 and 3). Bull Creek enters Beals Creek from the southwest at 11 km.

Average conductivities calculated from stream-axis airborne survey data show that the Dugout Creek segment is the least conductive of the Beals Creek segments despite some local conductivity highs (table 5; fig. 28). Average conductivities for the segment are below the averages for Beals Creek at all five frequencies. Maps of apparent conductivity at single frequencies depict minor areas of elevated conductivity, such as just upstream from Dugout Creek (at 3 km), between 4 and 5 km, and near 10 km, but most of the segment is poorly conductive (fig. 28). Combined-frequency images show that the highest conductivities are most extensive at the lowest frequency (fig. 29). At the highest frequency, elevated conductivities are found only downstream from Bull Creek (11 to 15 km).

There is little evidence for significant ground salinization along this segment. Some minor near-surface salinization may be present at and below Bull Creek, which drains a southern continuation of the Snyder Oil Field.

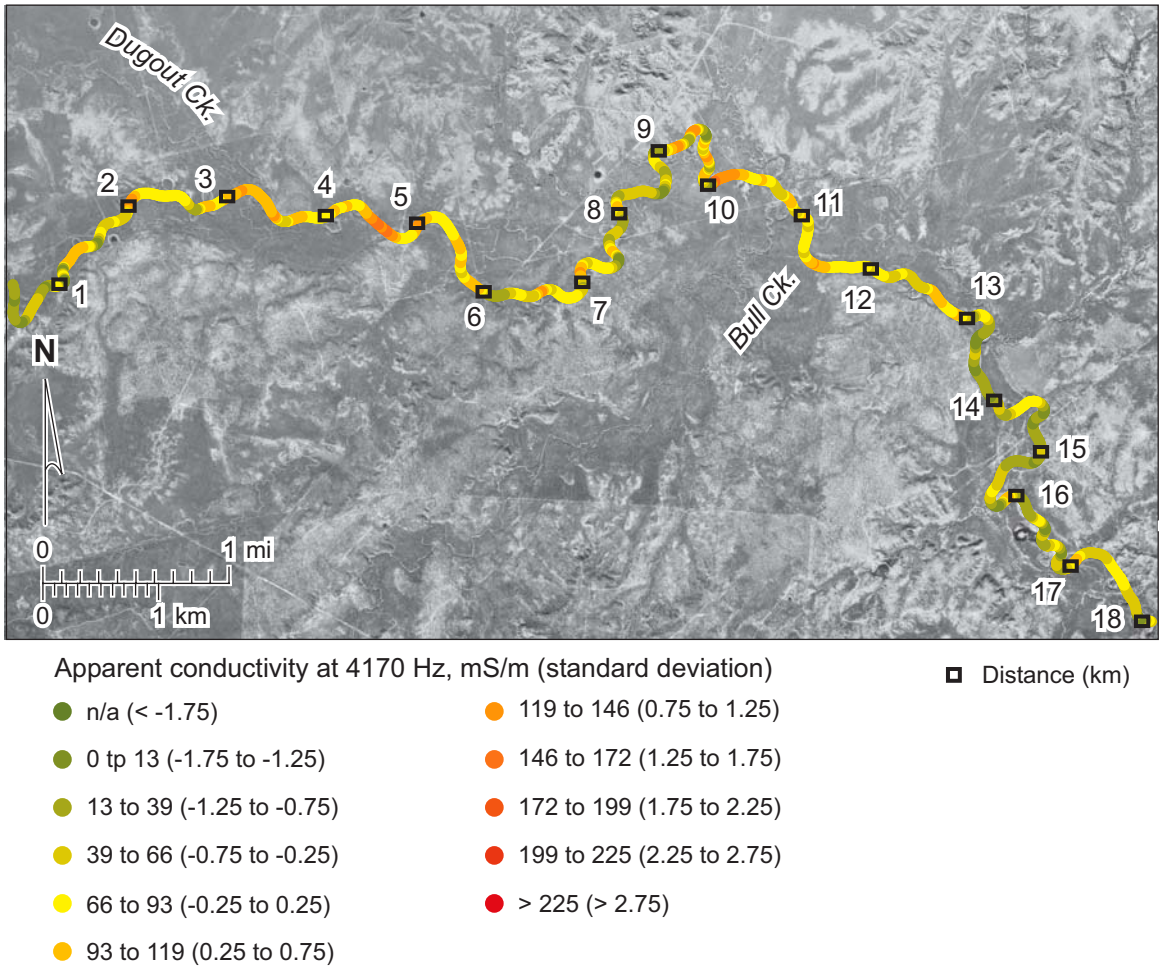

Figure 28. Map of the Dugout Creek area (fig. 16) along Beals Creek depicting apparent conductivity measured at 4170 Hz (colored dots). The numbered points are the distance (in km) along the stream segment. The 4170-Hz frequency explores from the land surface to an average depth of about 28 m, estimated from average conductivity measured at this frequency along Beals Creek (table 5).

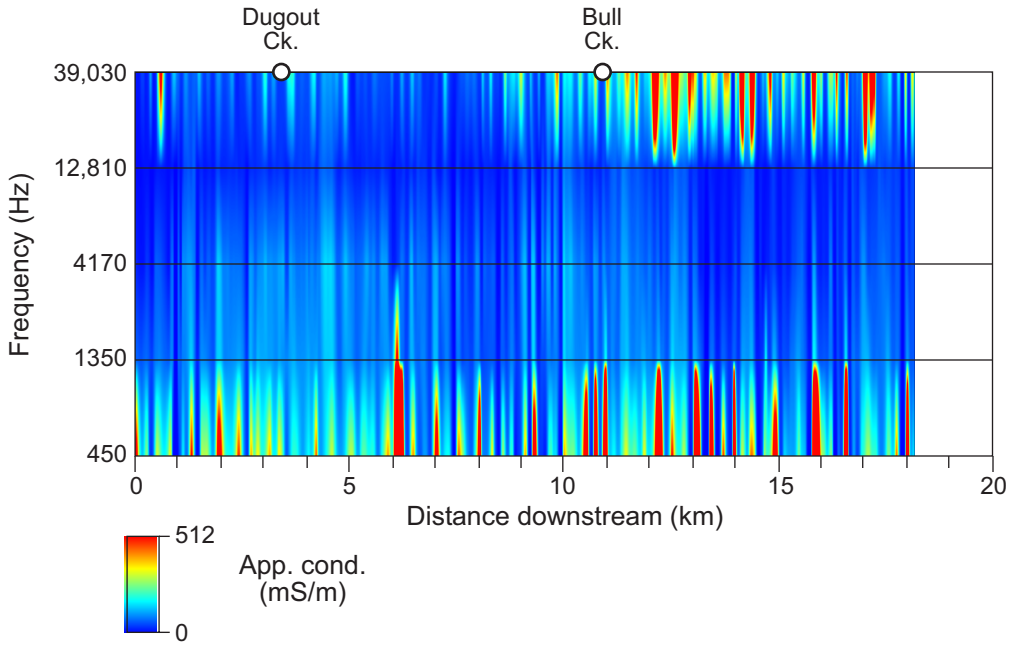

Figure 29. Combined apparent conductivity pseudosection along the Dugout Creek segment of Beals Creek from all airborne survey frequencies. The shallowest-exploring frequency is along the top of the image and the deepest-exploring frequency is along the bottom.

Spade Ranch Area, Beals Creek

The Spade Ranch segment of Beals Creek is the longest (25 km) and most downstream of the highly conductive Beals Creek segments, beginning downstream from Texas 163 and ending at the confluence with the Colorado River (figs. 16 and 17). Dockum Group sandstone and mudstone floor Beals Creek in this area (fig. 2 and 3). Wildcat Creek (at 4 km), Renderbrook Creek (at 12 km), and Geneva Creek (at 16 km) join Beals Creek from the south (fig. 30).

Compared to other Beals Creek segments, the Spade Ranch area had the highest average conductivity for both the highest two (12,810 and 39,030 Hz) and the lowest (450 Hz) frequencies (table 5). At high frequencies, much of the segment is highly conductive (figs. 30 and 31), particularly between Wildcat Creek and Geneva Creek. Elevated conductivities at the lowest frequencies begin upstream from Renderbrook Creek at 10 km and continue to the Colorado River.

Apparent conductivity data show evidence of significant shallow and deep salinization. Deep salinization likely reflects the presence of naturally saline ground water below the creek. The most likely areas where saline ground water might contribute to Beals Creek flow include the segment between Wildcat Creek and Renderbrook Creek (4 to 12 km) and downstream from 14 km. With the exception of a small number of wells near Wildcat Creek, oil-field development is sparse in this area. This suggests that, except for local near-surface salinization near Wildcat Creek, most salinization in this area is caused by surface contribution from sources farther upstream and by discharge of naturally saline ground water in the middle to lower part of this segment.

Colorado River Below Spence Reservoir (Segment 1426)

The stream-axis airborne survey flew over 144 km of the Colorado River downstream from Spence Reservoir, including the entire length of segment 1426 (fig. 32). In addition, we acquired airborne EM data in the Machae Creek block southeast of Robert Lee (figs. 1 and 32). Data from the airborne EM instrument showed that the Colorado River downstream from Spence Reservoir tends to have much lower ground conductivities at all measured frequencies than were measured along the

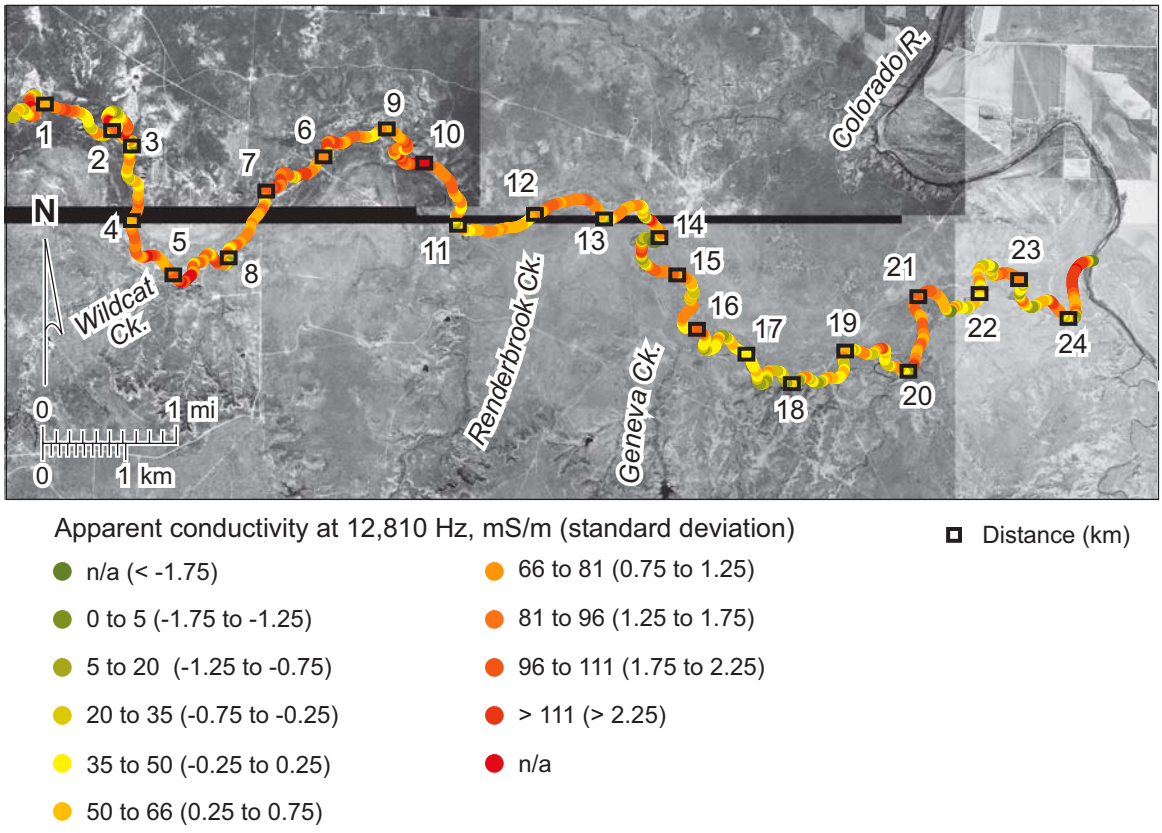

Figure 30. Map of the Spade Ranch area (fig. 17) along Beals Creek depicting apparent conductivity measured at 12,810 Hz (colored dots). The numbered points are the distance (in km) along the stream segment. The 12,810-Hz frequency explores from the land surface to an average depth of about 21 m, estimated from average conductivity measured at this frequency along Beals Creek.

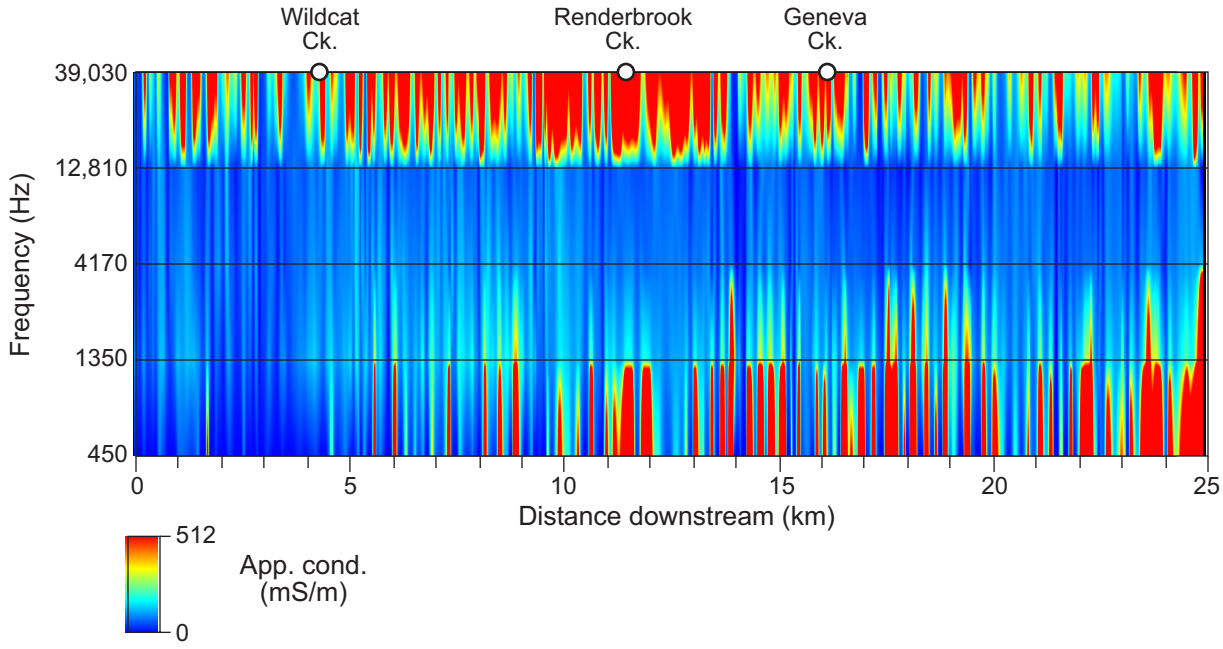

Figure 31. Combined apparent conductivity pseudosection along the Spade Ranch segment of Beals Creek from all airborne survey frequencies. The shallowest-exploring frequency is along the top of the image and the deepest-exploring frequency is along the bottom.

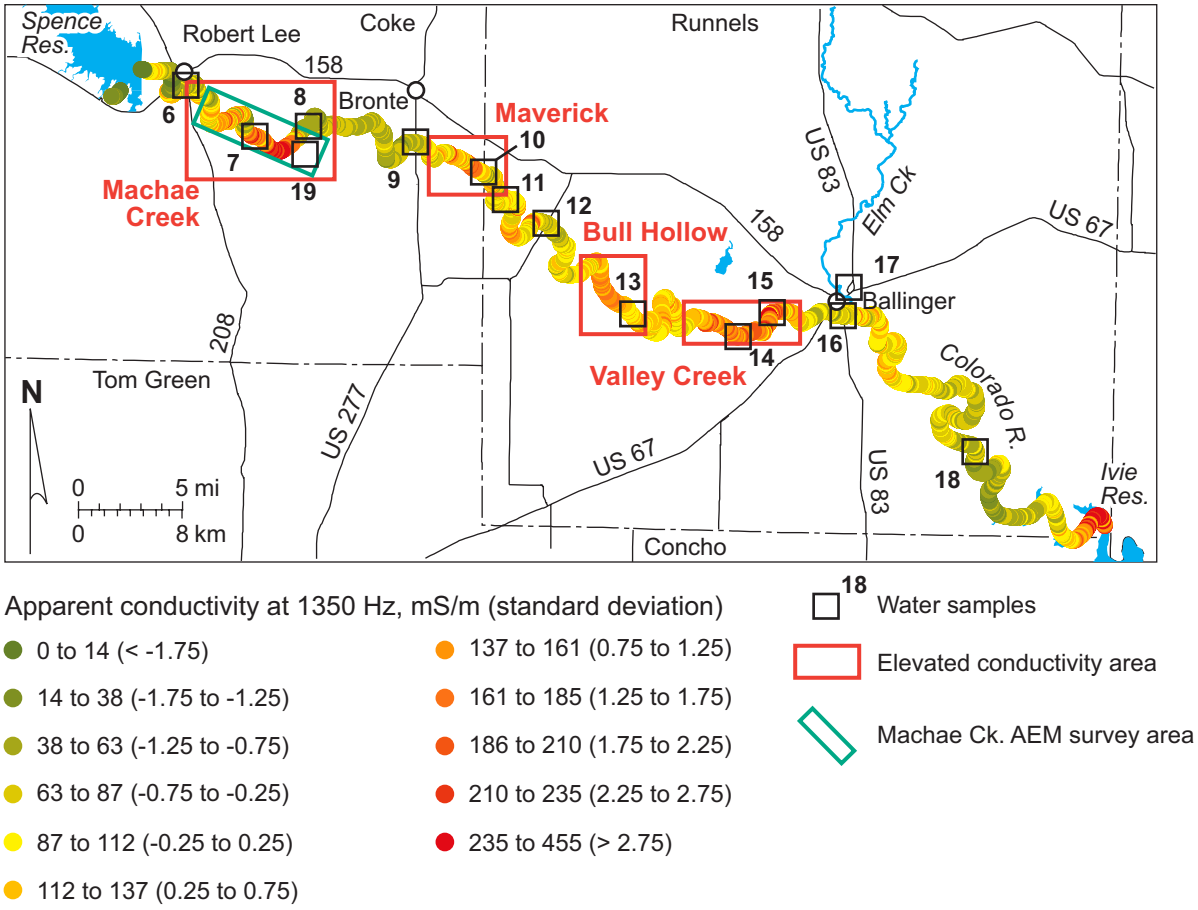

Figure 32. Apparent conductivity (colored dots) measured at 1350 Hz along the axis of the Colorado River between Spence and Ivie Reservoirs. Also shown are the Machae Creek, Maverick, Bull Hollow, and Valley Creek high-conductivity areas (red rectangles) and Colorado River area surface- and produced-water sampling sites (appendix C). The 1350-Hz frequency explores from the land surface to an average depth of about 43 m, estimated from average conductivity measured at this frequency along the Colorado River below Spence Reservoir (table 5).

Colorado River upstream from Spence Reservoir, confirming reconnaissance results from ground-based measurements. With the exception of the highest (shallowest-exploring) frequency, average apparent conductivities increase with exploration depth from a low of 43 mS/m measured at 12,810 Hz to a high of 195 mS/m at 450 Hz (table 5). This general trend of downward-increasing conductivity suggests that ground-water salinity increases with depth within the exploration range of this instrument, implying general upward-migration of saline ground water toward discharge areas along the river. High average conductivities at the highest frequency are likely to be responding to surface- and near-surface salinization caused by concentration of dissolved solids through evaporation, plant activity, and near-surface discharge of saline water from natural and oil-field sources.

Apparent conductivity trends plotted from the multi-frequency data acquired along the Colorado River axis allow delineation of four areas of generally elevated apparent ground conductivity (figs. 32 to 34). From upstream to downstream, these include (1) the Machae Creek area near Robert Lee, the Maverick area near Bronte, the Bull Hollow area below FM 3115, and the Valley Creek area between FM 2111 and Ballinger. These areas enclose the stream segments most likely to be receiving significant amounts of saline ground water that degrades Colorado River water quality.

Machae Creek Area

The Machae Creek area is the most upstream conductive river reach within segment 1426 (figs. 32 to 34). It begins about 2.4 km below the Texas 208 bridge at Robert Lee and extends downstream a total river length of 12.4 km (about 2 to 15 km, fig. 35). Several intermittent streams intersect the Colorado River along this segment, including Jack Miles, Machae, Buffalo, and Indian creeks. The river flows adjacent to the Wendkirk Oil Field at the downstream end of the segment. In the Machae Creek area, the Colorado River cuts the lower Blaine and upper San Angelo Formations (figs. 2 and 4). Blaine deposits, commonly thin-bedded, consist of shale, sandstone, gypsum, and dolomite. The San Angelo Formation is sandstone, shale, and conglomerate. A study of the surface geology by Beede and Bentley (1918) shows that the western part of this area contains interbedded shale and sandstone, and

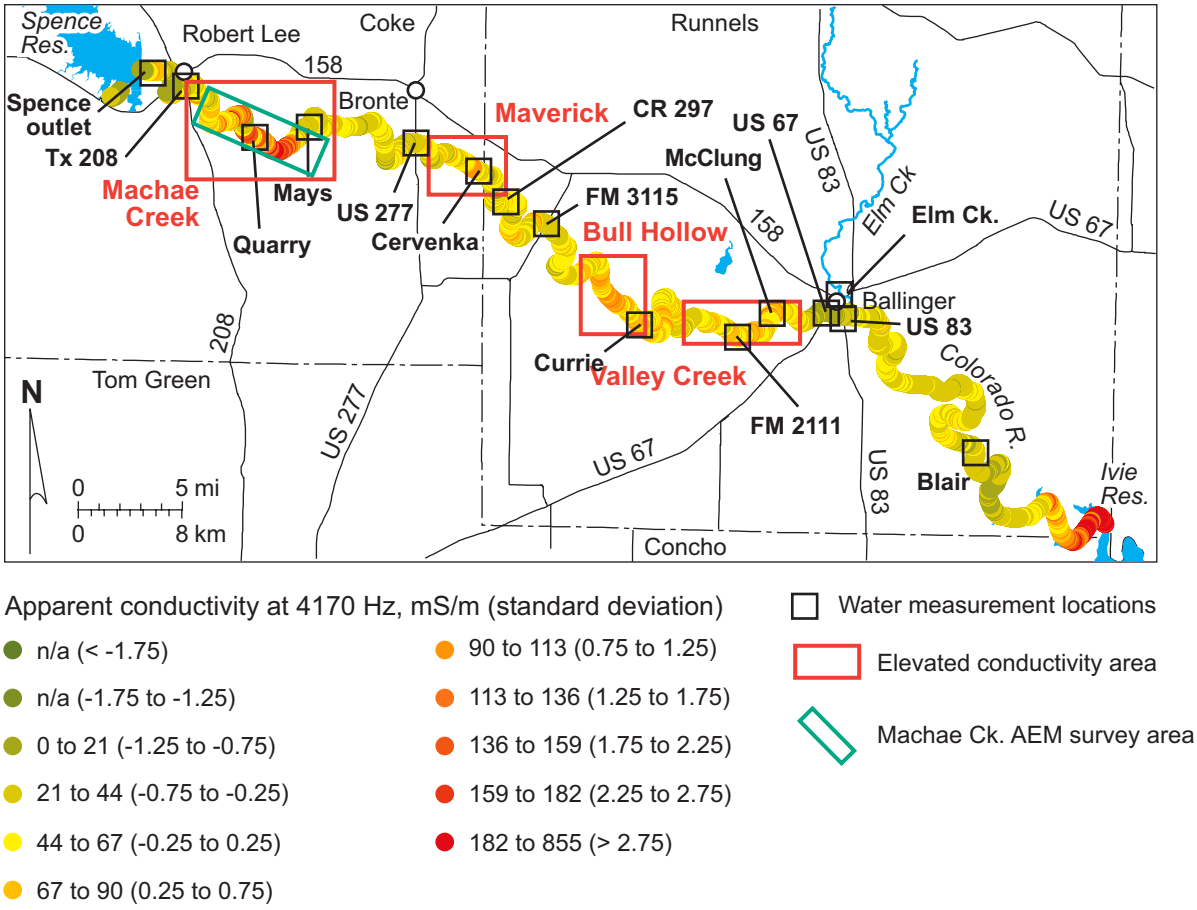

Figure 33. Apparent conductivity (colored dots) measured at 4170 Hz along the axis of the Colorado River between Spence and Ivie Reservoirs. Also shown are the Machae Creek, Maverick, Bull Hollow, and Valley Creek high-conductivity areas (red rectangles) and the names of Colorado River water-measurement sites. The 4170-Hz frequency explores from the land surface to an average depth of about 33 m, estimated from average conductivity measured at this frequency along the Colorado River below Spence Reservoir (table 5).

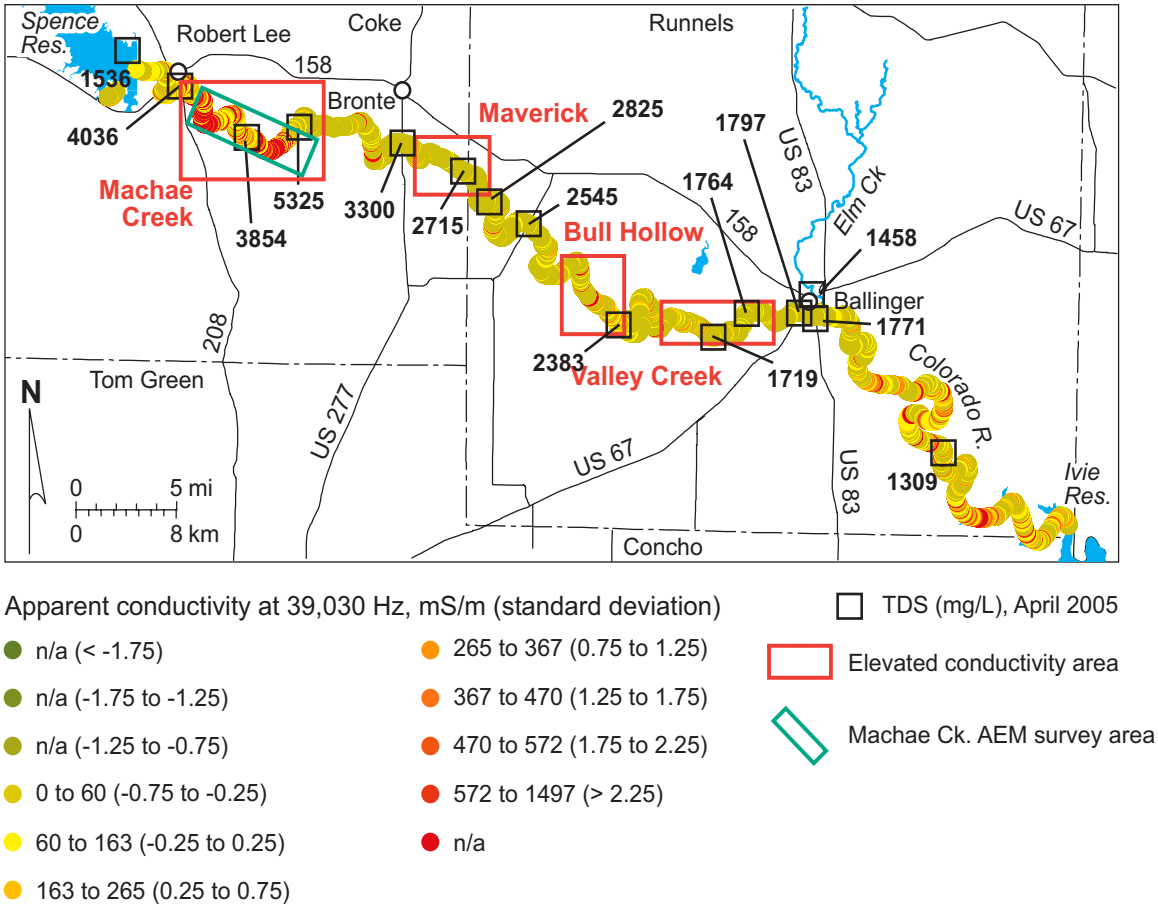

Figure 34. Apparent conductivity (colored dots) measured at 39,030 Hz along the axis of the Colorado River between Spence and Ivie Reservoirs. Also shown are the Machae Creek, Maverick, Bull Hollow, and Valley Creek high-conductivity areas (red rectangles) and Colorado River TDS concentrations measured in April 2005. The 39,030-Hz frequency explores from the land surface to an average depth of about 8 m, estimated from average conductivity measured at this frequency along the Colorado River below Spence Reservoir (table 5).

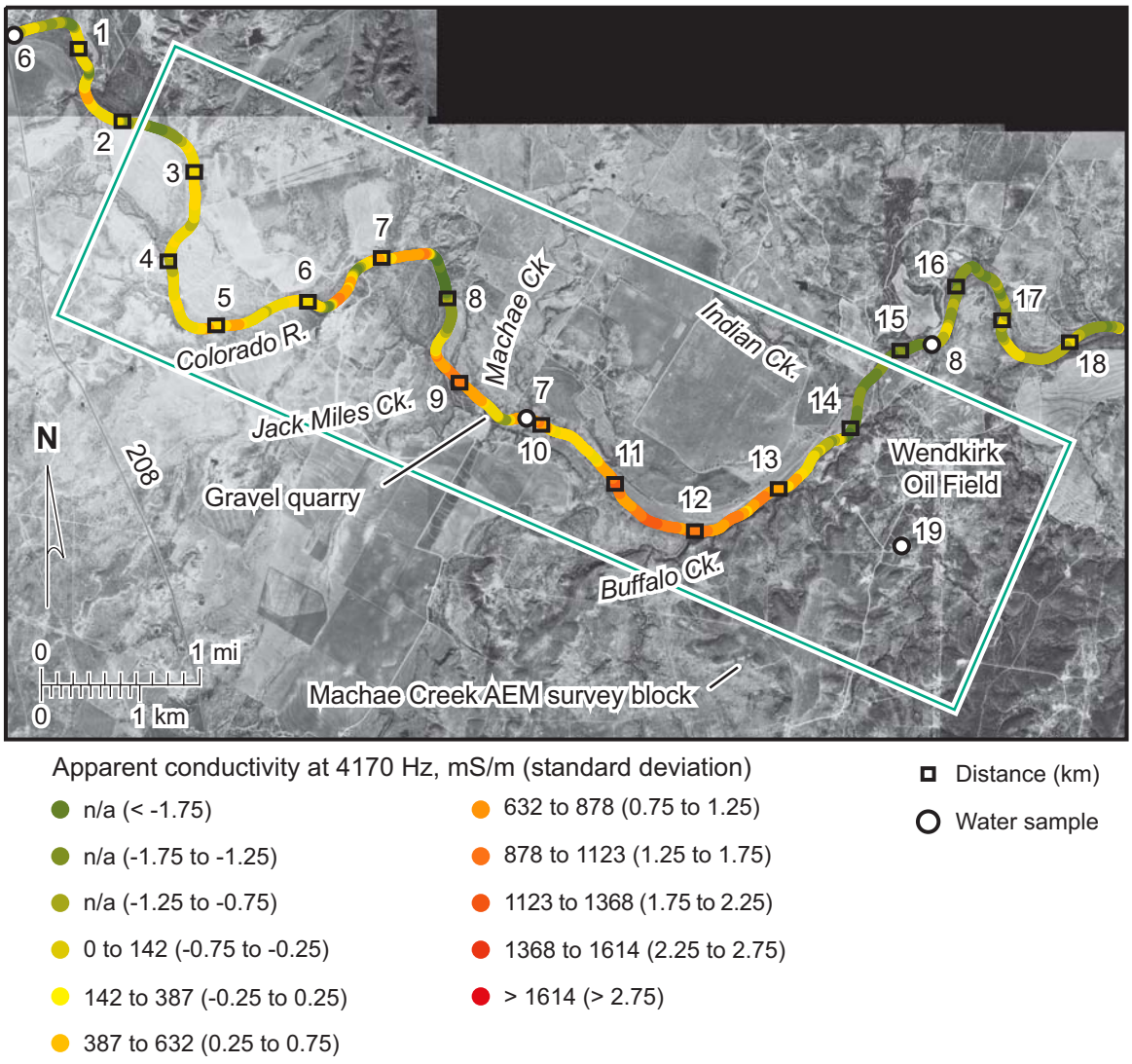

Figure 35. Map of the Machae Creek area depicting apparent conductivity measured at 4170 Hz during the airborne geophysical survey (colored dots). The numbered points are the distance (in km) along the stream segment. The 4170-Hz frequency explores from the land surface to an average depth of about 33 m, estimated from average conductivity measured at this frequency along the Colorado River below Spence Reservoir (table 5).

lesser gypsum beds (fig. 36). The eastern part of this area is within sandstone, conglomerate, and lesser shale. Bedrock units at the surface in the Machae Creek area lie at depths of about 500 to 600 ft (152 to 183 m) at the Seaboard Oil Company-Marvin Simpson No. 1 well, located about 14 km west of the study segment. The geophysical log for this well, reflecting some of the physical properties of the Blaine and San Angelo deposits, shows resistivity to be generally low (high conductivity) for rocks approximately equivalent to the surface deposits (fig. 37).

Elevated apparent conductivities in this area appear in both the shallowest-exploring frequency (39,030 Hz) and the two deepest-exploring frequencies (450 and 1350 Hz). At the highest frequencies, elevated conductivities are found between 2 and 5 km at the upstream end of the segment and between about 10 and 14 km at the downstream end (fig. 35). These include areas where we found evidence of near-surface salinization during ground-based studies, and likely represent near-surface accumulations of saline pore water from local sources. Elevated conductivities evident in deeper, low-frequency data between about 9 and 14 km downstream (fig. 38) suggest that this is an area where saline ground water may contribute to degradation of surface-water quality.

We used airborne survey results to identify the high-conductivity segments and choose follow-up water measurement and sampling sites (figs. 32 to 34). We combined these data with sampling and analysis done by CRMWD to estimate salinity loading along these segments. Considering data from early April 2005, we estimate an incoming flow of 0.56 ft^3 to the Machae Creek area at the Texas 208 bridge and an outgoing flow of about 1.16 ft^3 near the Double Barrel Road crossing. We measured an increase in stream salinity from 4036 mg/L at Texas 208 to 5325 mg/L at Mays Ranch. Combining flow and TDS concentrations at these sites translates to an increase in TDS load across the Machae Creek from 5517 kg/day at Texas 208 to 15,145 kg/day at Mays Ranch, a total increase of about 9600 kg/day under these flow conditions (fig. 39; table 6).

Major-ion concentrations for upstream (location 6, figs. 32 and 35; appendix C) and downstream (location 8) Colorado River water samples depict proportionally large increases in sodium and chloride concentrations and a smaller increase in sulfate concentrations (fig. 40). Combining these concentrations with stream flow yields a chloride load increase of 3830 kg/day (table 6) that is more than twice the

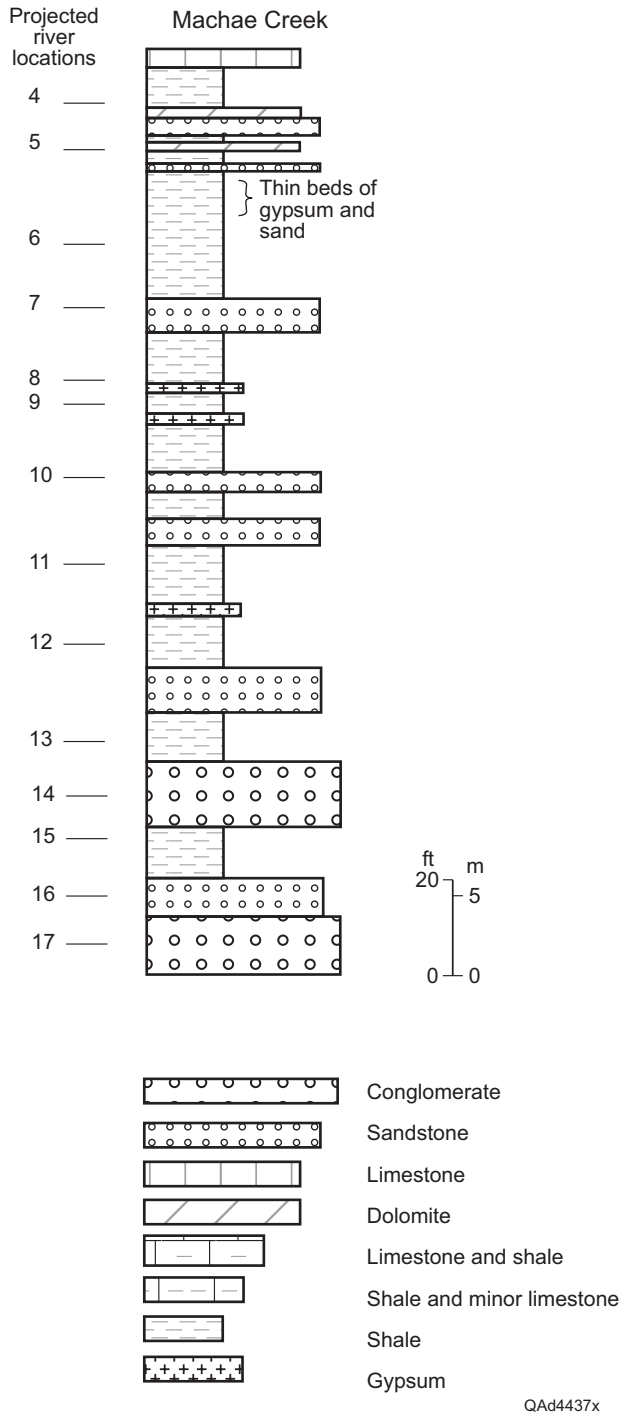

Figure 36. Stratigraphic section illustrating rock types of the Machae Creek area. Numbers correspond to positions along the river shown in fig. 35. Lithologic data from Beede and Bentley (1918).

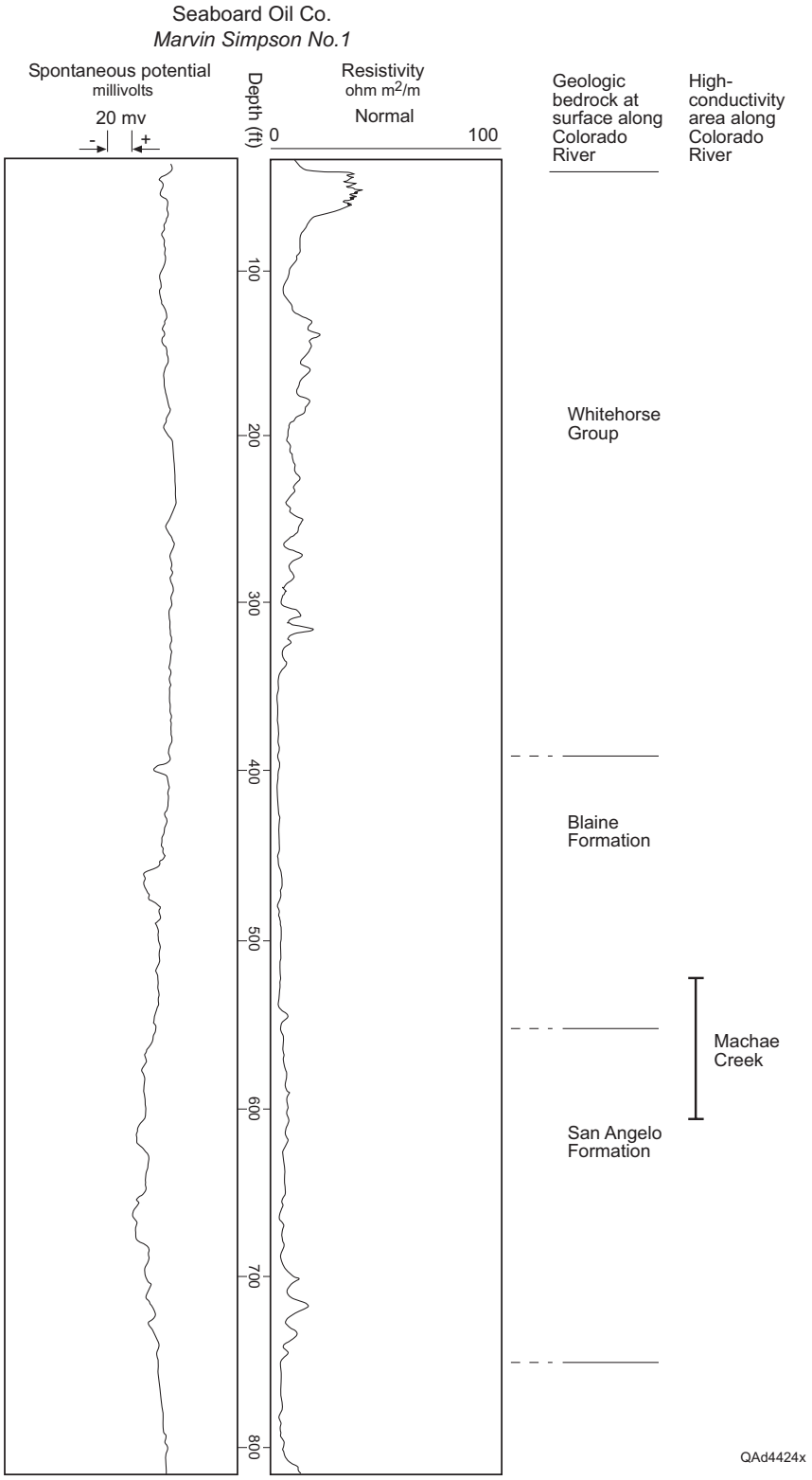

Figure 37. Geophysical log of the Seaboard Oil Company-Marvin Simpson No.1 well illustrating the resistivity log pattern for subsurface rocks that are approximately equivalent to the surface geologic deposits at the Machae Creek area.

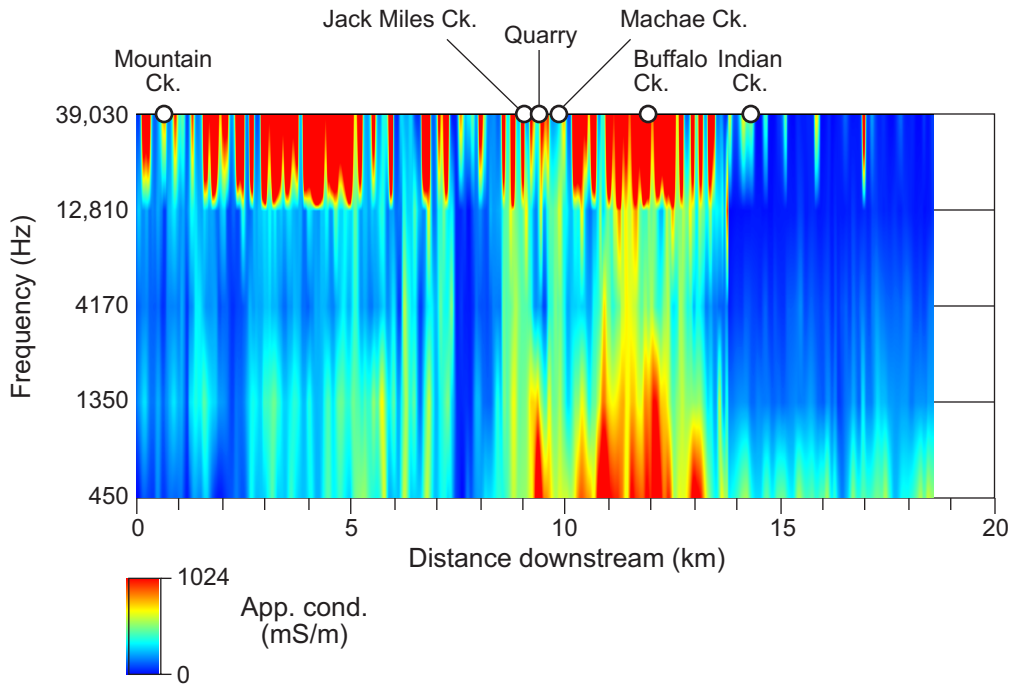

Figure 38. Combined apparent conductivity pseudosection along the Machae Creek segment from all frequencies acquired during the airborne geophysical survey. The shallowest-exploring frequency is along the top of the image and the deepest-exploring frequency is along the bottom.

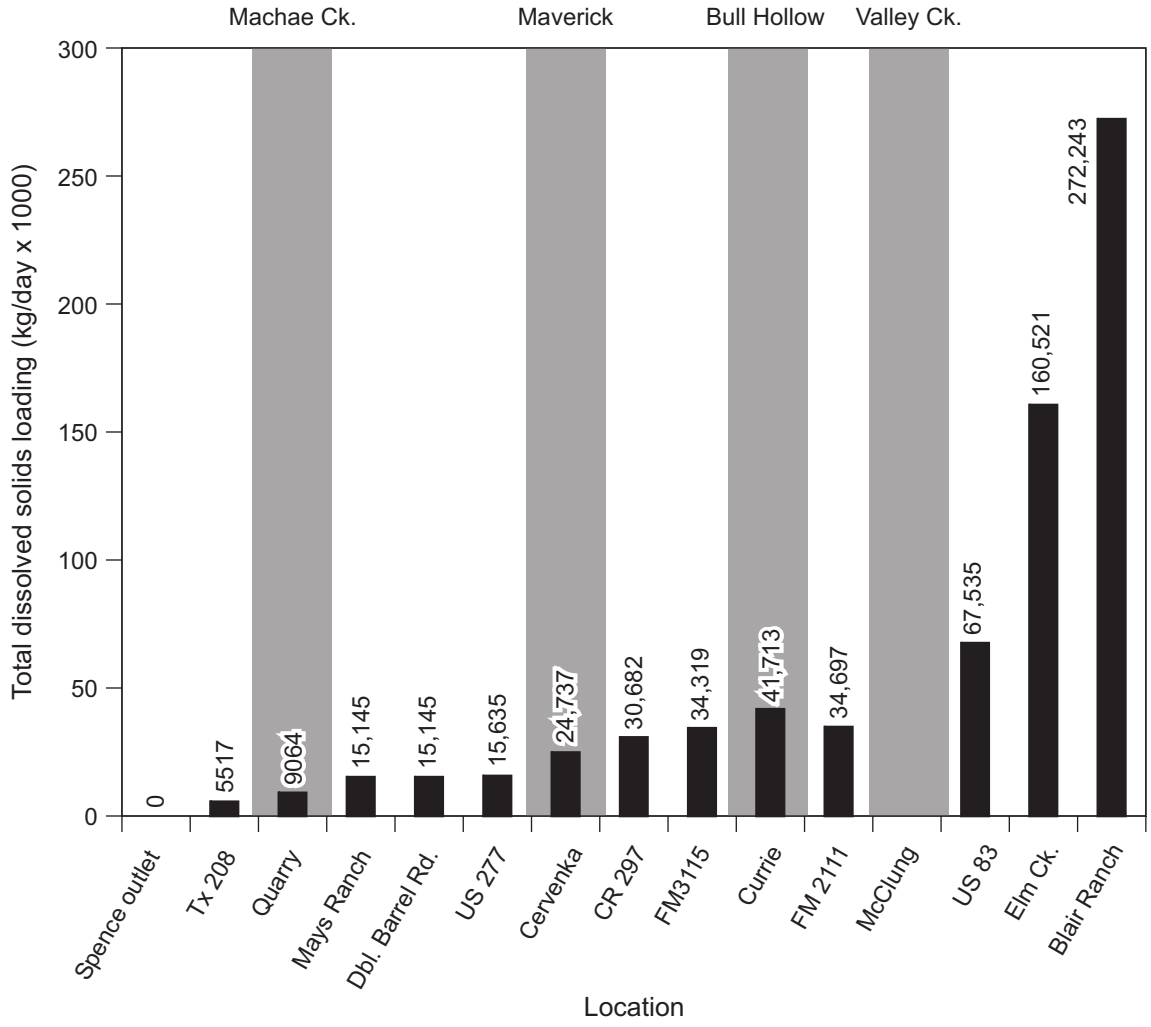

Figure 39. Colorado River TDS loading estimates for the Machae Creek, Maverick, Bull Hollow, and Valley Creek high-conductiviy areas. Estimates are based on April 2005 streamflow measured by CRMWD and salinity concentrations measured by the Bureau.

Table 6. Estimated Colorado River TDS, chloride, and sulfate loading changes for at the Machae Creek, Maverick, Bull Hollow, and Valley Creek high-conducitivity areas. Estimates based on April 2005 flow and water-quality data. Flow data provided by CRMWD. Station numbers represent CRMWD monitoring sites. Asterisk denotes an interpolated flow measurement from the two nearest CRMWD sites.

Location	**TDS (kg/day)**	**Chloride (kg/day)**	**Sulfate (kg/day)**
Machae Creek area			
Incoming(station 18338, S. H. 208)	5517	2057	1177
Outgoing (station 16900, Double Barrel Road)	15,145	5887	2929
Change	+ 9628	+ 3830	+ 1752
Maverick area			
Incoming (station 12432, U.S. 277)	15,635	4918	4785
Outgoing (Cervenka Ranch)*	24,737	5804	10,843
Change	+ 9102	+ 886	+ 6058
Bull Hollow area			
Incoming (station 16901, FM 3115)	34,319	8617	13,094
Outgoing (Currie Ranch)*	41,713	11,115	14,844
Change	+ 7394	+ 2498	+ 1750
Valley Creek area			
Incoming (station 13651, FM 2111)	34,697	7731	12,292
Outgoing (McClung property)*	45,104	9537	17,515
Change	+ 10,407	+ 1806	+ 5223

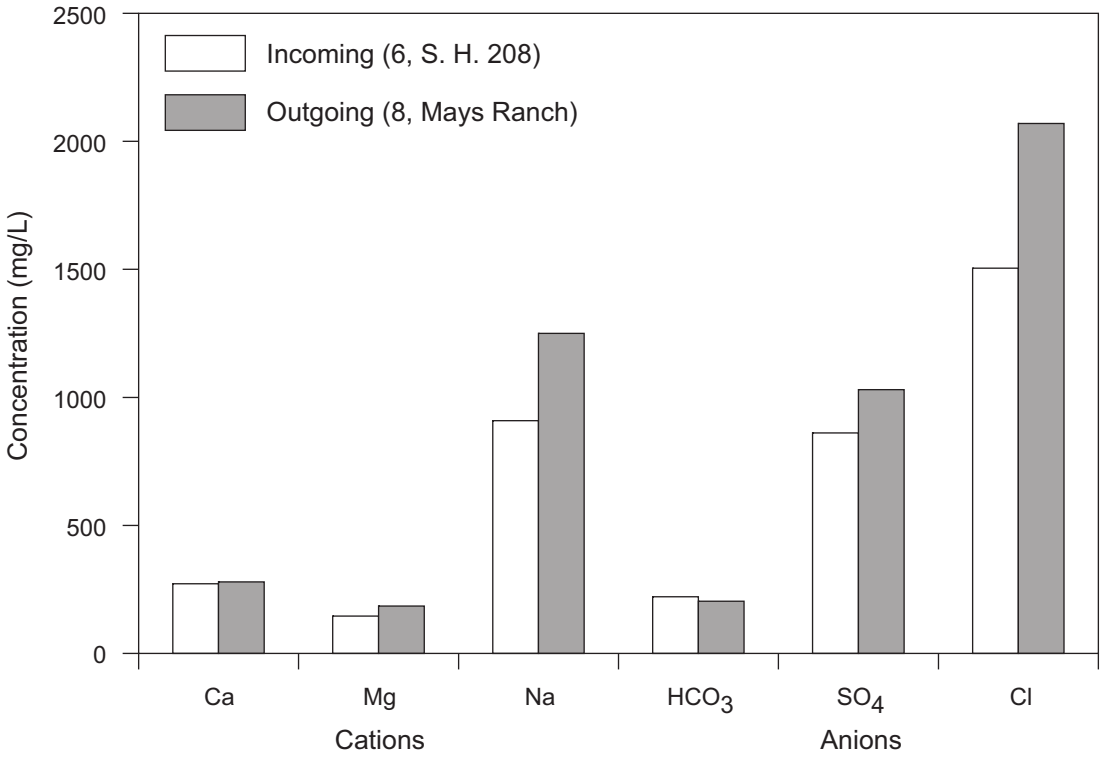

Figure 40. Major-ion concentrations in Colorado River samples taken upstream (incoming, location 6, figs. 32 and 35) and downstream (outgoing, location 8) from the Machae Creek high-conductivity area in April 2005 (appendix C).

sulfate load increase of 1752 kg/day. These concentration and loading changes are consistent with an increase in river salinity dominated by baseflow contributions to the river. Shallow, naturally saline ground water that contributes to stream flow has been relatively enriched in chloride that is likely to be caused by infiltration of produced water from the adjacent Wendkirk Oil Field.

Chemical analyses of subsurface brine produced from the Wendkirk Oil Field (location 19, figs. 32 and 35; appendix C) allow examination of whether the chemical characteristics of elevated-salinity Colorado River water flowing out of the Machae Creek area are consistent with the addition of local produced water to the river. Conservative mixing models use the high solubility of chloride and bromide to demonstrate the potential that water samples with significant differences in salinity have mixed to produce water of intermediate salinities. Chloride and bromide are conservative in that they tend to remain in solution while other common ionic species (Ca^{2+}, Mg^{2+}, Na^{+}, HCO_3^{-}, and SO_4^{2-}) are more prone to participate in chemical reactions or other complexing behavior that affect their concentration in solutions through precipitation as solids or absorption to electrically charged particulate matter (such as clay). The concentration of nonconservative ionic species in a mixture may not be the simple sum of the relative contributions from each of the end-member waters, but the concentration of conservative species will more faithfully reflect the proportions of the component end-members.

Using new and previously existing chloride and bromide analyses, we constructed chemical models (fig. 41) that mixed varying proportions of Wendkirk produced water with shallow groundwater from a nearby water well (well 43-16-603; Slade and Buszka, 1994). Mixing lines from these two end members pass near or through the concentrations analyzed for the Colorado River sample downstream from the Machae Creek area (location 8), representing a mixture of 99.3 percent groundwater and 0.7 percent produced water. This mixing line also passes through one of the analyses reported for a spring along the Colorado River just downstream from the Wendkirk Oil Field (spring 43-14-102; Slade and Buzka, 1994). This supports the proposition that the composition of the Colorado River at location 8 and that of water sampled at the spring downstream from the Wendkirk Oil Field is consistent with mixing between water similar to that sampled from well 43-13-603 and water similar to the Wendkirk brine sample. Further, the separate mixing model curve that fits river samples at locations 6, 7, and 8

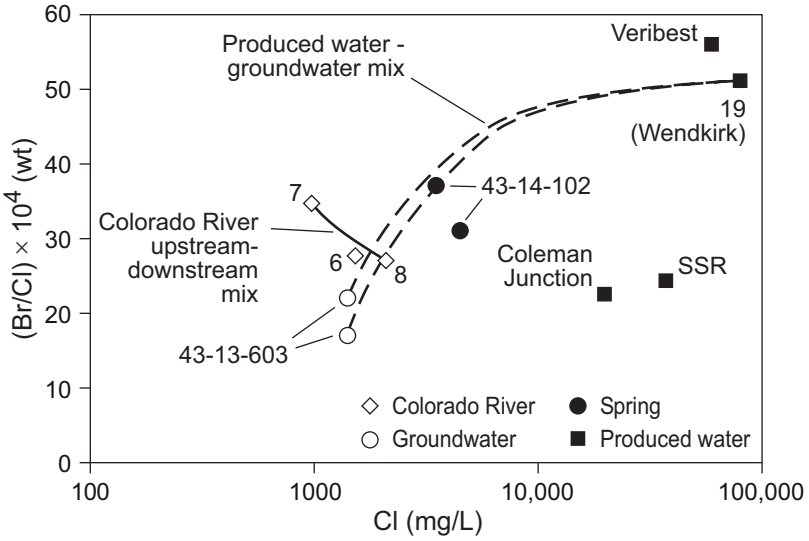

Figure 41. Bromide/chloride ratios (by weight) for Colorado River, groundwater, and produced water samples from the Machae Creek area. The solid line represents a mixture between Colorado River water upstream (location 7, fig. 35) and downstream (location 8) from the Wendkirk Oil Field. The dashed lines represent a mixture between produced water sampled from the Wendkirk Oil Field (location 19) and two separate analyses of groundwater sampled from a nearby water well (well 43-13-603; Slade and Buzska, 1994). Also shown are bromide/chloride ratios for samples from (a) a spring located downstream from the Wendkirk Oil Field, and (b) other produced waters in the area (Slade and Buzka, 1994).

(figs. 35 and 41) intersects the groundwater and produced water mixing curve at sample 8, supporting the proposition that sample 8 is a mixture between upstream water and a separate mixture of produced brine and local groundwater.

Maverick Area

The Maverick high-conductivity area begins about 1 km below the U.S. 277 bridge near Bronte and extends downstream a total creek length of about 8.3 km (figs. 32 and 42). Hog Creek, a small intermittent drainage, intersects the Colorado at the downstream end of the Maverick segment. The segment is within the upper part of the Clear Fork Group, which comprises shale, dolomite, limestone, and some gypsum (figs. 2 and 3). Sand, clay, and gravel terrace deposits lie adjacent to the river. Outcrop descriptions by Beede and Waite (1918) indicate that the river intersects shale and some dolomite beds across the Maverick segment (fig. 43). Deposits at the eastern downstream end of the study area were concealed from the early workers. Dolomite and shale that outcrop east of this study segment gently dip westward and are 12 to 35 m beneath the river across the Maverick area. Surface deposits of the Maverick area lie at depths of about 250 to 300 ft (76 to 91 m) at the Ambassador Oil Corporation-J. R. Smith No. 1 well, located about 12 km west of the study segment. The geophysical log for this well, reflecting the properties of Clear Fork deposits, shows resistivity increasing at rocks approximately equivalent to the deposits at the eastern part of the Maverick study segment and downstream (fig. 44).

Apparent conductivity measurements superimposed on maps of the Maverick area show little evidence of elevated salinity at the highest and shallowest-exploring frequencies (12,810 and 39,030 Hz). Hog Creek is not associated with a high-frequency conductivity anomaly, suggesting there is no near-surface salinization associated with this Colorado tributary. Higher apparent ground conductivities are evident on the maps and sections at lower frequencies and greater exploration depths (450, 1350, and 4170 Hz), particularly from 2 to 5 km and from 6 to 8 km downstream from the beginning of the segment (figs. 42 and 45). Increasing apparent conductivities with increasing exploration depth along

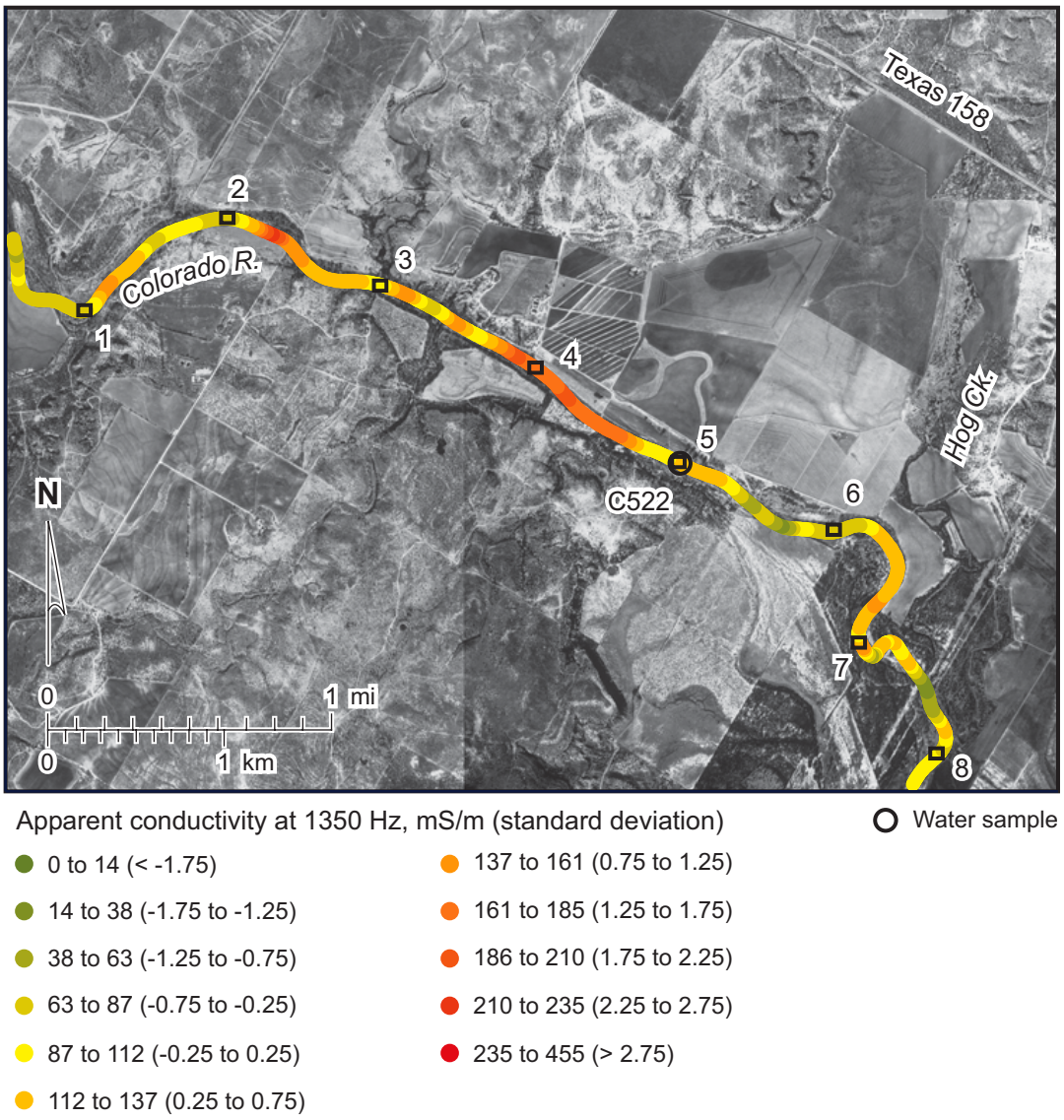

Figure 42. Map of the Maverick area depicting apparent conductivity measured at 1350 Hz during the airborne geophysical survey (colored dots). The numbered points are the distance (in km) along the stream segment. The 1350-Hz frequency explores from the land surface to an average depth of about 43 m, estimated from average conductivity measured at this frequency along the Colorado River below Spence Reservoir (table 5) .

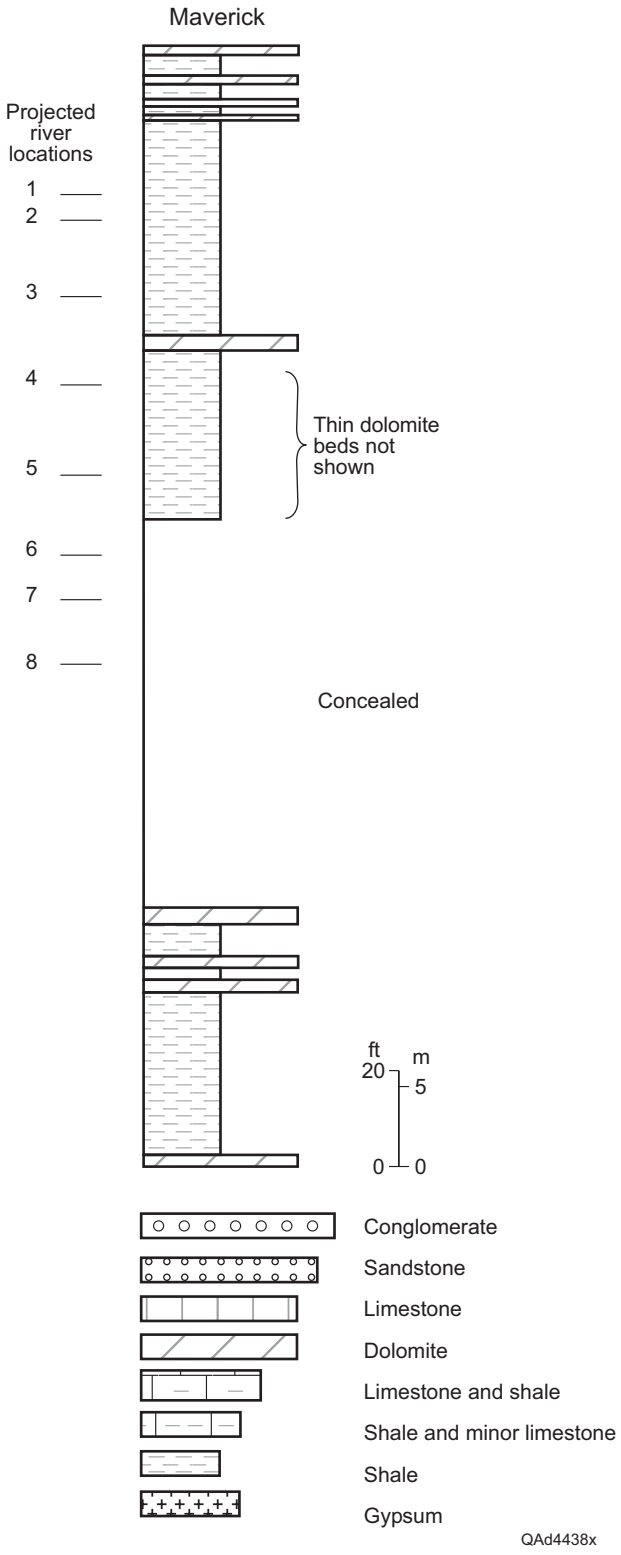

Figure 43. Stratigraphic section illustrating rock types of the Maverick study area. Numbers correspond to positions along the river shown in fig. 42. Lithologic data from Beede and Waite (1918).

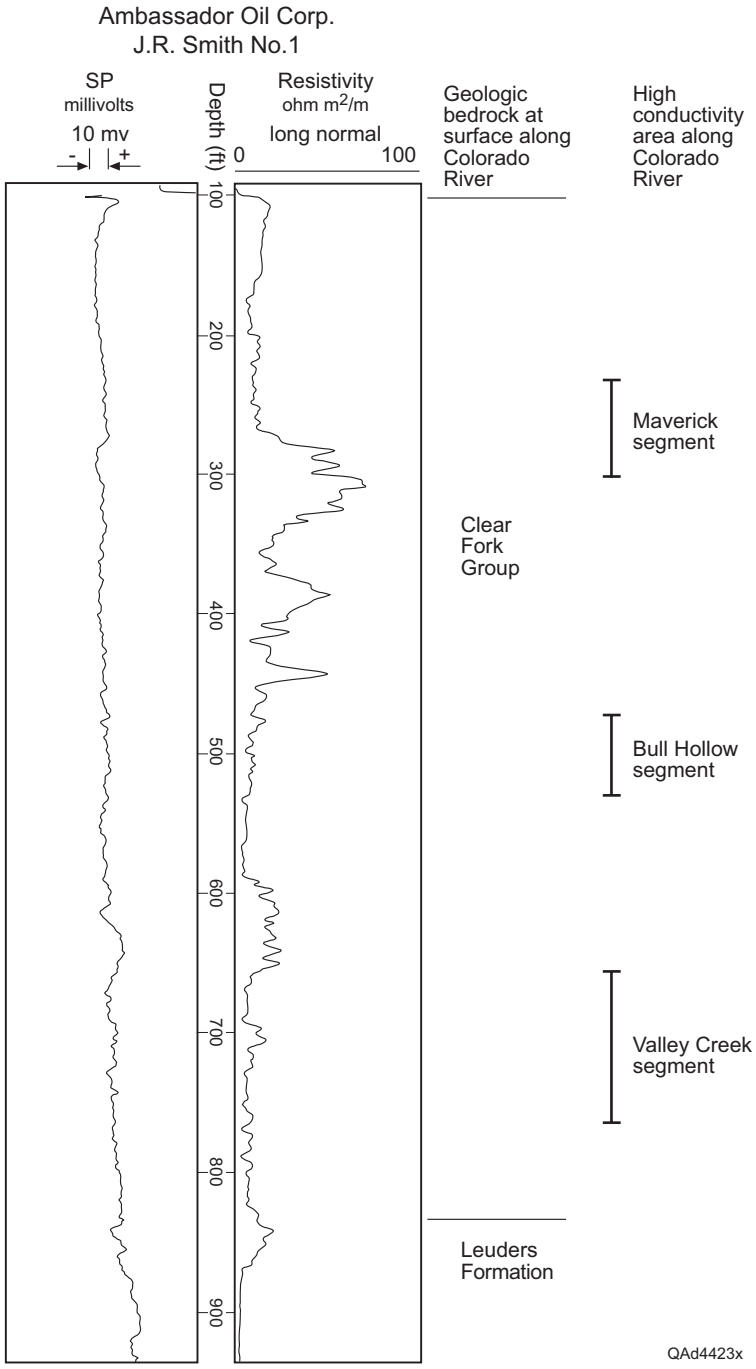

Figure 44. Geophysical log of the Ambassador Oil Corporation-J. R. Smith No. 1 well illustrating the resistivity log pattern for subsurface rocks that are approximately equivalent to the surface geologic deposits at the Maverick, Bull Hollow, and Valley Creek areas.

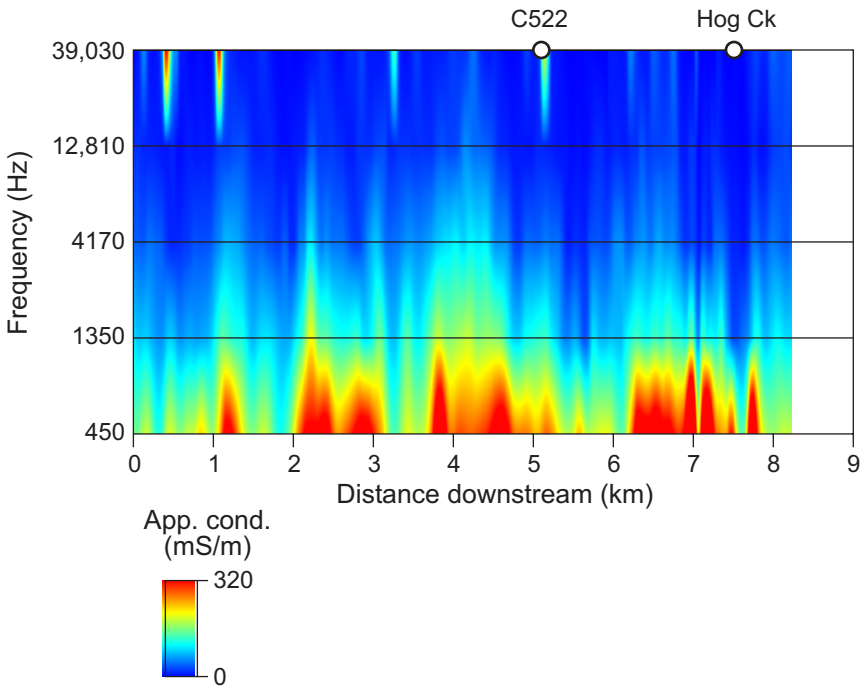

Figure 45. Combined apparent conductivity pseudosection along the Maverick segment from all frequencies acquired during the airborne geophysical survey. The shallowest-exploring frequency is along the top of the image and the deepest-exploring frequency is along the bottom.

these segments, combined with little evidence of elevated conductivities associated with surface salinization, suggest that increases in salinity loading along this segment arise from baseflow contributions.

Combined CRMWD and Bureau surface-water measurements show evidence of an increase in salinity loading along this segment (fig. 39). Colorado River TDS concentrations in early April 2005 fell from 3300 mg/L at the U.S. 277 bridge just upstream from the Maverick segment to 2715 mg/L at the Cervenka ranch located about 5 km from the beginning of the segment, then rose to 2825 mg/L at Runnels County Road 297 less than 2 km downstream from the end of the segment (fig. 34). Estimated flow increased downstream from 1.94 ft^3 at U.S. 277 to 4.44 ft^3 at County Road 297, translating to an increase in TDS load from 8234 kg/day at U.S. 277 to 30,682 kg/day at Country Road 297, nearly quadrupling the total load.

Major-ion concentrations determined from an upstream sample at U.S. 277 (location 9, fig. 32) and a downstream sample at the Cervenka ranch (location 10) show a downstream decrease in sodium and chloride concentrations accompanying an increase in sulfate and calcium concentrations (fig. 46). Combined with flow, chloride load increased less than 900 kg/day while sulfate load increased more than 6000 kg/day along the Maverick segment (table 6). We conclude that the significant increase in salinity load observed along the Maverick segment arises mostly from sulfate-rich baseflow contributions from ground water containing elevated concentrations of constituents naturally dissolved from Permian evaporite strata.

Bull Hollow Area

The Bull Hollow area encloses an 8.6-km-long river segment of generally elevated apparent ground conductivity that extends downstream from a point about 6 km downstream from the FM 3115 bridge (figs. 32 and 47). Two small, intermittent streams, Mesquite Creek and Bull Hollow, intersect the Colorado near the upstream end of this segment. Antelope Creek, another small intermittent drainage, intersects the river at the downstream end of the segment. The river cuts the middle part of the Clear Fork Group at the Bull Hollow area (figs. 2 and 4). Near the river, terrace deposits comprising sand,

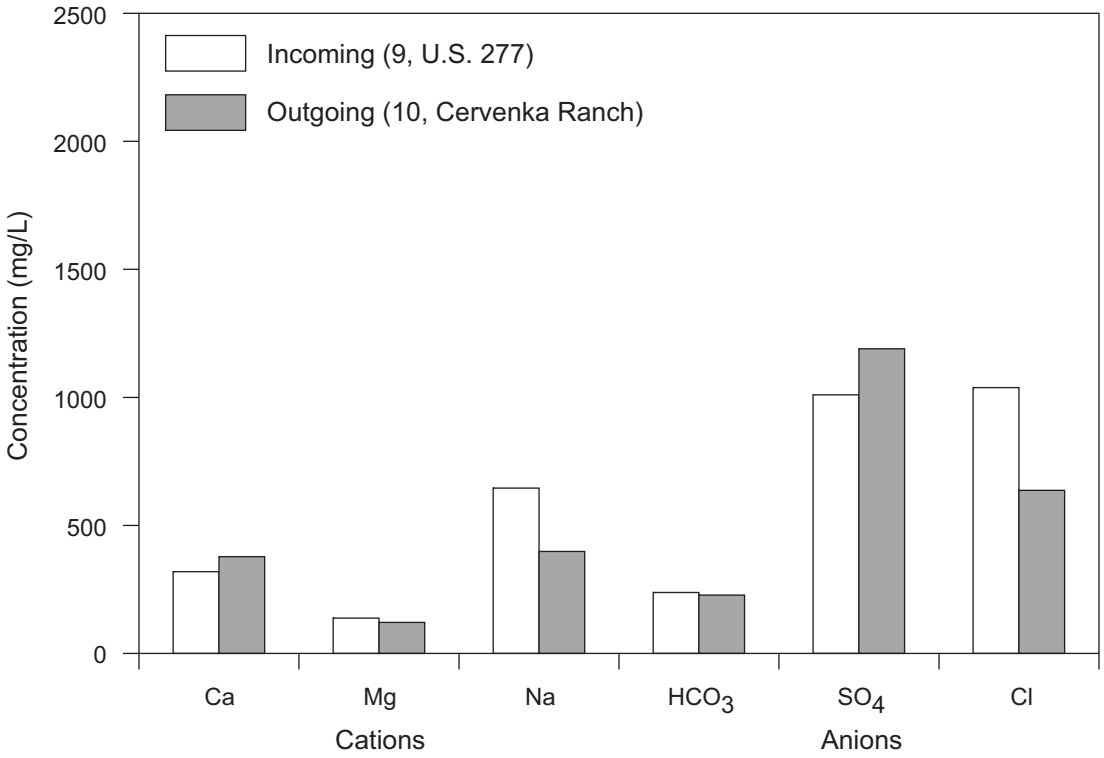

Figure 46. Major-ion concentrations in Colorado River samples taken upstream (incoming, location 9, fig. 32) and downstream (outgoing, location 10) from the Maverick high-conductivity area in April 2005 (appendix C).

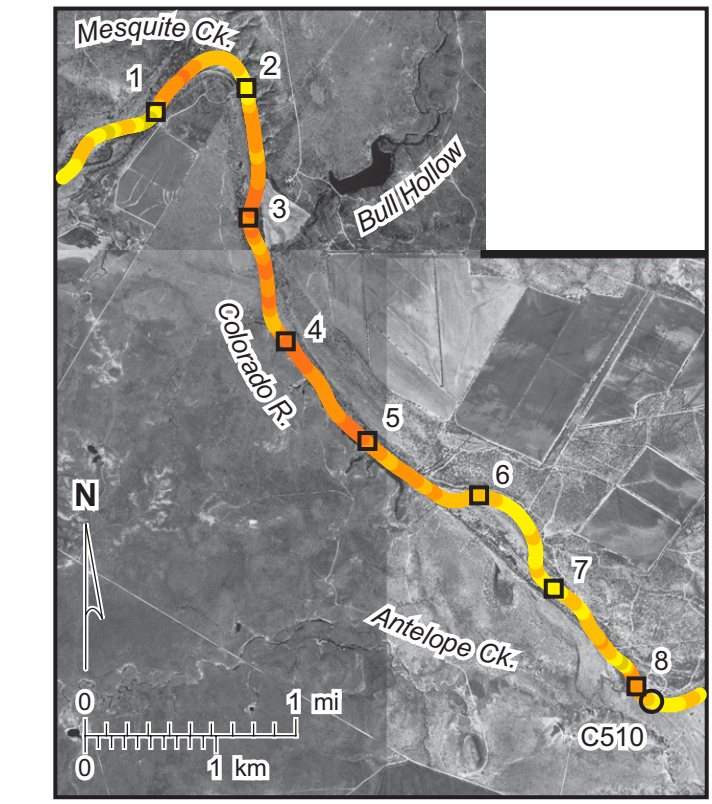

Figure 47. Map of the Bull Hollow area depicting apparent conductivity measured at 1350 Hz during the airborne geophysical survey (colored dots). The numbered points are the distance (in km) along the stream segment. The 1350-Hz frequency explores from the land surface to an average depth of about 43 m, estimated from average conductivity measured at this frequency along the Colorado River below Spence Reservoir (table 5).

clay, and gravel overlie bedrock. Bedrock strata (Beede and Waite, 1918) are mostly shale and some dolomite and limestone (fig. 48). Surface deposits of the Bull Hollow area lie at depths of about 450 to 500 ft (137 to 152 m) at the Ambassador Oil Corporation-J. R. Smith No. 1 well, located about 28 km west of the study segment. The geophysical log for this well, reflecting the properties of Clear Fork deposits, shows resistivity to be generally low for rocks that are approximately equivalent to the surface deposits of the Bull Hollow area (fig. 44).

At high, shallow-exploring frequencies, elevated apparent conductivities were measured in several local areas between Mesquite and Antelope Creeks that may indicate local shallow salinization (fig. 49). High apparent conductivities are more extensive at lower frequencies and deeper exploration depths, particularly at 4170 Hz and lower. At these frequencies, elevated conductivities are observed along most (about 1 to 8 km) of the Bull Hollow segment. Increases in salinity loading within the Bull Hollow area are thus likely to be dominantly caused by baseflow contributions of saline ground water.

Salinity loading estimates for the Bull Hollow segment are hindered by limited access to the river. The closest river access upstream from the segment is at the FM 3115 bridge, where we used early April flow (5.51 ft^3) and TDS concentration (2545 mg/l, fig. 34) to estimate an incoming TDS load of 34,319 kg/day (fig. 39; table 6). TDS at the Currie site, located within about 0.5 km of the end of the segment, was slightly lower at 2383 mg/L. Using an estimated flow at this site of 7.15 ft^3, we estimate an outgoing TDS load of 41,713 kg/day, and increase of more than 7,000 kg/day.

Major-ion concentrations are similar upstream (location 12, fig. 32) and downstream (location 13) from the Bull Hollow segment (fig. 50). Sulfate concentration changes little, resulting in a 50 percent larger increase in chloride load than in sulfate load (table 6). Baseflow contributions are dominated by naturally occurring, sulfate-rich ground water, but local salinity sources are supplying relatively minor volumes of chloride-enriched water. The most likely additional salinity source is brine produced from sparse oil-field activities along this segment.

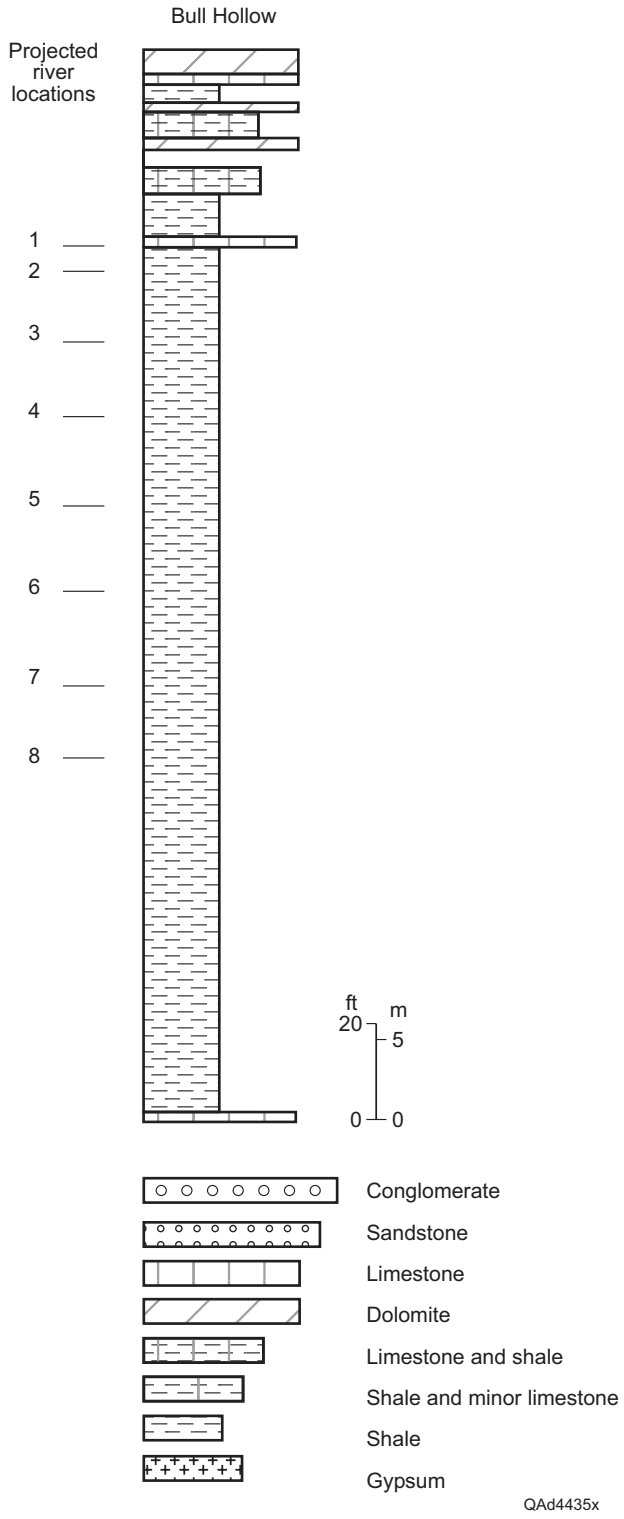

Figure 48. Stratigraphic section illustrating rock types of the Bull Hollow study area. Numbers correspond to positions along the river shown in fig. 47. Lithologic data from Beede and Waite (1918).

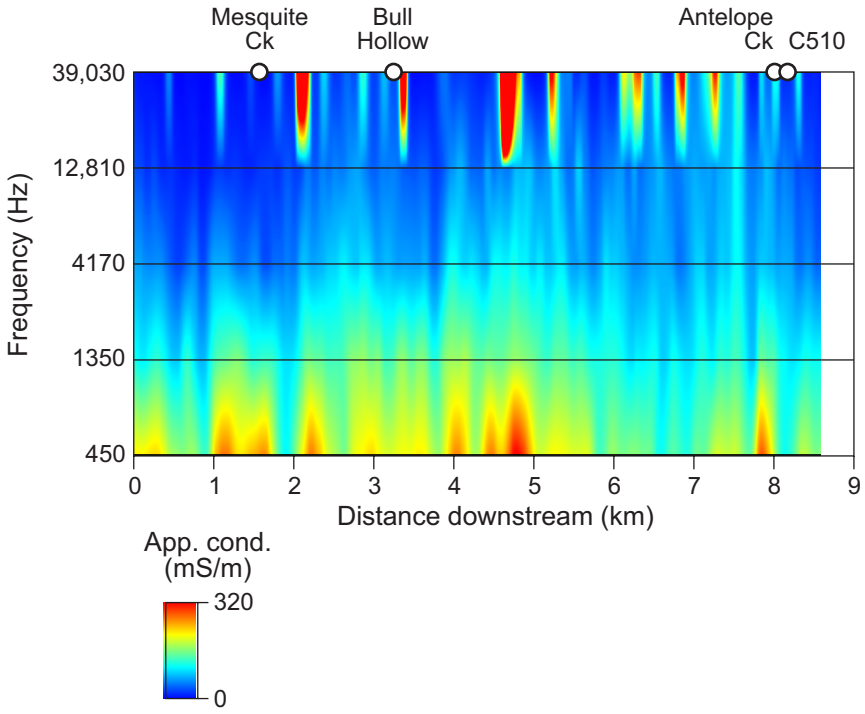

Figure 49. Combined apparent conductivity pseudosection along the Bull Hollow segment from all frequencies acquired during the airborne survey. The shallowest-exploring frequency is along the top of the image and the deepest-exploring frequency is along the bottom.

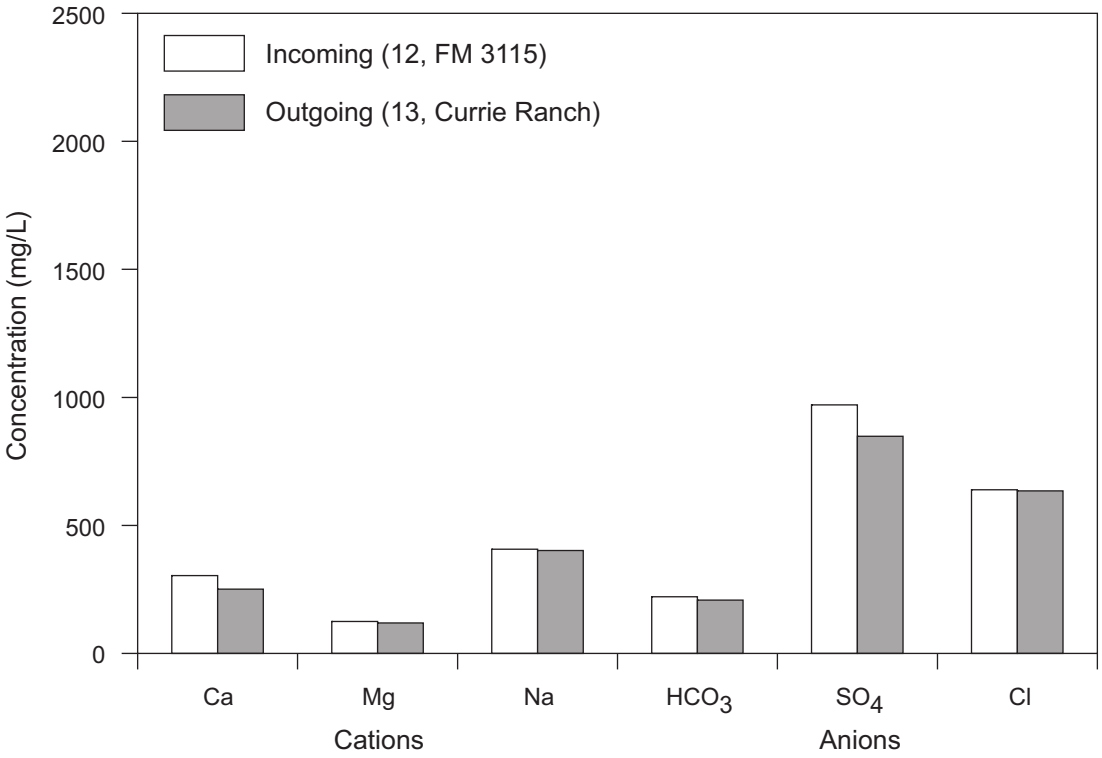

Figure 50. Major-ion concentrations in Colorado River samples taken upstream (incoming, location 12, fig. 32) and downstream (outgoing, location 13) from the Bull Hollow high-conductivity area in April 2005 (appendix C).

Valley Creek Area

The Valley Creek area is the most downstream zone of generally elevated apparent conductivity along segment 1426 (figs. 32 to 34). It is nearly 12 km long, beginning about 5 km upstream from the FM 2111 bridge and extending about 7 km downstream from that bridge toward Ballinger. Minor drainages intersecting the river along this segment include Indian and Valley creeks (fig. 51). The Valley Creek study segment is within the lower part of the Clear Fork Group. The eastern edge of the segment is at the Clear Fork Group-Leuders Formation contact. In general, bedrock consists of shale, limestone, dolomite, and gypsum (figs. 2 and 3). Terraces of sand, clay, and gravel are relatively well developed along the river at this area. Previous study of the surface geology by Beede and Waite (1918) indicate the river cuts through interbedded shale and limestone, and lesser sandstone and gypsum (fig. 52). Limestone at the east edge of the study area dips gently westward and is about 55 m beneath the river at the western margin of the area. Surface deposits of the Valley Creek area lie at depths of about 650 to 800 ft (198 to 244 m) at the Ambassador Oil Corporation-J. R. Smith No. 1 well, located about 37 km west of the study segment. The geophysical log for this well, reflecting the properties and conductivity of Clear Fork and Leuders deposits, shows relatively low resistivity for rocks approximately equivalent to those at the surface in the study area (fig. 44).

Apparent conductivity measurements show only minor, local areas of elevated ground conductivity at the shallowest-exploring frequencies (12,810 and 39,030 Hz, fig. 53), suggesting there is no pervasive shallow salinization along this segment. Apparent conductivities at lower, deeper-exploring frequencies (450, 1350, and 4170 Hz) are higher and more extensive, particularly between 2 and 10 km downstream along this segment. The positions of the Indian Creek and Valley Creek confluences appear to have no geographic relationship to the high-conductivity zones. The apparent increase in conductivity with exploration depth, the lack of elevated shallow or deep apparent conductivity associated with the minor tributaries, and the negligible flow contribution from the tributaries suggest that any increase in salinity loading along this segment is dominated by baseflow contributions.

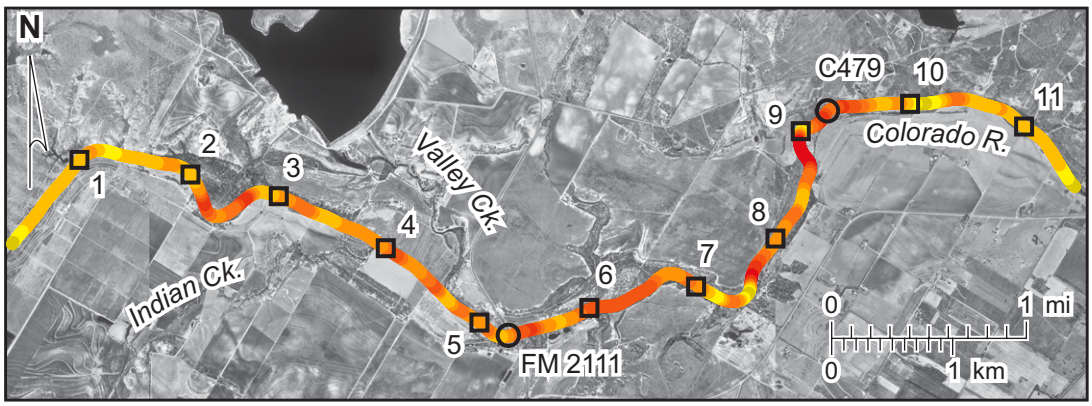

Apparent conductivity at 1350 Hz, mS/m (standard deviation)

- 0 to 14 (< -1.75)
- 14 to 38 (-1.75 to -1.25)
- 38 to 63 (-1.25 to -0.75)
- 63 to 87 (-0.75 to -0.25)
- 87 to 112 (-0.25 to 0.25)
- 112 to 137 (0.25 to 0.75)
- 137 to 161 (0.75 to 1.25)
- 161 to 185 (1.25 to 1.75)
- 186 to 210 (1.75 to 2.25)
- 210 to 235 (2.25 to 2.75)
- 235 to 455 (> 2.75)

Water sample

Figure 51. Map of the Valley Creek area depicting apparent conductivity measured at 1350 Hz during the airborne geophysical survey (colored dots). The numbered points are the distance (in km) along the stream segment. The 1350-Hz frequency explores from the land surface to an average depth of about 43 m, estimated from average conductivity measured at this frequency along the Colorado River below Spence Reservoir (table 5).

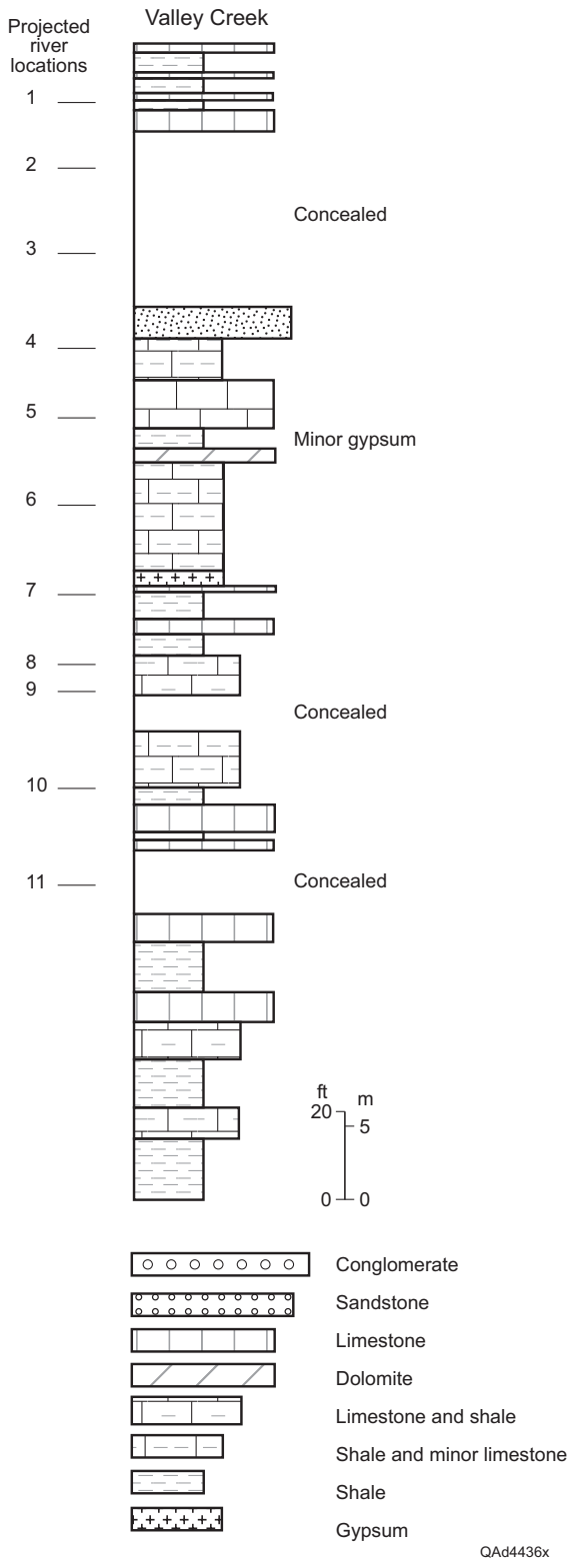

Figure 52. Stratigraphic section illustrating rock types of the Valley Creek area. Numbers correspond to positions along the river shown in fig. 51. Lithologic data from Beede and Waite (1918).

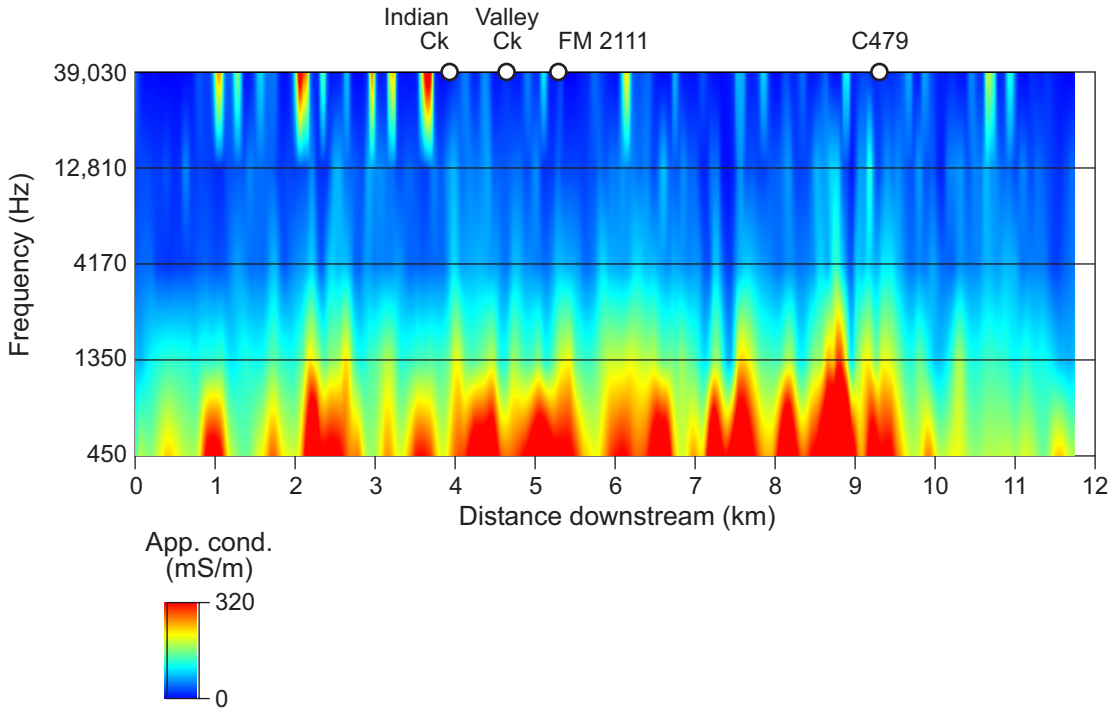

Figure 53. Combined apparent conductivity pseudosection along the Valley Creek segment from all frequencies acquired during the airborne survey. The shallowest-exploring frequency is along the top of the image and the deepest-exploring frequency is along the bottom.

Surface-water data from early April 2005 indicate lower TDS concentrations along this segment than were measured farther upstream (fig. 34). Calculated TDS concentration dropped from 2383 mg/L at the downstream end of the Bull Hollow area to 1719 mg/L at FM 2111 and 1764 mg/L at the McClung property near the downstream end of the Valley Creek segment. Using estimated flows of 8.3 ft^3 at FM 2111 and 15.6 ft^3 at the U.S. 83 bridge, we calculate an increase in TDS loading from 34,697 kg/day to 67,535 kg/day, most of which probably occurs within the eastern half of the Valley Creek segment.

Analyses of major-ion concentrations from samples taken at upstream (FM 2111, location 14, fig. 32) and downstream (location 15) sites within the Valley Creek segment reveal higher sulfate and lower chloride concentrations at the downstream site (fig. 54). Consequently, load increase for sulfate more than doubles that of chloride, reinforcing the sulfate dominance of river water (table 6). Baseflow contributions of naturally sulfate-rich ground water appear to be the dominant mechanism increasing the salinity load of the Colorado River in the Valley Creek segment.

Using April 2005 surface-water data as an example, the Machae Creek, Maverick, Bull Hollow, and Valley Creek high-conductivity segments account incrementally for a total dissolved solids loading of no more than 72,300 kg/day. During the same sampling period, Elm Creek contributed an estimated additional 160,521 kg/day as surface flow to the Colorado River at Ballinger, more than doubling the TDS load carried by the Colorado River (fig. 39).

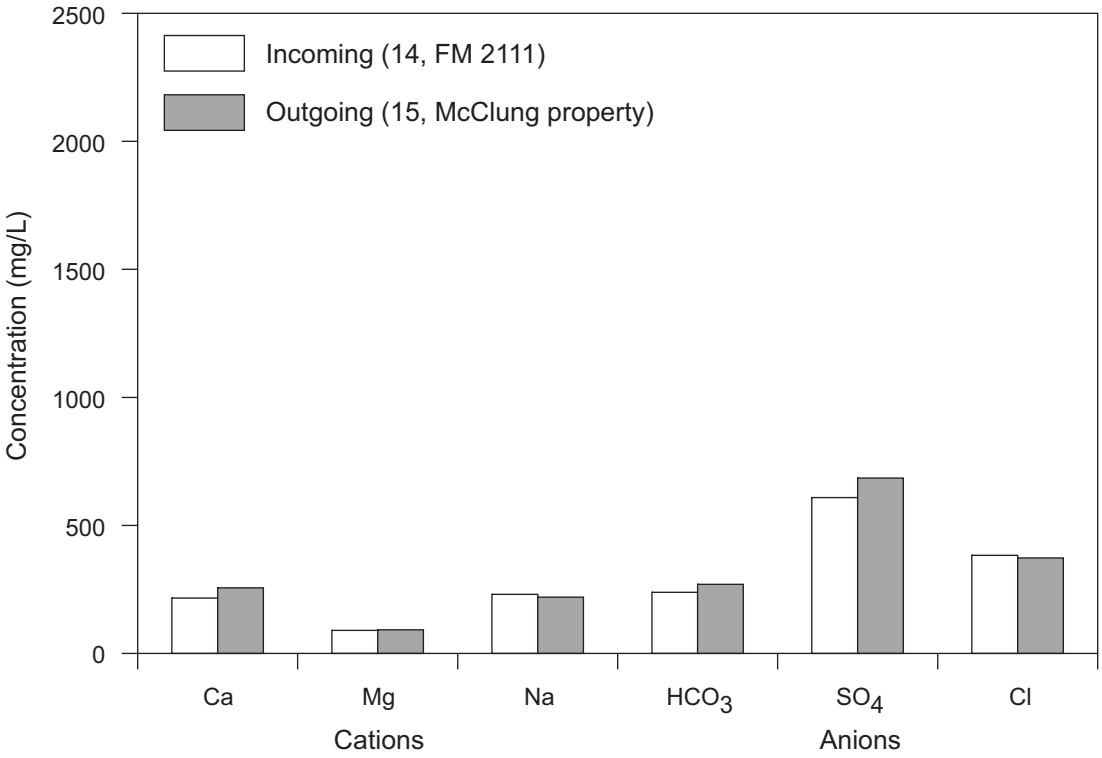

Figure 54. Major-ion concentrations in Colorado River samples taken upstream (incoming, location 14, fig. 32) and downstream (outgoing, location 15) from the Valley Creek high-conductivity area in April 2005 (appendix C).

CONCLUSIONS

We employed ground-based and airborne EM methods and supporting geological and hydrochemical analyses to delineate areas of ground salinization that increase the salinity, chloride, and sulfate loads of the upper Colorado River between Lake Thomas and Ivie Reservoir.

Geophysical methods identified four high-conductivity segments of the Colorado River along segment 1426 that are characterized by dominant baseflow contributions to the salinity load of the river. All segments receive significant natural salinity contributions from local and regional dissolution of Permian sulfate-bearing minerals. Two of the high-conductivity segments below Spence Reservoir also receive chloride-enriched baseflow or surface contributions, most likely from brine once produced in local oil fields.

Seven additional high-conductivity areas were identified upstream from Spence Reservoir that are likely to increase the salinity load of the Colorado River on its way to Spence Reservoir. These areas have higher conductivities than those below Spence Reservoir, suggesting a generally greater degree of ground salinization along the river. Four of the seven areas are located within or adjacent to major oil fields that may augment natural sources of salinity by having introduced subsurface brine into the near-surface environment over their long history of operation.

ACKNOWLEDGMENTS

This project was funded under Service Order No. 6, Framework Agreement No. 582-4-56385 between the Texas Commission on Environmental Quality (TCEQ) and the Bureau of Economic Geology, The University of Texas at Austin, Jeffrey G. Paine, principal investigator. Kerry Niemann served as TCEQ's project manager.

Alex Oren, Dak Darbha, Frank Funak, and Haoping Huang of Geophex acquired and processed airborne geophysical data. Ron Stewart and Tim Cole flew and maintained the helicopter used in the airborne survey. Don Horner and Brian Floyd of the Railroad Commission of Texas (District 7C) and Okla Thornton and Wendell Barber of the Colorado River Municipal Water District helped guide field

investigations and provided oil-field and surface-water data, Raed El-Farhan and Robert Oakes of The Louis Berger Group provided GIS data, and Deborah Flados of the Railroad Commission of Texas provided oil and gas well data. Coke County resident Bud Johnson led field tours of the area and provided many helpful suggestions on area geology and hydrology. Steve Walden facilitated the project and reviewed work plans and deliverables.

REFERENCES

Beede, J. W., and Waite, V. V., 1918, The geology of Runnels County: University of Texas, Bureau of Economic Geology and Technology, Bulletin 1816, 64 p.

Beede, J. W., and Bentley, W. P., 1918, The geology of Coke County: University of Texas, Bureau of Economic Geology and Technology, Bulletin 1850, 81 p.

EA Engineering, Science, and Technology, Inc., 2002, Historical data assessment for river segment 1426 of the Colorado River: Final report prepared for Texas Natural Resource Conservation Commission, Total Maximum Daily Load Requisition No. 582-1-30480, 28 p.

Eifler, G. K., Jr., Frye, J.C., Leonard, A.B., Hentz, T.F., and Barnes, V.E., 1974, Big Spring sheet: The University of Texas at Austin, Bureau of Economic Geology, Geologic Atlas of Texas: scale 1:250,000; revised and reprinted 1994.

Eifler, G. K., Jr., Hentz, T. F., and Barnes, V. E.,1975, San Angelo sheet: The University of Texas at Austin, Bureau of Economic Geology, Geologic Atlas of Texas: scale 1:250,000.

Frischknecht, F. C., Labson, V. F., Spies, B. R., and Anderson, W. L., 1991, Profiling using small sources, in Nabighian, M. N., ed., Electromagnetic methods in applied geophysics—applications, part A and part B: Tulsa, Society of Exploration Geophysicists, p. 105–270.

Geophex, 2005, Helicopter electromagnetic and magnetic survey in Texas: Geophex, Ltd., Raleigh, N.C., final report, 21 p.

Johnson, R. S., 2002, Aquifers of Coke County, Texas: 40 p. + illustrations.

Kier, R. S., Brown, L. F., Jr., and Harwood, P., 1976, Brownwood sheet: The University of Texas at Austin, Bureau of Economic Geology, Geologic Atlas of Texas: scale 1:250,000.

Lehman, T. M., 1994, The saga of the Dockum Group and the case of the Texas/New Mexico boundary fault, *in* Ahlen, Jack, Peterson, John, and Bowsher, Arthur L., Geologic activities in the 90s, Southwest Section of AAPG 1994: New Mexico Bureau of Mines & Mineral Resources, Bulletin 150, p. 37–52.

Leifeste, D. K., and Lansford, M. W., 1968, Reconnaissance of the chemical quality of surface waters of the Colorado River basin, Texas: Texas Water Development Board, Report 71, 78 p.

Lucas, S.G., Anderson, O.J., and Hunt, A.P., 1994, Triassic stratigraphy and correlations, southern High Plains of New Mexico-Texas, *in* Ahlen, Jack, Peterson, John, and Bowsher, Arthur L., Geologic activities in the 90s, Southwest Section of AAPG 1994: New Mexico Bureau of Mines & Mineral Resources, Bulletin 150, p. 105–126.

McNeill, J. D., 1980a, Electrical conductivity of soils and rocks, Geonics Ltd., Mississauga, Ont.,Technical Note TN-5, 22 p.

McNeill, J. D., 1980b, Electromagnetic terrain conductivity measurement at low induction numbers, Geonics Ltd., Mississauga, Ont.,Technical Note TN-6, 15 p.

Mear, C.E., 1963, Stratigraphy of Permian outcrops, Coke County, Texas: Bulletin of the American Association of Petroleum Geologists, v. 47, no. 11, p. 1952–1962.

Mount, J. R., Rayner, F. A., Shamburger, V. M., Jr., Peckham, R. C., and Osborne, F. L. Jr., 1967, Reconnaissance investigation of the ground-water resources of the Colorado River Basin, Texas: Texas Water Development Board, Report 51, 107 p.

Paine, J. G., Dutton, A. R., and Blüm, M. U., 1999, Using airborne geophysics to identify salinization in West Texas: The University of Texas at Austin, Bureau of Economic Geology, Report of Investigations No. 257, 69 p.

Parasnis, D. S., 1986, Principles of applied geophysics: Chapman and Hall, 402 p.

Richter, B. C., Dutton, A. R., and Kreitler, C. W., 1990, Identification of sources and mechanisms of salt-water pollution affecting ground-water quality: a case study, West Texas: The University of Texas at Austin, Bureau of Economic Geology, Report of Investigations No. 191, 43 p.

Robinove, C. J., Langford, R. H., and Brookhart, J. W., 1958, Saline-water resources of North Dakota: U. S. Geological Survey Water-Supply Paper 1428, 72 p.

Sengpiel, K. P., 1988, Approximate inversion of airborne EM data from a multi-layered ground: Geophysical Prospecting, v. 36, p. 446–459.

Shamburger, V. M. Jr., 1967, Ground-Water resources of Mitchell and western Nolan Counties, Texas, Texas Water Development Board, Report 50, 175 p.

Slade, R. M., and Buszka, P. M., 1994, Characteristics of streams and aquifers and processes affecting the salinity of water in the upper Colorado River basin, Texas: U.S. Geological Survey, Water Resources Investigation Report 94-4036, 81 p.

Sullivan, Jeri, Nava, Robin, Paine, Jeffrey, Dutton, Alan, and Smyth, Rebecca, 1999, Investigation of the Snyder Field Site, Howard County, Texas: The University of Texas at Austin, Bureau of Economic Geology, final report prepared for the Railroad Commission of Texas under interagency contract no. UTA98-0380, 49 p. + appendices (2 vols).

Telford, W. M., Geldart, L. P., and Sheriff, R. E., 1990, Applied Geophysics, 2nd edition, New York, Cambridge University Press, 770 p.

West, G. F., and Macnae, J. C., 1991, Physics of the electromagnetic induction exploration method, in Nabighian, M. N., ed., Electromagnetic methods in applied geophysics—applications, part A and part B: Tulsa, Society of Exploration Geophysicists, p. 5–45.

West Texas-San Angelo Geological Societies, 1961, Upper Permian to Pliocene-San Angelo Area field trip guidebook: Publication 61-46, 99 p.Wilson, C. A., 1973, Ground-water resources of Coke County, Texas: Texas Water Development Board, Report 166, 87 p.

Wilson, C. A., 1973, Ground-water resources of Coke County, Texas: Texas Water Development Board, Report 166, 87 p.

Won, I. J., Oren, Alex, and Funak, Frank, 2003, GEM-2A: A programmable broadband helicopter-towed electromagnetic sensor: Geophysics, v. 68, no.6, p. 1888–1895.

APPENDIX A: APPARENT GROUND CONDUCTIVITY MEASUREMENTS

Apparent conductivity measured in the upper Colorado River area, July, August, and October 2004 and March 2005 (fig. 9). Conductivities (in millisiemens per meter, or mS/m) were measured using the Geonics EM31 ground conductivity meter in the vertical (VD) and horizontal (HD) dipole configurations. Location coordinates, determined using a GPS receiver, are in decimal degrees using the 1984 World Geodetic System (WGS 1984).

Location	Latitude (degrees)	Longitude (degrees)	Date	App. Con. (VD, mS/m)	App. Con (HD, mS/m)	Notes
C003	31.91093	-100.52301	7/20/05	93	80	Lake Spence; Lakeview Rec. Area
C004	31.91091	-100.52313	7/20/05	90	74	Lake Spence; Lakeview Rec. Area
C005	31.91091	-100.52325	7/20/05	89	80	Lake Spence; Lakeview Rec. Area
C006	31.91091	-100.52334	7/20/05	83	93	Lake Spence; Lakeview Rec. Area
C007	31.91089	-100.52341	7/20/05	107	105	Lake Spence; Lakeview Rec. Area
C008	31.91088	-100.52355	7/20/05	121	115	Lake Spence; Lakeview Rec. Area
C009	31.91084	-100.52363	7/20/05	122	123	Lake Spence; Lakeview Rec. Area
C010	31.91083	-100.52374	7/20/05	115	118	Lake Spence; Lakeview Rec. Area
C011	31.91083	-100.52388	7/20/05	127	133	Lake Spence; Lakeview Rec. Area
C012	31.91086	-100.52397	7/20/05	112	140	Lake Spence; Lakeview Rec. Area
C013	31.90407	-100.51304	7/20/05	82	80	Messbox Creek; under power line
C014	31.90417	-100.51302	7/20/05	65	75	Messbox Creek
C015	31.90425	-100.51298	7/20/05	90	77	Messbox Creek
C016	31.90434	-100.51292	7/20/05	98	90	Messbox Creek
C017	31.90444	-100.51289	7/20/05	118	89	Messbox Creek; gravel bar
C018	31.90449	-100.51281	7/20/05	121	100	Messbox Creek
C020	31.87333	-100.51915	7/20/05	85	61	Wildcat Creek
C021	31.87340	-100.51908	7/20/05	68	51	Wildcat Creek
C022	31.87344	-100.51898	7/20/05	59	49	Wildcat Creek
C023	31.87352	-100.51892	7/20/05	65	45	Wildcat Creek
C024	31.87359	-100.51886	7/20/05	70	55	Wildcat Creek
C025	31.87364	-100.51876	7/20/05	64	61	Wildcat Creek
C026	31.87369	-100.51868	7/20/05	67	60	Wildcat Creek
C027	31.87376	-100.51859	7/20/05	61	51	Wildcat Creek
C028	31.91257	-100.58280	7/20/05	71	149	Salt Creek
C029	31.91249	-100.58288	7/20/05	96	159	Salt Creek
C030	31.91241	-100.58292	7/20/05	116	166	Salt Creek
C031	31.91233	-100.58297	7/20/05	102	155	Salt Creek
C032	31.91227	-100.58306	7/20/05	106	152	Salt Creek
C033	31.91219	-100.58311	7/20/05	103	146	Salt Creek
C034	31.91207	-100.58326	7/20/05	101	134	Salt Creek
C035	31.91193	-100.58341	7/20/05	90	122	Salt Creek; boat dock
C036	31.91182	-100.58358	7/20/05	82	181	Salt Creek
C037	31.91172	-100.58376	7/20/05	87	192	Salt Creek
C038	31.91158	-100.58391	7/20/05	96	170	Salt Creek
C039	31.91144	-100.58403	7/20/05	109	152	Salt Creek
C041	31.90674	-100.61230	7/20/05	71	67	Salt Creek; Dripping Springs
C042	31.92918	-100.66157	7/20/05	54	46	Pecan Creek; power line
C043	31.92912	-100.66166	7/20/05	48	40	Pecan Creek
C044	31.92909	-100.66176	7/20/05	46	43	Pecan Creek
C045	31.92905	-100.66188	7/20/05	48	44	Pecan Creek

C046	31.90317	-100.56874	7/20/05	53	39	Paint Creek
C047	31.90325	-100.56876	7/20/05	47	32	Paint Creek
C048	31.90334	-100.56873	7/20/05	46	36	Paint Creek
C049	31.91828	-100.52989	7/20/05	8	8	Lake Spence; Lakeview Rec. Area; caliche-cemented alluvium
C050	31.91822	-100.53010	7/20/05	9	8	Lake Spence; Lakeview Rec. Area; caliche-cemented alluvium
C051	31.91814	-100.53028	7/20/05	8	7	Lake Spence; Lakeview Rec. Area; caliche-cemented alluvium
C052	31.91804	-100.53046	7/20/05	8	7	Lake Spence; Lakeview Rec. Area; caliche-cemented alluvium
C053	31.98457	-100.54439	7/20/05	47	30	Yellow Wolf Creek
C054	31.98453	-100.54445	7/20/05	58	39	Yellow Wolf Creek
C055	31.89191	-100.49170	7/20/05	87	59	Colorado River; Robert Lee
C056	31.89173	-100.49165	7/20/05	66	50	Colorado River; Robert Lee
C057	31.89155	-100.49170	7/20/05	84	112	Colorado River; Robert Lee
C058	31.89137	-100.49176	7/20/05	83	119	Colorado River; Robert Lee
C059	31.89119	-100.49173	7/20/05	93	104	Colorado River; Robert Lee
C060	31.89101	-100.49181	7/20/05	108	109	Colorado River; Robert Lee
C061	31.89084	-100.49184	7/20/05	102	61	Colorado River; Robert Lee
C062	31.89067	-100.49189	7/20/05	96	74	Colorado River; Robert Lee
C063	31.89048	-100.49185	7/20/05	76	48	Colorado River; Robert Lee
C064	31.89026	-100.49191	7/20/05	64	75	Colorado River; Robert Lee
C065	31.89554	-100.48186	7/21/05	78	55	Mountain Creek; Robert Lee
C066	31.89544	-100.48169	7/21/05	77	54	Mountain Creek; Robert Lee
C067	31.89527	-100.48160	7/21/05	66	49	Mountain Creek; Robert Lee
C068	31.89511	-100.48148	7/21/05	73	55	Mountain Creek; Robert Lee
C069	31.89495	-100.48139	7/21/05	77	51	Mountain Creek; Robert Lee
C070	31.89481	-100.48126	7/21/05	94	87	Mountain Creek; Robert Lee
C071	31.89464	-100.48115	7/21/05	120	120	Mountain Creek; Robert Lee
C072	31.89455	-100.48099	7/21/05	101	67	Mountain Creek; Robert Lee
C073	31.89449	-100.48073	7/21/05	80	67	Mountain Creek; Robert Lee
C074	31.89442	-100.48049	7/21/05	80	50	Mountain Creek; Robert Lee
C075	31.89432	-100.48033	7/21/05	89	67	Mountain Creek; Robert Lee
C077	31.85091	-100.42461	7/21/05	126	95	Colorado River; gravel quarry
C078	31.85089	-100.42441	7/21/05	131	102	Colorado River; gravel quarry
C079	31.85089	-100.42420	7/21/05	145	122	Colorado River; gravel quarry
C080	31.85095	-100.42398	7/21/05	157	142	Colorado River; gravel quarry
C081	31.85097	-100.42377	7/21/05	210	156	Colorado River; gravel quarry
C082	31.85109	-100.42359	7/21/05	267	454	Colorado River; gravel quarry; efflorescence
C083	31.85114	-100.42349	7/21/05	176	528	Colorado River; gravel quarry; efflorescence
C084	31.85115	-100.42339	7/21/05	200	440	Colorado River; gravel quarry; efflorescence
C085	31.85095	-100.42355	7/21/05	252	212	Colorado River; gravel quarry
C086	31.85096	-100.42345	7/21/05	264	210	Colorado River; gravel quarry
C087	31.85093	-100.42336	7/21/05	217	177	Colorado River; gravel quarry
C088	31.85092	-100.42325	7/21/05	247	192	Colorado River; gravel quarry
C089	31.85077	-100.42306	7/21/05	199	155	Colorado River; gravel quarry
C091	31.85333	-100.42340	7/21/05	131	80	Machae Creek
C092	31.85323	-100.42322	7/21/05	155	127	Machae Creek
C093	31.85303	-100.42318	7/21/05	205	151	Machae Creek
C094	31.85290	-100.42302	7/21/05	189	144	Machae Creek

C095	31.85273	-100.42296	7/21/05	205	153	Machae Creek
C096	31.85265	-100.42304	7/21/05	198	223	Machae Creek
C097	31.85251	-100.42299	7/21/05	171	224	Machae Creek
C098	31.85249	-100.42288	7/21/05	190	170	Machae Creek
C099	31.85353	-100.42349	7/21/05	113	88	Machae Creek
C100	31.85366	-100.42364	7/21/05	97	77	Machae Creek
C101	31.85374	-100.42378	7/21/05	73	62	Machae Creek
C102	31.87520	-100.36633	7/21/05	85	62	Turkey Creek
C103	31.87495	-100.36625	7/21/05	72	47	Turkey Creek
C104	31.87521	-100.35274	7/21/05	55	31	Double Barrel Creek
C105	31.87506	-100.35288	7/21/05	60	40	Double Barrel Creek
C106	31.86697	-100.29258	7/21/05	73	54	Kickapoo Creek; U.S. 277
C107	31.86701	-100.29279	7/21/05	78	54	Kickapoo Creek; U.S. 277
C108	31.86707	-100.29287	7/21/05	79	63	Kickapoo Creek; U.S. 277
C109	31.86714	-100.29297	7/21/05	83	58	Kickapoo Creek; U.S. 277
C110	31.84702	-100.28923	7/21/05	90	78	Colorado River; U.S. 277 to Kickapoo Creek
C111	31.84709	-100.28920	7/21/05	88	100	Colorado River; U.S. 277 to Kickapoo Creek
C112	31.84697	-100.28788	7/21/05	115	211	Kickapoo Creek; mouth
C113	31.84700	-100.28811	7/21/05	137	120	Kickapoo Creek; mouth
C114	31.84667	-100.28677	7/21/05	99	46	Kickapoo Creek; mouth
C115	31.84716	-100.28682	7/21/05	108	130	Kickapoo Creek
C116	31.84710	-100.28683	7/21/05	136	97	Kickapoo Creek
C117	31.84679	-100.28734	7/21/05	69	120	Colorado River; near Kickapoo Creek confluence
C118	31.84684	-100.28718	7/21/05	128	115	Colorado River; near Kickapoo Creek confluence
C119	31.84679	-100.28714	7/21/05	121	131	Colorado River; near Kickapoo Creek confluence
C120	31.84670	-100.28703	7/21/05	118	116	Colorado River; near Kickapoo Creek confluence
C121	31.84668	-100.28692	7/21/05	101	129	Colorado River; near Kickapoo Creek confluence
C123	31.84791	-100.29660	7/21/05	109	80	Colorado River; upstream from U.S. 277
C124	31.84792	-100.29650	7/21/05	91	76	Colorado River; upstream from U.S. 277
C125	31.84792	-100.29639	7/21/05	88	78	Colorado River; upstream from U.S. 277
C126	31.84789	-100.29628	7/21/05	96	85	Colorado River; upstream from U.S. 277
C127	31.84789	-100.29617	7/21/05	90	90	Colorado River; upstream from U.S. 277
C128	31.84789	-100.29606	7/21/05	85	85	Colorado River; upstream from U.S. 277
C129	31.84437	-100.22253	7/22/05	60	42	Hog Creek
C130	31.84418	-100.22266	7/22/05	53	41	Hog Creek
C131	31.84406	-100.22276	7/22/05	57	48	Hog Creek
C132	31.84392	-100.22290	7/22/05	56	40	Hog Creek
C133	31.80920	-100.21784	7/22/05	102	98	Colorado River; county road crossing
C134	31.80934	-100.21771	7/22/05	88	79	Colorado River; county road crossing

C135	31.80937	-100.21767	7/22/05	92	82	Colorado River; county road crossing
C136	31.80937	-100.21755	7/22/05	88	82	Colorado River; county road crossing
C137	31.80941	-100.21738	7/22/05	96	94	Colorado River; county road crossing
C138	31.84610	-100.19607	7/22/05	107	89	Oak Creek
C139	31.84600	-100.19590	7/22/05	106	92	Oak Creek
C140	31.84588	-100.19573	7/22/05	101	89	Oak Creek
C141	31.84577	-100.19557	7/22/05	106	95	Oak Creek
C142	31.84561	-100.19545	7/22/05	113	115	Oak Creek
C143	31.84543	-100.19542	7/22/05	114	129	Oak Creek
C144	31.84526	-100.19548	7/22/05	114	118	Oak Creek;; seep
C145	31.84507	-100.19554	7/22/05	126	124	Oak Creek
C146	31.84491	-100.19573	7/22/05	100	124	Oak Creek
C147	31.84479	-100.19589	7/22/05	106	95	Oak Creek
C148	31.84472	-100.19615	7/22/05	102	103	Oak Creek
C149	31.84464	-100.19638	7/22/05	114	122	Oak Creek
C150	31.79261	-100.18478	7/22/05	80	93	Colorado River; upstream from FM 3115 bridge; in river
C151	31.79271	-100.18545	7/22/05	83	71	Colorado River; upstream from FM 3115 bridge
C152	31.79266	-100.18532	7/22/05	73	65	Colorado River; upstream from FM 3115 bridge
C153	31.79268	-100.18523	7/22/05	79	77	Colorado River; upstream from FM 3115 bridge
C154	31.79267	-100.18513	7/22/05	81	71	Colorado River; upstream from FM 3115 bridge
C155	31.79267	-100.18502	7/22/05	81	68	Colorado River; upstream from FM 3115 bridge
C156	31.79263	-100.18493	7/22/05	86	81	Colorado River; upstream from FM 3115 bridge
C157	31.79236	-100.18434	7/22/05	62	79	Colorado River; downstream from FM 3115 bridge
C158	31.79234	-100.18426	7/22/05	65	78	Colorado River; downstream from FM 3115 bridge
C159	31.79231	-100.18417	7/22/05	72	88	Colorado River; downstream from FM 3115 bridge
C160	31.81908	-100.05254	7/22/05	99	75	Valley Creek
C161	31.81926	-100.05264	7/22/05	110	78	Valley Creek
C162	31.81942	-100.05273	7/22/05	113	116	Valley Creek
C163	31.81959	-100.05277	7/22/05	114	112	Valley Creek
C164	31.81977	-100.05283	7/22/05	125	105	Valley Creek
C165	31.77918	-100.03287	7/22/05	88	63	Valley Creek
C166	31.77900	-100.03284	7/22/05	87	72	Valley Creek
C167	31.77883	-100.03289	7/22/05	89	66	Valley Creek
C168	31.77864	-100.03293	7/22/05	88	57	Valley Creek
C169	31.75831	-100.05142	7/22/05	106	88	Quarry Creek
C170	31.75847	-100.05156	7/22/05	109	85	Quarry Creek
C171	31.75853	-100.05175	7/22/05	92	65	Quarry Creek
C173	31.71485	-100.02673	7/22/05	86	74	Colorado River; downstream from FM 2111 bridge
C174	31.71486	-100.02673	7/22/05	78	76	Colorado River; downstream from FM 2111 bridge

C175	31.71484	-100.02666	7/22/05	88	101	Colorado River; downstream from FM 2111 bridge; in river
C176	31.71494	-100.02651	7/22/05	86	114	Colorado River; downstream from FM 2111 bridge
C177	31.73634	-99.98963	7/22/05	97	147	Los Arroyos
C178	31.73635	-99.98944	7/22/05	105	112	Los Arroyos
C179	31.73635	-99.98921	7/22/05	98	101	Los Arroyos
C180	31.73653	-99.98903	7/22/05	104	115	Los Arroyos
C181	31.78535	-99.94610	7/22/05	55	50	Elm Creek
C182	31.78547	-99.94595	7/22/05	64	41	Elm Creek
C183	31.78559	-99.94579	7/22/05	62	45	Elm Creek
C184	31.73000	-99.94186	7/22/05	90	62	Colorado River; U.S. 83 bridge; on terrace 1m above river
C185	31.73004	-99.94210	7/22/05	90	68	Colorado River; U.S. 83 bridge; on terrace 1m above river
C186	31.73258	-99.95472	7/22/05	163	105	Colorado River; U.S. 67 bridge; under bridge
C199	31.73876	-99.88884	8/3/04	85	78	Bears Foot Creek; County Road 122
C200	31.73860	-99.88874	8/3/04	93	97	Bears Foot Creek; County Road 122
C201	31.70955	-99.83671	8/3/04	83	60	Mustang Creek; county road
C202	31.70941	-99.83673	8/3/04	70	49	Mustang Creek; county road
C203	31.70905	-99.83675	8/3/04	86	69	Mustang Creek; county road
C204	31.70879	-99.83680	8/3/04	75	60	Mustang Creek; county road
C205	31.70856	-99.83681	8/3/04	75	53	Mustang Creek; county road
C207	31.63603	-99.83225	8/3/04	56	46	Colorado River; County Road 129
C209	31.69229	-99.91707	8/3/04	89	81	Spur Creek; County Road 114
C210	31.69237	-99.91681	8/3/04	102	111	Spur Creek; County Road 114
C211	31.71016	-100.02246	8/3/04	72	56	Rocky Creek; County Road 287
C212	31.71011	-100.02256	8/3/04	78	54	Rocky Creek; County Road 287
C213	31.70768	-100.06100	8/3/04	101	84	Indian Creek; County Road 287
C214	31.71207	-100.10652	8/3/04	111	129	Red Bank Creek
C215	31.71233	-100.10643	8/3/04	98	103	Red Bank Creek
C216	31.72561	-100.14081	8/3/04	71	56	Antelope Creek
C217	31.72539	-100.14096	8/3/04	55	58	Antelope Creek
C218	31.76844	-100.21734	8/3/04	85	65	Mule Creek
C219	31.76839	-100.21769	8/3/04	75	60	Mule Creek
C220	31.79256	-100.25263	8/3/04	63	65	Juniper Creek
C221	31.79248	-100.25251	8/3/04	87	76	Juniper Creek
C222	31.79243	-100.25244	8/3/04	88	95	Juniper Creek
C223	31.82520	-100.31650	8/3/04	34	26	Live Oak Creek tributary
C224	31.82504	-100.31648	8/3/04	34	30	Live Oak Creek tributary
C225	31.82854	-100.32744	8/3/04	25	24	Live Oak Creek
C226	31.82865	-100.32747	8/3/04	30	22	Live Oak Creek
C227	31.82889	-100.32743	8/3/04	28	20	Live Oak Creek
C229	31.84775	-100.43790	8/3/04	94	66	Jack Miles Creek
C230	31.84783	-100.43791	8/3/04	99	74	Jack Miles Creek
C231	31.83588	-100.43149	8/3/04	80	38	Buffalo Creek
C232	31.83607	-100.43146	8/3/04	50	34	Buffalo Creek
C233	31.83615	-100.43152	8/3/04	42	37	Buffalo Creek
C234	31.83631	-100.43151	8/3/04	48	46	Buffalo Creek
C235	31.83649	-100.43153	8/3/04	74	51	Buffalo Creek

C237	32.01964	-100.73653	8/3/04	170	200	Colorado River; RR 2059 bridge
C238	32.01964	-100.73627	8/3/04	180	298	Colorado River; RR 2059 bridge
C239	31.97891	-100.58553	8/3/04	71	64	Rough Creek
C240	31.97896	-100.58539	8/3/04	84	79	Rough Creek
C241	31.97906	-100.58527	8/3/04	95	84	Rough Creek
C242	31.97919	-100.58524	8/3/04	135	107	Rough Creek
C243	31.97929	-100.58512	8/3/04	127	98	Rough Creek
C245	32.62784	-101.28577	10/26/04	56	47	Colorado River; FM 1205 bridge
C246	32.62872	-101.28560	10/26/04	146	154	Colorado River; FM 1205 bridge
C250	32.58429	-101.13025	10/26/04	121	153	Colorado River; FM 1298 bridge
C251	32.59886	-101.09421	10/26/04	142	122	Bull Creek; FM 2085 bridge
C252	32.59947	-101.09413	10/26/04	109	158	Bull Creek; FM 2085 bridge
C253	32.59221	-101.05031	10/26/04	114	101	Bluff Creek; FM 1606 bridge
C254	32.59240	-101.05027	10/26/04	109	98	Bluff Creek; FM 1606 bridge
C255	32.53889	-101.05501	10/26/04	425	275	Colorado River; Texas 350 bridge
C257	32.51109	-101.05679	10/26/04	103	97	Willow Creek; FM 1229 bridge
C258	32.54445	-100.96855	10/26/04	246	203	Colorado River; FM 2835 bridge
C259	32.57486	-100.96207	10/26/04	78	92	Canyon Creek; FM 1606 bridge
C260	32.54425	-100.88492	10/26/04	138	125	Deep Creek; Scurry County Road 4138
C261	32.54414	-100.88489	10/26/04	136	107	Deep Creek; Scurry County Road 4138
C262	32.47826	-100.94913	10/26/04	220	260	Colorado River; FM 1808 bridge
C263	32.44178	-100.94920	10/26/04	207	155	Colorado River; Mitchell County Road 167; Cedar Bend bridge
C265	32.39344	-100.85077	10/27/04	83	102	Lone Wolf Creek; Ruddick Park, Colorado City
C266	32.39331	-100.85095	10/27/04	110	110	Lone Wolf Creek; Ruddick Park, Colorado City
C267	32.39261	-100.85111	10/27/04	84	45	Lone Wolf Creek; Ruddick Park, Colorado City
C268	32.39262	-100.85120	10/27/04	61	56	Lone Wolf Creek; Ruddick Park, Colorado City
C269	32.38928	-100.87327	10/27/04	286	158	Colorado River; State Spur 377 bridge
C270	32.38940	-100.87319	10/27/04	166	186	Colorado River; State Spur 377 bridge
C271	32.38952	-100.87319	10/27/04	154	180	Colorado River; State Spur 377 bridge
C272	32.38515	-100.86510	10/27/04	124	137	Colorado River; Texas 163 bridge
C273	32.31600	-100.91794	10/27/04	205	215	Morgan Creek; Texas 163 bridge
C275	32.24941	-100.97229	10/27/04	61	60	Wildhorse Creek; Mitchell County Road 337
C276	32.19927	-101.01380	10/27/04	128	139	Beals Creek; downstream fromTexas 163 bridge
C277	32.19921	-101.01378	10/27/04	137	123	Beals Creek; downstream fromTexas 163 bridge
C278	32.20992	-100.87275	10/27/04	123	139	Colorado River; Mitchell County Road 337
C281	32.12869	-100.73418	10/27/04	70	47	Walnut Creek; Texas 208
C284	32.20338	-100.78577	10/27/04	100	81	Red Bank Creek; Mitchell County Road 337
C286	32.25701	-101.41743	10/28/04	389	407	Beals Creek; Midway Road
C287	32.25714	-101.41743	10/28/04	428	474	Beals Creek; Midway Road

C288	32.24896	-101.36224	10/28/04	174	138	Beals Creek; Moss Lake Road
C289	32.24897	-101.36217	10/28/04	166	153	Beals Creek; Moss Lake Road
C290	32.24899	-101.36213	10/28/04	135	215	Beals Creek; Moss Lake Road
C293	32.21249	-101.21040	10/28/04	280	206	Beals Creek; FM 821 bridge
C294	32.14169	-101.18821	10/28/04	74	62	Bull Creek; FM 2183
C295	32.14190	-101.18822	10/28/04	87	57	Bull Creek; FM 2183
C296	32.17102	-101.02146	10/28/04	150	132	Hackberry Creek; FM 2183
C297	32.17099	-101.02149	10/28/04	134	93	Hackberry Creek; FM 2183
C298	32.39965	-100.89426	10/28/04	265	376	Colorado River; I-20 bridge
C299	32.39981	-100.89428	10/28/04	258	290	Colorado River; I-20 bridge
C300	32.39987	-100.89425	10/28/04	204	238	Colorado River; I-20 bridge
C301	32.39996	-100.89427	10/28/04	250	316	Colorado River; I-20 bridge
C304	32.25777	-101.43190	10/28/04	214	367	Beals Creek; FM 700 bridge
C305	32.25784	-101.43209	10/28/04	225	397	Beals Creek; FM 700 bridge
C402	31.84681	-100.39250	3/8/05	192	244	Colorado River bank, Wendkirk oil field
C403	31.84674	-100.39256	3/8/05	211	320	Colorado River bank, Wendkirk oil field
C404	31.84665	-100.39260	3/8/05	242	272	Colorado River bank, Wendkirk oil field
C405	31.84658	-100.39266	3/8/05	211	385	Colorado River bank, Wendkirk oil field
C406	31.84653	-100.39275	3/8/05	230	285	Colorado River bank, Wendkirk oil field
C407	31.84646	-100.39283	3/8/05	239	279	Colorado River bank, Wendkirk oil field
C408	31.84640	-100.39288	3/8/05	212	263	Colorado River bank, Wendkirk oil field
C409	31.84929	-100.37647	3/8/05	42	38	Plugged oil well, Wendkirk oil field
C410	31.84936	-100.37651	3/8/05	46	36	Plugged well, Wendkirk oil field
C411	31.84945	-100.37655	3/8/05	56	44	Plugged well, Wendkirk oil field
C412	31.84953	-100.37661	3/8/05	51	44	Plugged well, Wendkirk oil field
C413	31.84961	-100.37665	3/8/05	47	37	Plugged well, Wendkirk oil field
C414	31.84971	-100.37666	3/8/05	50	38	Plugged well, Wendkirk oil field
C415	31.85400	-100.38147	3/8/05	90	71	Barren area, Wendkirk oil field
C416	31.85409	-100.38149	3/8/05	94	54	Barren area, Wendkirk oil field
C417	31.85418	-100.38153	3/8/05	155	161	Barren area, Wendkirk oil field
C418	31.85426	-100.38157	3/8/05	191	351	Barren area, Wendkirk oil field
C419	31.85435	-100.38158	3/8/05	336	369	Barren area, Wendkirk oil field
C420	31.85444	-100.38159	3/8/05	204	287	Barren area, Wendkirk oil field
C421	31.85453	-100.38161	3/8/05	98	93	Barren area, Wendkirk oil field
C422	31.85463	-100.38164	3/8/05	78	59	Barren area, Wendkirk oil field
C423	31.85471	-100.38167	3/8/05	58	46	Barren area, Wendkirk oil field
C424	31.85479	-100.38174	3/8/05	54	40	Barren area, Wendkirk oil field
C425	31.85487	-100.38177	3/8/05	55	42	Barren area, Wendkirk oil field
C426	32.05315	-100.75306	3/9/05	36	20	Gypsum beds, Jameson-Strawn oil field
C427	32.05330	-100.75309	3/9/05	38	25	Gypsum beds, Jameson-Strawn oil field
C428	32.05345	-100.75301	3/9/05	28	20	Gypsum beds, Jameson-Strawn oil field
C431	32.00957	-100.71117	3/9/05	105	81	Colorado River, Silver Loop Road
C432	32.00957	-100.71127	3/9/05	105	76	Colorado River, Silver Loop Road

C433	32.00959	-100.71138	3/9/05	97	71	Colorado River, Silver Loop Road
C434	32.00958	-100.71149	3/9/05	93	68	Colorado River, Silver Loop Road
C435	32.00961	-100.71159	3/9/05	97	70	Colorado River, Silver Loop Road
C436	32.00964	-100.71169	3/9/05	103	69	Colorado River, Silver Loop Road
C437	32.00937	-100.71137	3/9/05	138	104	Colorado River, Silver Loop Road
C438	32.00936	-100.71126	3/9/05	188	185	Colorado River, Silver Loop Road
C439	32.00934	-100.71116	3/9/05	166	117	Colorado River, Silver Loop Road
C440	32.00932	-100.71105	3/9/05	179	151	Colorado River, Silver Loop Road
C441	32.00934	-100.71095	3/9/05	171	135	Colorado River, Silver Loop Road
C480	31.73182	-99.99932	3/10/05	101	85	Colorado River below McClung residence
C481	31.73172	-99.99933	3/10/05	85	66	Colorado River below McClung residence
C482	31.73164	-99.99938	3/10/05	73	66	Colorado River below McClung residence
C483	31.73156	-99.99942	3/10/05	74	53	Colorado River below McClung residence
C484	31.73147	-99.99943	3/10/05	67	53	Colorado River below McClung residence
C485	31.73141	-99.99953	3/10/05	72	56	Colorado River below McClung residence
C486	31.73133	-99.99958	3/10/05	73	56	Colorado River below McClung residence
C487	31.73126	-99.99967	3/10/05	71	56	Colorado River below McClung residence
C488	31.73119	-99.99971	3/10/05	77	58	Colorado River below McClung residence
C489	31.73111	-99.99983	3/10/05	80	53	Colorado River below McClung residence
C490	31.73105	-99.99992	3/10/05	74	57	Colorado River below McClung residence
C491	31.73096	-100.00012	3/10/05	79	63	Colorado River below McClung residence
C492	31.73090	-100.00039	3/10/05	75	59	Colorado River below McClung residence
C493	31.73086	-100.00059	3/10/05	81	59	Colorado River below McClung residence
C494	31.73091	-100.00089	3/10/05	66	47	Colorado River below McClung residence
C495	31.73095	-100.00111	3/10/05	85	93	Colorado River below McClung residence
C496	31.73075	-100.00130	3/10/05	87	63	Colorado River below McClung residence
C498	31.73119	-100.00111	3/10/05	70	54	Colorado River below McClung residence
C499	31.73142	-100.00095	3/10/05	88	70	Colorado River below McClung residence
C500	31.73152	-100.00076	3/10/05	101	76	Colorado River below McClung residence
C501	31.73169	-100.00058	3/10/05	106	78	Colorado River below McClung residence
C502	31.73182	-100.00038	3/10/05	100	96	Colorado River below McClung residence

C503	31.73191	-100.00016	3/10/05	116	100	Colorado River below McClung residence
C504	31.73198	-99.99993	3/10/05	130	102	Colorado River below McClung residence
C505	31.73202	-99.99977	3/10/05	125	113	Colorado River below McClung residence
C506	31.73210	-99.99974	3/10/05	177	155	Colorado River below McClung residence
C507	31.73212	-99.99960	3/10/05	186	222	Colorado River below McClung residence
C512	31.72418	-100.10864	3/10/05	68	44	Colorado River; Currie Ranch
C513	31.72411	-100.10872	3/10/05	63	45	Colorado River; Currie Ranch
C514	31.72402	-100.10876	3/10/05	53	47	Colorado River; Currie Ranch
C515	31.72392	-100.10873	3/10/05	84	53	Colorado River; Currie Ranch; pipeline
C516	31.72383	-100.10872	3/10/05	145	57	Colorado River; Currie Ranch; pipeline
C517	31.72382	-100.10871	3/10/05	67	49	Colorado River; Currie Ranch
C518	31.72366	-100.10851	3/10/05	61	44	Colorado River; Currie Ranch
C523	31.83154	-100.24641	3/11/05	82	60	Colorado River; Cervenka Ranch
C524	31.83158	-100.24654	3/11/05	81	68	Colorado River; Cervenka Ranch
C525	31.83160	-100.24662	3/11/05	85	67	Colorado River; Cervenka Ranch
C526	31.83165	-100.24671	3/11/05	85	72	Colorado River; Cervenka Ranch
C527	31.83170	-100.24681	3/11/05	92	72	Colorado River; Cervenka Ranch
C528	31.83173	-100.24690	3/11/05	88	71	Colorado River; Cervenka Ranch
C529	31.83182	-100.24697	3/11/05	85	74	Colorado River; Cervenka Ranch

Page intentionally blank

APPENDIX B: SURFACE WATER TEMPERATURE, CONDUCTIVITY, AND SALINITY

Temperature, apparent conductivity, and calculated total dissolved solids (TDS) concentration measured in surface-water samples from the upper Colorado River area (figs. 7 and 8) in August and October 2004. Values were measured using a Corning Checkmate 90 Conductivity and TDS Probe. Location coordinates, determined using a GPS receiver, are in decimal degrees using the 1984 World Geodetic System (WGS 1984).

Location	Latitude (degrees)	Longitude (degrees)	Date	Temp. (deg. C)	App. Con. (mS/m)	TDS (mg/L)	Notes
C187	31.91060	-100.52474	8/2/04	32.2	295	1470	Lake Spence; Lakeview Recreation Area (ponded)
C188	31.91212	-100.58331	8/2/04	37.3	702	3510	Salt Creek (ponded)
C189	31.89188	-100.49169	8/2/04	35.4	298	1490	Colorado River; Robert Lee
C190	31.85075	-100.42468	8/2/04	31.9	305	1520	Colorado River; gravel quarry; upstream from efflorescence
C191	31.85092	-100.42321	8/2/04	32.0	307	1520	Colorado River; gravel quarry; downstream from efflorescence
C192	31.84788	-100.29204	8/2/04	34.6	259	1290	Colorado River; U.S. 277 bridge
C193	31.80924	-100.21784	8/2/04	35.1	295	1470	Colorado River; county road crossing
C194	31.79256	-100.18473	8/2/04	34.2	225	1120	Colorado River; FM 3115 bridge
C195	31.71484	-100.02668	8/2/04	34.7	285	1430	Colorado River; downstream from FM 2111 bridge
C196	31.78535	-99.94621	8/2/04	34.5	151	810	Elm Creek at county road
C197	31.74993	-99.94532	8/2/04	31.3	146	732	Elm Creek at Ballinger City Park
C198	31.73241	-99.95474	8/3/04	29.5	259	1370	Colorado River; U.S. 67 bridge
C203	31.70905	-99.83675	8/3/04	28.2	84	426	Mustang Creek at county road (ponded)
C206	31.63588	-99.83225	8/3/04	31.9	156	777	Colorado River; County Road 129
C213	31.70768	-100.06100	8/3/04	30.7	44	218	Indian Creek; County Road 287 (ponded)
C228	31.82847	-100.32753	8/3/04	37.2	20	100	Live Oak Creek (ponded)
C236	32.01974	-100.73617	8/3/04	33.2	118	590	Colorado River; RR 2059 bridge
C244	32.21888	-101.47628	10/25/04	19.4	48	247	Big Spring historic site, Cosden Lake area (ponded)
C246	32.62872	-101.28560	10/26/04	18.5	299	1500	Colorado River; FM 1205 bridge
C248	32.57993	-101.13673	10/26/04	20.0	63	314	Lake J. B. Thomas; south end of dam (ponded)
C249	32.57742	-101.14325	10/26/04	20.2	62	313	Lake J. B. Thomas; south end of dam (ponded)
C250	32.58429	-101.13025	10/26/04	19.5	29	149	Colorado River; FM 1298 bridge (ponded)
C251	32.59886	-101.09421	10/26/04	21.3	327	1670	Bull Creek; FM 2085 bridge
C256	32.53888	-101.05494	10/26/04	24.0	681	3400	Colorado River; Texas 350 bridge

C257	32.51109	-101.05679	10/26/04	22.8	57	284	Willow Creek; FM 1229 bridge (ponded)
C258	32.54445	-100.96855	10/26/04	24.2	736	3690	Colorado River; FM 2835 bridge
C260	32.54425	-100.88492	10/26/04	20.0	83	415	Deep Creek; Scurry County Road 4138
C262	32.47826	-100.94913	10/26/04	23.5	489	2450	Colorado River; FM 1808 bridge
C263	32.44178	-100.94920	10/26/04	23.3	421	2111	Colorado River at Mitchell County Road 167; Cedar Bend bridge
C264	32.39378	-100.85053	10/27/04	20.2	162	807	Lone Wolf Creek at Ruddick Park, Colorado City
C269	32.38928	-100.87327	10/27/04	20.7	687	3460	Colorado River; State Spur 377 bridge
C272	32.38515	-100.86510	10/27/04	19.7	635	3170	Colorado River; Texas 163 bridge
C273	32.31600	-100.91794	10/27/04	20.6	572	2870	Morgan Creek; Texas 163 bridge (ponded)
C274	32.33939	-100.92881	10/27/04	20.6	427	2150	Lake Colorado City State Park (ponded)
C276	32.19927	-101.01380	10/27/04	21.6	338	1690	Beals Creek; downstream fromTexas 163 bridge
C278	32.20992	-100.87275	10/27/04	21.3	450	2250	Colorado River; Mitchell County Road 337
C279	31.91054	-100.52452	10/27/04	21.2	267	1330	Lake Spence; Lakeview Recreation Area (ponded)
C280	32.01966	-100.73613	10/27/04	21.5	307	1540	Colorado River; RR 2059 bridge
C285	32.25676	-101.41756	10/28/04	20.9	1630	8160	Beals Creek; Midway Road
C288	32.24896	-101.36224	10/28/04	19.4	910	4550	Beals Creek; Moss Lake Road
C291	32.24375	-101.31224	10/28/04	20.6	299	1490	Moss Creek Reservoir (ponded)
C293	32.21249	-101.21040	10/28/04	20.6	1003	5040	Beals Creek; FM 821 bridge
C302	32.39986	-100.89420	10/28/04	26.5	1205	6030	Colorado River; I-20 bridge
C303	32.44176	-100.94902	10/28/04	21.9	479	2390	Colorado River at Mitchell County Road 167; Cedar Bend Bridge
C305	32.25784	-101.43209	10/28/04	23.2	–	> 10,000	Beals Creek; FM 700 bridge

APPENDIX C: HYDROCHEMICAL ANALYSES

Laboratory analytical results for samples collected from the upper Colorado River basin. Locations shown on figs. 16 and 32.

Sample	Lat. (deg)	Long. (deg)	Date	Sp. C. uS/cm	Lab. pH	SiO2 (mg/L)	Ca (mg/L)	Mg (mg/L)	Na (mg/L)	K (mg/L)	Sr (mg/L)	CO3 (mg/L)	HCO3 (mg/L)	SO4 (mg/L)	Cl (mg/L)	NO3-N (mg/L)	Br (mg/L)	B (mg/L)	TDS (mg/L)
1	32.5389	-101.0549	2/2/05	13,600	8.05	<1.3	392	160	2,480	6.6	6.45	0.00	299	1,280	3,950	0.32	3.86	<0.53	8,430
2	32.3999	-100.8942	2/2/05	11,000	8.15	<1.3	266	133	2,080	7.7	5.83	0.00	224	1,090	3,090	0.16	3.39	<0.53	6,790
3	32.1993	-101.0138	2/1/05	11,300	8.10	9.4	425	358	1,720	22.0	9.45	0.00	344	1,500	3,060	0.38	14.3	0.92	7,280
4	32.2099	-100.8728	2/1/05	7,310	8.20	3.6	347	161	1,150	8.2	5.33	0.00	312	1,460	1,604	0.18	2.25	0.50	4,890
5	32.0197	-100.7362	2/1/05	8,420	8.05	7.3	397	174	1,310	10.7	7.25	0.00	271	1,370	2,080	0.20	4.50	0.51	5,500
6	31.8854	-100.4808	4/11/05	6,120	8.05	4.2	272	146	909	16.5	5.54	0.00	221	861	1,505	0.29	4.19	0.51	3,830
7	31.8509	-100.4232	2/1/05	4,420	8.05	4.3	205	113	607	13.1	4.06	0.00	213	700	974	0.09	3.37	0.39	2,730
8	31.8581	-100.3796	4/13/05	8,000	7.95	1.1	279	185	1,250	16.8	6.24	0.00	204	1,030	2,070	0.23	5.63	0.74	4,950
9	31.8479	-100.2920	4/11/05	5,060	8.00	4.7	319	138	646	12.0	8.60	0.00	238	1,010	1,038	0.86	3.03	0.83	3,300
10	31.8288	-100.2404	4/12/05	4,060	8.00	6.2	378	121	398	9.2	10.4	0.00	228	1,190	637	1.31	2.00	0.80	2,870
11	31.8092	-100.2178	1/31/05	4,170	8.05	5.9	342	125	474	9.5	8.83	0.00	263	1,030	728	1.67	2.29	0.66	2,860
12	31.7926	-100.1846	4/11/05	3,820	8.05	3.2	304	125	407	8.4	8.18	0.00	221	971	639	0.68	2.05	0.77	2,580
13	31.7227	-100.1074	4/12/05	3,570	8.30	1.9	251	119	402	8.7	6.64	0.00	208	848	635	0.29	1.94	0.67	2,380
14	31.7147	-100.0274	4/11/05	2,550	8.05	5.3	216	90	231	6.5	4.24	0.00	239	609	383	0.63	1.11	0.44	1,667
15	31.7318	-99.9993	4/12/05	2,630	7.95	8.4	256	92	220	3.8	5.01	0.00	270	685	373	3.14	1.16	0.42	1,792
16	31.7299	-99.9416	2/1/05	4,000	8.05	5.2	350	133	408	7.5	7.85	0.00	262	1,030	659	2.78	2.21	0.57	2,750
17	31.7499	-99.9453	1/31/05	2,520	8.20	8.6	156	103	248	4.7	3.34	0.00	362	402	411	5.44	1.73	0.41	1,540
18	31.6359	-99.8323	1/31/05	2,710	8.20	6.1	201	97	267	4.6	4.54	0.00	291	566	433	3.48	1.64	0.38	1,739
19	31.8394	-100.3826	10/27/05	172,000	6.65	12.4	8,790	1,630	39,200	244	415	0.00	121	356	80,680	na	412	7.45	131,800